THESIS

SEISMIC PERFORMANCE EVALUATION OF FULL-SCALE MASS TIMBER STRUCTURES: COMPARATIVE INSIGHTS FROM TALL AND MID-RISE SHAKE TABLE TEST PROGRAMS

Submitted by

Prashanna Mishra

Department of Civil and Environmental Engineering

In partial fulfillment of the requirements

For Degree of Master of Science

Colorado State University

Fort Collins, Colorado

Fall 2025

Master's Committee:

Advisor: John W. van de Lindt

Gaofeng Jia
Martin Shields

ABSTRACT

SEISMIC PERFORMANCE EVALUATION OF FULL-SCALE MASS TIMBER STRUCTURES: COMPARATIVE INSIGHTS FROM TALL AND MID-RISE SHAKE TABLE TEST PROGRAMS

This thesis presents an overview of the design, construction, and testing of full-scale mass timber building specimens as part of two major multi-university projects - the NHERI TallWood and NHERI Converging Design research projects. These projects both focused on ensuring resilience for tall and mid-rise wood buildings in high seismic regions, with one focusing on structural and non-structural design for resilience and the other adding considerations for sustainability. Over the past decade, advances in materials, manufacturing, components, and building systems have enabled taller mass timber construction. However, most existing tall wood buildings still rely on concrete cores or steel bracing for lateral force-resisting systems due to limited code-approved mass timber options and industry reliance on traditional systems.

The NHERI TallWood test building incorporated a post-tensioned mass timber rocking wall system, a low-damage gravity framing system, and drift-compatible non-structural components. Standing 34.4 m (113 ft) tall with a uniform 84 m² (900 ft²) floor plan, it was constructed and tested on the NHERI@UCSD outdoor shake table in Miramar, California. The system was designed to meet standard office loading criteria, with a 2-hour fire rating, and featured a range of floor systems including nail-laminated timber (NLT), dowel-laminated timber (DLT), and 5-ply cross-laminated timber (CLT) panels. Connections at the column bases at ground level were designed to allow free rotation up to 5% drift, ensuring damage-free performance during seismic events. The NHERI Converging Design structure, constructed by deconstructing the top four floors of the TallWood building, was 20.4 m (67 ft) tall and used a similar post-tensioned rocking wall system but with a modified lateral force-resisting design approach. It was also tested on the NHERI@UCSD

shake table, providing valuable comparative data on the seismic performance of both designs since they had the exact same footprint and very similar relative lateral force resistance to weight.

This research represents the first time post-tensioned rocking walls have been physically tested at full scale in such tall buildings. The results from these shake table tests, representing the tallest mass timber buildings ever tested, provided critical data for validating seismic design methodologies and supporting the adoption of resilient mass timber lateral systems in tall and mid-rise wood buildings in seismic region

ACKNOWLEDGEMENTS

I would like to express my gratitude to my advisor and mentor, Dr. John W. van de Lindt, whose unwavering support, encouragement, and guidance have been instrumental throughout this journey. His mentorship has shaped not only the direction of this research but also my growth as a researcher. I dedicate this thesis to him in appreciation of everything he has done for me.

I am profoundly thankful to my family my grandfather, the late Mr. Devendra Sharma Mishra; my father, Binod Mishra; and my mother, Rajeshwori Mishra and my sister Aashmi Mishra for the countless sacrifices they made, both known and unknown, to support me and help me reach where I am today. Their strength and love have been my constant foundation.

I am also grateful to the NHERI TallWood and NHERI Converging Design project teams for their collaborative spirit and constant support throughout this research. I would like to sincerely thank Dr. Shiling Pei, Dr. Andre R. Barbosa, Steve Pryor, Dr. Jeffrey Berman, Dr. Barbara G. Simpson, Dr. Keri L. Ryan, Dr. Arijit Sinha, Patricio A. Uarac P., Morgan McBain, Tanner Field, Steven Kontra, Shokrullah Sorosh, Sir Lathan Wynn, and all the researchers, engineers, students, and collaborators involved in these groundbreaking projects. I would also like to thank Alex Sherman, Buckey Rutherford, Koorosh Lorfizadeh, Abdullah Hamid, Robert Beckley from the NHERI shake table team for their support.

The structural system scope of the NHERI TallWood Project was supported by NSF Grants No. 1635227, 1634628, and 1634204. The non-structural component scope was supported by NSF Grant No. CMMI-1635363 and USFS Grant No. 19-DG-11046000-16. Use and operation of the NHERI shake table facility were supported by NSF Grant No. CMMI-2227407. The project also benefited from generous technical, financial, and material support from industry leaders in the U.S. and internationally. A full list of sponsors is available at http://nheriTallWood.mines.edu/collaboration.html. The project team is deeply grateful for this support.

The NHERI Converging Design Project is supported by the National Science Foundation under CMMI award numbers 2120683, 2120684, and 2120692. Additional support from the TallWood Design Institute and the USDA Agricultural Research Service Award 58-0204-9-165 is also gratefully acknowledged. The findings, opinions, recommendations, and conclusions expressed in this thesis are those of the author and do not necessarily reflect the views of the sponsors. A full list of supporting partners is available at https://TallWoodinstitute.org/converging-design-partners.

TABLE OF CONTENTS

LIST OF FIGURES

LIST OF TABLES

Chapter 1 Literature Review and Background

1.1 Background

The use of mass timber products as lateral shear wall elements in buildings is gradually gaining popularity. A new lateral resisting system, known as the mass timber rocking wall system, has been found suitable for timber buildings in high seismic regions and significant research and development efforts have been made to understand this system's behavior and limitations. This section summarizes major research findings on mass timber rocking wall systems and highlights some of the gaps between current research and practical applications.

To understand the mechanical behavior of wood rocking lateral systems, researchers conducted experimental studies, including component-level pushover tests and full-scale shake table tests. New Zealand, situated on the boundary between the Pacific Plate and the Australian Plate, has seen substantial growth in the mass timber market, leading to extensive research on suitable lateral resisting systems for mass timber construction. Palermo et al. (2006a) demonstrated that controlled rocking concepts in bridge systems offer an effective alternative to traditional systems. Subsequent research programs investigated the seismic performance of this innovative rocking concept for multi-story LVL (Laminated Veneer Lumber) buildings. Their research applied innovative jointed ductile connections to LVL beam-column, LVL wall-to-foundation, and column-to-foundation joints.

The new system mainly consists of three components: prefabricated structural elements, unbonded post-tensioning, and innovative jointed ductile connections. The unbonded post-tensioning provides re-centering capabilities, ensuring that inelastic seismic demands are accommodated within the connection itself through the opening and closing of gaps. Comprehensive numerical and experimental investigations revealed that the controlled rocking motion governs the system's behavior, while the flag-shaped hysteresis loop shows

that the system can endure large inelastic displacements, limiting structural damage and ensuring full re-centering after seismic events.

The first phase of that research program involved quasi-static cyclic testing at the University of Canterbury (Palermo et al., 2006). Specifically, beam-column joints, column-to-foundation, and wall-to-foundation specimens were tested under uni- and bi-directional quasi-static lateral loading. Horizontal loads were applied at the top of the specimens, with a constant axial load of 120 kN to simulate gravity loads. The results showed that the beam-column response, in terms of lateral force versus inter-story drift, exhibited a flag-shaped pattern. The column specimen could reach a drift of 2.75%, and the column-to-foundation specimen could reach 4.5% drift without damage or apparent stiffness degradation. Additionally, pseudo-dynamic testing was conducted on cantilever column-to-foundation specimens, investigating various levels of initial post-tensioning and different dissipation capacities. Full re-centering capability was maintained regardless of the earthquake's intensity.

Loo et al. (2014) introduced slip-friction connectors to mass timber shear wall systems. Unlike post-tensioned mass timber rocking walls, this system does not apply post-tension to provide self-centering capacity. Instead, it relies on the self-weight of the wall panel, with forces on the wall capped by the slip-friction connectors to give self-centering ability. A series of quasi-static tests were conducted to evaluate the performance of rigid timber shear walls equipped with this novel connector. A method was proposed to quantify the influence of shear key friction, wall panel, and slip-threshold on the overall moment resistance of the wall. The slip-friction connectors enabled the wall to rock with one end descending and the other uplifting, resulting in excellent self-centering performance under minimal vertical loads.

Following the component-level tests conducted at the University of Canterbury, Iqbal et al. (2015a) extended the research to coupled mass timber walls using U-shaped Flexural Plates (UFPs) as energy dissipation devices. UFPs are commonly used in rocking coupled timber wall systems and were first proposed by Kelly et al. (1972). Baird et al. (2014) performed detailed studies on UFPs to determine their

key characteristics, such as initial and post-yield stiffness, dissipation ratio, and maximum force. Experimental tests of UFPs validated an ABAQUS finite element model that simulated the force-displacement behavior of UFPs, helping to summarize parameters such as yield force and initial stiffness.

In the quasi-static cyclic and pseudo-dynamic tests conducted by Iqbal et al. (2015a), the coupled LVL walls were connected using UFPs. The UFP connectors were first tested separately to better calibrate their cyclic behavior, yielding and ductility. Different UFP sizes and arrangements were investigated. The LVL walls, tested at 2/3 scale, measured 2.46 meters in height, 0.78 meters in width, and 195 mm in thickness, constructed from three layers of 65 mm thick Hyspan LVL. Six coupled LVL wall specimens were tested, both with and without UFPs. The results were used to validate two numerical models: the lumped plasticity model and the multi-spring model. While the lumped plasticity model was simple and effective, it was less effective in accounting for axial deformation of elements.

The multi-spring model requires more experience for developing spring values but has the capacity to predict local behaviors, such as neutral axis position, stresses, strains, and axial deformation effects. Both the numerical and experimental results demonstrated the feasibility of post-tensioned timber walls coupled with UFP dampers for seismic applications. In further research, Iqbal et al. (2015b) conducted additional research on a coupled LVL rocking wall system at the University of Canterbury, New Zealand. In that project, the LVL rocking wall was coupled with plywood sheets. Plywood sheets, used as externally attached dissipaters, offer the advantage of being replaceable after an earthquake and are easily accessible for maintenance during the building's service life. Iqbal et al. tested the coupled LVL rocking walls subjected to both quasi-static cyclic and pseudo-dynamic seismic testing protocols. They also tested different nail arrangements used to connect the plywood coupling panels with the PT (post-tensioned) timber walls to compare their energy dissipation characteristics.

Three different nail arrangements were used during the testing. Specimens HP1 and HP2 had nails spaced at 100 mm and 50 mm center-to-center, respectively, along the outer edge of the plywood sheets. HP3 had

nails spaced at 50 mm center-to-center across the entire area of the plywood sheets. The LVL wall was constructed to a two-thirds scale of the prototype building, with each wall measuring 2.46 m in height, 0.78 m in width, and 195 mm in thickness. PT bars were placed at the centers of the outer ducts. The testing results showed that as nailing spacing was reduced, the system's energy dissipation and strength increased. Using nailed plywood sheets as a hysteretic damper to couple PT rocking LVL walls proved efficient. Although this form of dissipative element does not provide the stable hysteretic behavior achievable with UFPs, the plywood sheet connectors are less expensive to implement and easier to install and replace.

In another study, a different type of damper was investigated. Wrzesniak et al. (2016) used High-Force-to-Volume (HF2V) damping devices in rocking timber structures, applying quasi-static tests to study the energy-dissipating and self-centering capacities. HF2V damping devices dissipate energy through reversible plastic extrusion of lead. The recrystallization temperature of lead is approximately -25°C, allowing the lead material to dynamically recover during the extrusion process. This unique rheological property means the device experiences no change in strength or stiffness under cyclic loading.

For testing, HF2V damping devices were attached at the bottom corners of a GLT (glulam) wall panel. The GLT wall specimen measured 2.95 m in height, 2 m in width, and 160 mm in thickness, made of glulam class GL24 according to Eurocode 5. The loading protocol was conducted in accordance with EN12512 standards for timber structures, ensuring the tests were defendable from a design standpoint. A maximum displacement of 60 mm was applied, with a test speed of 0.4 mm/s. Displacement was applied at the top right corner of the wall by an actuator, while a uniform vertical load of 25 kN/m was applied during one of the tests.

Results showed that the system could sustain up to 1.3% horizontal drift without damage across all connections and maintained good self-centering capabilities. However, for drifts greater than 1.3% without vertical load, the self-centering ability was lost.

In another series of experiments, six specimens with and without UFPs were set up for quasi-static cyclic and pseudo-dynamic tests. Two different post-tensioned initial forces were applied to the specimens. The comparison between the PT rocking wall system with boundary columns and a more traditional single-wall configuration revealed that boundary columns significantly help avoid displacement incompatibility issues, thereby preventing diaphragm damage.

Ganey et al. (2017) conducted quasi-static experimental tests on six self-centering CLT wall specimens to investigate their response to cyclic lateral loading and the effects of various design parameters on global behavior. The specimens used 5-ply CLT wall panels with different PT bar sizes, UFP configurations, and boundary conditions consisting of either steel or CLT foundations. Both single walls and coupled walls were studied. The results showed that self-centering CLT walls exhibited ductile responses, recentering capabilities, and demonstrated strength and energy dissipation. The hysteretic response of the walls became significantly pinched only at large drifts due to CLT damage and PT bar yielding. A desirable hierarchy of limit states was identified: UFP yielding, CLT crushing, PT bar yielding, and CLT splitting.

Hashemi et al. (2017, 2018) proposed a novel type of friction joint, termed the Resilient Slip Friction (RSF) joint, for use in mass timber rocking wall systems. This new joint functions as both an energy dissipation mechanism and a self-centering device. The RSF joint consists of grooved outer cap plates and slotted center plates clamped together by high-strength bolts and Belleville springs. When the applied force on the joint exceeds the frictional resistance between the surfaces, the center slotted plates begin to slip, dissipating energy through friction. The grooves' shape, combined with the Belleville springs, facilitates self-centering. The reversing force due to the spring's compression is higher than the friction force between the sliding surfaces, causing the center plates to return to their original positions. This provides the RSF joint with the characteristic flag-shaped hysteresis behavior.

The RSF joints were attached to the bottom corners of CLT rocking wall panels, and quasi-static tests were conducted on the system. The CLT walls used in the tests were 5-layer panels, each measuring 6 meters

high, 2025 mm wide, and 200 mm thick. Analytical predictions for the lateral strength of the rocking CLT wall with RSF joints were compared with the load-deformation behavior observed during the seven tests. The results showed that the walls exhibited flag-shaped hysteretic behavior, confirming their fully self-centering capabilities. The proposed system offers a robust solution for seismic resilience, with no additional vertical load needed to achieve full self-centering behavior.

A similar concept to the Resilient Slip Friction (RSF) joint was investigated by Fitzgerald et al. (2020), who tested a novel Slip-Friction Connection (SFC) for CLT rocking walls. The SFC employed Belleville springs and brass shims to provide stable slip forces, yielding equivalent viscous damping ratios between 0.28 and 0.63. In half of the tests, a short post-tensioned restoring rod with Belleville washers was added for additional restoring forces. The SFCs were connected to the CLT walls using inclined self-tapping screws (STS), designed to dissipate energy effectively while protecting the rocking walls from damage. This configuration showed promise for enhancing the seismic resilience of mass timber structures.

In parallel, significant efforts have been made by research organizations to push the boundaries of mass timber high-rise buildings. A key initiative is the NHERI TallWood project. In 2017, as part of that project, a full-scale two-story CLT building with post-tensioned coupled rocking walls was tested at the UCSD outdoor shake table facility (Pei et al. 2019), essentially as a proof of concept. This two-story building was designed to inform future analysis and testing of taller structures, including a ten-story mass timber building highlighted in this thesis. For the lateral force-resisting system, the two-story building utilized CLT coupled rocking walls connected with U-shaped Flexural Plates (UFPs). An innovative diaphragm-to-wall connection was developed and tested to ensure effective shear force transfer between diaphragms and rocking walls, while allowing vertical movement and providing out-of-plane bracing.

The two-story building was subjected to 14 earthquake excitations scaled to various hazard levels for a San Francisco site. The findings from these tests provided valuable insights into the behavior of the lateral

system and highlighted potential improvements for future designs of taller structures, including the planned ten-story building.

Following the tests on the two-story structure, the researchers reconfigured the CLT rocking wall system for the next phase of testing. In the new configuration, a center anchor was introduced as a hold-down mechanism for the walls, and inter-panel connectors were used as energy dissipation devices, with replaceable crushing blocks added at the toe of the wall panels. This updated design was subjected to 13 earthquake motions ranging from Service-Level Earthquakes (SLE) to Maximum Considered Earthquake Risk Targeted (MCER+) intensities as defined by ASCE 7 (ASCE 2017), based on seismic hazard values near Seattle, Washington. These hazard levels were informed by the probabilistic seismic hazard analysis and site-specific spectra described in Blomgren et al. (2022), which guided the selection and scaling of the input motions to match performance-based seismic design objectives.

The test results demonstrated that the rocking shear wall system was able to remain damage-free during service-level earthquakes, with repairable damage confined to the sacrificial components—namely the crushing blocks and inter-panel connectors that can be easily replaced after a significant seismic event. This approach to design and testing provides a clear pathway toward creating seismically resilient mass timber buildings capable of withstanding significant earthquake forces while remaining both repairable and functional after major events.

At Oregon State University, researchers explored the use of different energy dissipation devices in Mass Plywood Panel (MPP) rocking walls, conducting both cyclic testing and numerical modeling. This research focused on using buckling-restrained braces (BRBs) as energy-dissipating hold-downs in MPP walls. A BRB-MPP spline assembly was developed as the lateral load-resisting system of a 3-story mass timber building segment, which was tested under cyclic quasi-static loading (Araújo et al. 2025). The study provided insights into the design of the BRB and the associated numerical model used to predict the system's behavior.

As experimental studies on mass timber rocking wall systems in New Zealand and North America have successfully demonstrated performance under lateral loads, the feasibility of adopting these systems in North American construction is being explored. A study conducted by Ahmed and Arocho (2021) assessed the practicality of mass timber as a construction material in the U.S. midstream market. Due to the sustainability advantages, speed of construction, and excellent dynamic behavior of mass timber, practical projects using mass timber lateral-resisting systems have been proposed.

One significant project in North America was the Framework building (Zimmerman and McDonnell 2017), a 12-story mixed use building proposed in Portland, Oregon. Although the project ultimately was not constructed due to financing issues, it remains significant as the first mass timber high-rise in the U.S. to receive full construction approval. The proposed design utilized mass timber for both its gravity and lateral systems. The lateral force-resisting system consists of CLT post-tensioned rocking walls with glulam columns at each wall end. The CLT walls are post-tensioned externally with threaded rods at the center of the wall and are connected to the bounding columns with U-shaped Flexural Plates (UFPs). The UFPs serve as the primary energy dissipation devices, while the post-tensioned (PT) rods provide re-centering capacity.

For the gravity system, glulam columns and beams, along with CLT floors, handle gravity loads. The beams and floors deliver gravity forces directly to the columns, allowing the CLT walls to move vertically without uplifting or damaging the floors. In other words, the CLT rocking wall system only transfers lateral loads to the foundation. Since the CLT rocking wall system is not included in the prescriptive design approach, performance-based design methodology was used for the building. A nonlinear response analysis using PERFORM 3D was conducted to evaluate the performance of the building under Maximum Considered Earthquake (MCE) hazard levels. The design also considered several serviceability limit states, such as drift and vibration under service-level wind events, as well as repairability following seismic events.

Another notable mass timber project was the Catalyst building (Zimmerman et al. 2020), a 5-story mixed-use educational and office building completed in 2020 in Spokane, WA. The building incorporated mass

timber shear walls equipped with buckling-restrained braces (BRBs) acting as energy-dissipating hold-downs at the toes of the wall panels, providing both self-centering and energy dissipation capabilities. Because the BRB-mass timber system is not included in the prescriptive provisions of the International Building Code (IBC), performance-based design (PBD) including nonlinear time history analysis were required to demonstrate code compliance. The successful implementation of this innovative lateral system further validates the feasibility of mass timber construction in high seismic regions and illustrates the expanding role of advanced analysis in enabling code approval for novel timber structural systems.

Chapter 2 Introduction

2.1 Motivation and Background

In the past decade, mass timber construction has emerged as a viable solution for sustainable, high-performance buildings. Recent changes to the International Building Code now allow mass timber buildings up to 18 stories in the U.S., increasing interest in using this renewable material, especially in seismic-prone regions like the Pacific Northwest (ICC 2021). While the use of exposed wood aesthetics and rapid construction techniques adds to its appeal, the primary challenge lies in developing effective lateral force-resisting systems (LFRS) that are compatible with tall mass timber structures.

Most existing tall timber buildings rely on conventional systems concrete cores or steel braced frames for lateral resistance. This trend stems from two key limitations: the familiarity of the construction industry with steel and concrete systems, and restrictive building code provisions. Specifically, ASCE 7-22 limits panelized mass timber shear wall systems to a building height of 65 feet, restricting their broader application (ASCE 7-22, 2022). Despite these limitations, the potential advantages of integrated mass timber lateral systems faster construction, lower embodied carbon, and enhanced seismic performance continue to drive innovation (van de Lindt et al., 2021).

Among various alternatives, post-tensioned mass timber rocking walls have shown significant promise as a low-damage lateral system. This system was initially explored in New Zealand and later studied extensively in the U.S. and Japan (Palermo et al., 2005; Iqbal et al., 2015). Research has shown its ability to provide full re-centering capacity and sustain seismic events with minimal structural damage, even under Maximum Considered Earthquake (MCE) demands. However, until recently, no tall building had been tested with this system at full scale.

This research builds upon earlier component-level and subassembly testing, advancing to the system-level evaluation of full-scale mass timber structures. A key area of interest has been the development of

reconfigurable, open-floor-plan mass timber buildings suited for the office and mixed-use markets. Large-scale testing programs including reverse cyclic tests, biaxial subassembly tests, and two-story shake table experiments have laid the groundwork for validating the performance of post-tensioned CLT rocking wall systems under seismic loading (Pei et al., 2019). These studies established deformation thresholds, damage state fragilities, and performance-based design methodologies.

The conceptual evolution and motivation behind this progression from early subassembly testing to full-scale system-level validation in the NHERI TallWood and Converging Design Projects are illustrated in Figure 1. This diagram summarizes the key phases of research and their influence on the development of resilient mass timber lateral systems.

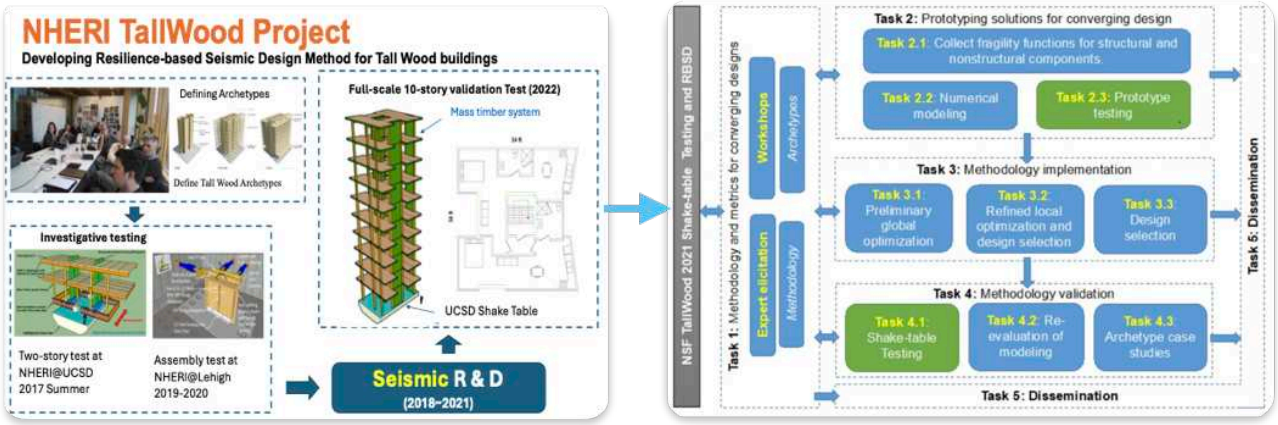

Figure 1: Motivation of NHERI TallWood Project and NHERI Converging design Project. (picture credit: Pei et al and Barbosa et al)

Building on this foundation, the current research forms part of an NSF-funded initiative under the NHERI program, focused on developing and validating a resilience-based seismic design methodology for tall wood buildings. The NHERI TallWood and NHERI Converging Design Projects include the design, construction, and full-scale shake table testing of 10-story and 6-story post-tensioned mass timber buildings, respectively. These tests assess structural resilience, lateral system behavior, and non-structural component performance under realistic seismic demands.

Both test specimens included gravity systems with low-damage detailing, drift-compatible non-structural elements, and prefabricated stair systems. The shake table tests, conducted at NHERI@UC San Diego—the only facility globally capable of testing buildings of this height represent the most extensive system-level seismic validation of mass timber structures to date.

This thesis presents the design process, construction, instrumentation, test setup, and results from both the NHERI TallWood and NHERI Converging Design Projects. Particular focus is placed on Phase 1 of the NHERI Converging Design and its comparison to the NHERI TallWood structure under similar ground motions. The comparative analysis aims to evaluate differences in seismic response due to structural configuration, lateral system detailing, and design philosophy, ultimately contributing to the advancement of resilient, sustainable, and code-compliant tall timber construction.

2.2 Introduction and Project Overview

The Natural Hazards Engineering Research Infrastructure (NHERI) TallWood and NHERI Converging Design projects are landmark research initiatives aimed at enhancing the seismic resilience and sustainability of mass timber structures. These projects, funded by the National Science Foundation (NSF), focus on the development and testing of advanced design paradigms for tall mass timber buildings in

earthquake-prone regions. They represent a significant step toward creating more resilient, sustainable, and cost-effective solutions for building in high seismicity areas Mishra et al (2025).

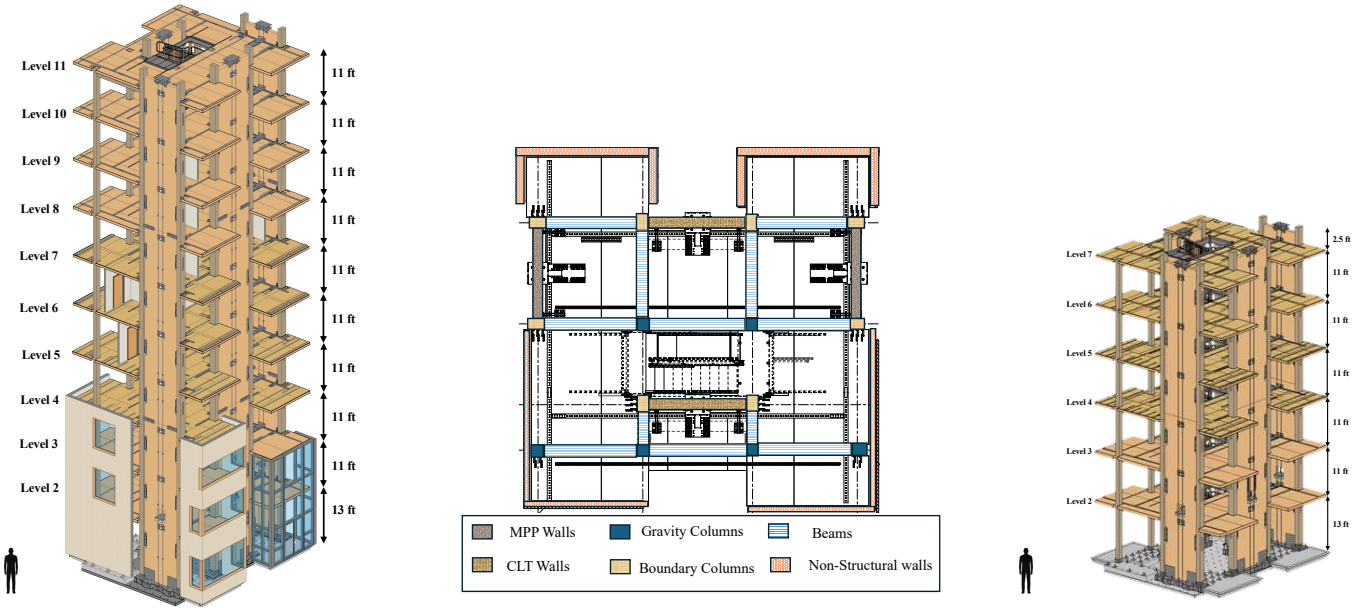

Figure 2: Project Overview

NHERI TallWood Project

The NHERI TallWood Project was a collaborative research effort led by Colorado School of Mines, Colorado State University, the University of Washington, and the University of Nevada, Reno, with support from various industry partners. The project aimed to develop and validate a resilience-based seismic design methodology for tall wood buildings through full-scale shake table testing of a 10-story mass timber structure. The building incorporated innovative systems, including post-tensioned mass timber rocking walls, and was designed to withstand a range of seismic intensities—from design-level events to the Maximum Considered Earthquake (MCER) while maintaining minimal damage. Testing was conducted at the NHERI@UCSD shake table facility, confirming that mass timber buildings can achieve high performance with minimal structural damage and repairable nonstructural damage. Figure 3 illustrates the

NHERI TallWood test structure during experimental setup at the shake table. A detailed review of this project is provided by Pei et al. (2024).

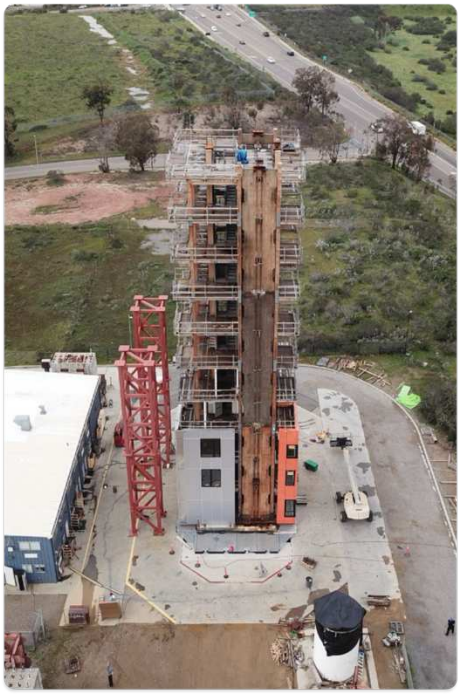

Figure 3: NHERI TallWood Specimen

NHERI Converging Design Project

Building on the foundation of the NHERI TallWood Project, the NHERI Converging Design Project sought to advance the understanding and design of mass timber structures further. The project focused on optimizing these structures to maximize functional recovery while incorporating sustainable building principles. A central innovation was the adoption of multi-objective optimization, a methodology that integrates various factors such as structural resilience, sustainability, cost-effectiveness, and constructability into the design process.

This collaborative effort brought together researchers and industry professionals from institutions such as Colorado State University, Oregon State University, Stanford University, and Penn State University. Through these collaborations, the project developed a novel design paradigm that leveraged advanced computational tools to enhance structural performance while prioritizing sustainable design elements. To

validate the proposed methodologies, full-scale shake-table testing was conducted, emphasizing the seismic resilience of mass timber structures, environmental sustainability, and construction cost efficiency. The NHERI Converging Design Project was implemented in three phases, each investigating distinct lateral force-resisting systems and energy dissipation mechanisms as illustrated in Figure 4.

Figure 4: NHERI Converging Design Test Specimen with Different Phases

Phase 1 focused on the application of U-shaped flexural plates (UFPs) as energy dissipators integrated with post-tensioned mass timber rocking walls. The inherited shear wall panels from the NHERI TallWood Project were repurposed, reduced from ten to six stories, and reconfigured into a new UFP-wall setup. Additionally, a novel post-tensioned (PT) rod arrangement was introduced, guided by the Direct Displacement-Based Design (DDBD) method. This innovative approach enabled the design to meet strain-limit- and drift-limit-based performance objectives. The UFPs were central to this phase, designed to operate in the inelastic range, ensuring energy dissipation while adhering to predefined performance criteria. The detailed review of this phase can be found in Uarac et al. (2025)

Phase 2 marked a significant shift by incorporating buckling-restrained braces (BRBs) into the lateral force-resisting system. These braces replaced the mass plywood panel (MPP) walls at the first story only in the N-S direction, which had previously served as the primary lateral system. The BRBs, designed based on prototype testing at Oregon State University, were strategically placed at the first-story wall boundaries as high-ductility hold-downs. The MPP walls above the base remained essentially elastic, with the BRBs anchoring compressive and tensile forces through gusset plates, steel side plates, and inclined, fully threaded screws. This system drew inspiration from prior research on steel frames and mass timber walls with buckling-restrained columns, blending innovative design with practical energy dissipation mechanisms. The detailed review of this phase can be found in McBain et al (2025).

Phase 3 explored hybrid steel–mass timber structural systems using Yield-Link® brace and moment connections developed by Simpson Strong-Tie. This phase replaced the N–S post-tensioned timber walls with a six-story resilient steel moment and braced frame system that utilized Simpson's replaceable fuse technology to absorb inelastic seismic demands while keeping the primary structural members elastic. Although early in the design process there were concerns that residual drifts might increase due to the steel frame configuration, the final system achieved a residual roof drift of less than 1.6 mm (1/16 inch) even under MCER-level shaking. This performance was achieved through enhanced design procedures that explicitly addressed higher mode effects and concentrated inelasticity in sacrificial yield links, resulting in a uniform drift profile and minimal permanent deformation. This phase served as an alternative to post-tensioned rocking wall systems, demonstrating the potential of hybrid steel–timber solutions in achieving both structural resilience and reparability. The detailed review of this phase can be found in Field et al. (2025).

The author played an integral graduate student role in both the NHERI TallWood and NHERI Converging Design research programs, providing a continuity of involvement across the two landmark full-scale seismic testing campaigns. Key responsibilities encompassed assisting with the planning and execution of

sensor layouts, coordination of instrumentation setup, and development of the camera instrumentation plan to capture detailed structural responses.

In the NHERI TallWood project, the author was involved in the installation and inspection of over 100 sensors during the 10-story shake table testing phase, managed data curation from accelerometers and cameras, and contributed to specialized tests such as the MTU Damper Payload phase (not part of this thesis). Following completion of the TallWood testing, the author directly participated in the deconstruction process, ensuring safe removal of instrumentation and structural components while documenting the transition to the next testing phase.

This experience extended into the NHERI Converging Design project, where the author again worked with the team on instrumentation planning, coordinated sensor installations with UC San Diego staff, and led the camera instrumentation setup. The author was actively engaged in the construction of the 6-story structure, its testing operations, and subsequent full deconstruction.

This continuous and hands-on involvement from the construction of the 10-story TallWood building, through its deconstruction and adaptation into the 6-story NHERI Converging Design test, and finally through the Converging Design testing and dismantling, provided the author with a unique longitudinal perspective. Such involvement enabled a comparative assessment of the seismic performance of tall and mid-rise mass timber buildings, which forms the core focus of this thesis.

Chapter 3 Design Overview for the Test Buildings

3.1 Overview

This chapter outlines the key design considerations involved in the development of both the NHERI TallWood Project and the NHERI Converging Design Project by the project teams. It describes the various components and systems that were incorporated into the structure, with a particular focus on gravity systems, lateral force-resisting systems, diaphragms, and their integration into the overall design.

3.2 Gravity System

The gravity system for the NHERI TallWood Project had main elements consisting of bounding columns, which are adjacent to the rocking wall, and gravity columns, which make up the remaining columns in the structure. All the beams and columns were designed assuming a live load of 65 psf, which is typical for an office building, including partition walls.

The design and drafting of the gravity system were carried out by the Colorado School of Mines team, in collaboration with industry partners KPFF, Holmes Structures, and Lever Architecture. The dead load was assumed to be 64.4 psf, based on the self-weight of the structural system. The mechanical properties used in the gravity design are summarized in Table 1. These design assumptions were made per floor, while the live load was used only for the design process and was not present during the testing phase. Detailed design calculations are available in Bush (2023).

Table 1: Design Parameters for Gravity System

Design Parameters	
Flexural Stress (F_b)	2650 psi
Compressive Stress (F_c)	3000 psi
True MOE (E)	1800000 psi
Apparent MOE ($E_{apparent}$)	1700000 psi

All columns and beams used in the building were designed to have a two-hour fire rating and were constructed in accordance with AWC (2018) standards. These elements were donated by Boise Cascade and are of grade 1.8E 2650 LVL. The final sizes of structural members were selected to satisfy both strength and fire design criteria. The key gravity member dimensions and their demand-to-capacity(D/C) ratios, both before and after fire reductions, are shown in Table 2.

Table 2: Detail Member sizes of Gravity System

Member Sizes				
Members	Thickness (in)	Length (ft)	D/C ratio before fire	D/C ratio after fire
Columns (Floor 1-2)	12.25 x 15	144 ft	0.576	1.041
Columns (Floor 3-6)	12.25 x 13.5	264 ft	0.512	1.031
Columns (Floor 7-10)	12.25 x 12	264 ft	0.288	0.677
Bounding Columns	12.25 x 18	896 ft	0.480	0.752
Beams	12.25 x 13.5	966 ft	0.459	0.732

The base connections for both the bounding columns and gravity columns were designed by Simpson Strong-Tie to provide a true pin connection, allowing movement in the X and Y directions. The bounding columns were bolted to the foundation beam, while the gravity columns were welded into the foundation.

The gravity frames and beam connections were customized with dowel connections, designed to minimize damage under lateral deformation as shown in the Figure 5.

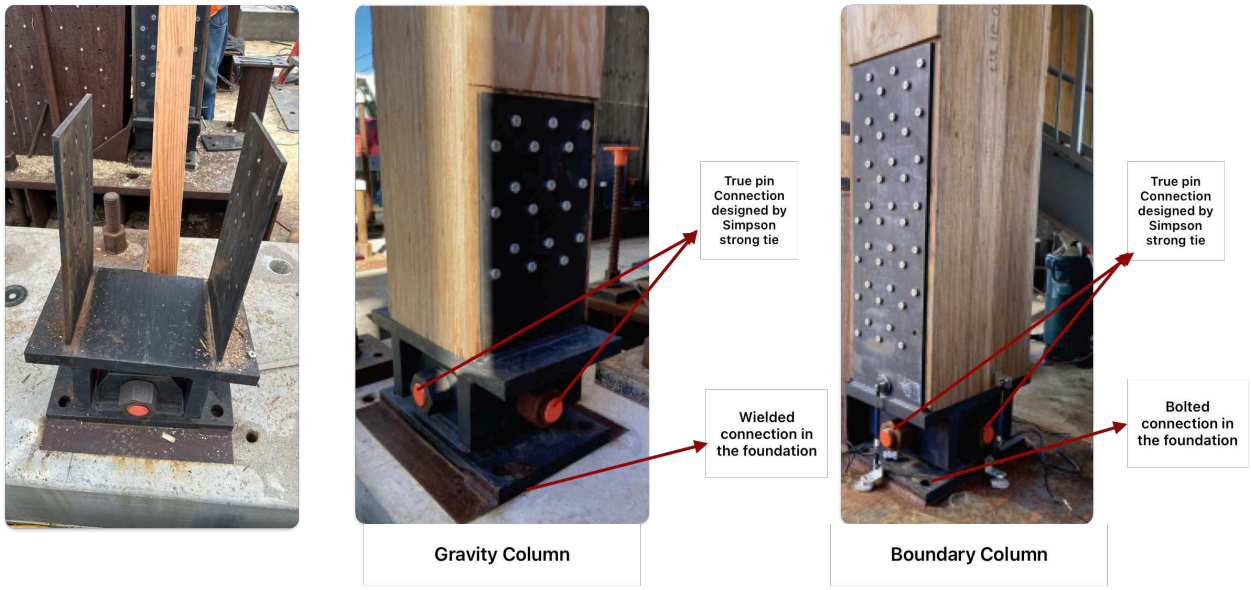

Figure 5: Columns and Its True Pin Connection

The designed axial tension capacity for these connections is 133 kN (30 kips) using LRFD, allowing for a 0.06 rad rotation about the primary axis without moment transfer while maintaining positive axial force. The detailed design performance of these connections is thoroughly documented in Pryor et al. (2024), Bush (2023), and Da Huang (2023). The gravity columns were strategically oriented for strong-axis bending in the east-west direction, while the bounding columns were oriented perpendicular to the corresponding wall's strong axis of bending to optimize structural performance.

For the beam-to-column connections, a beam hanger with slotted holes was employed. This design facilitated shear transfer while permitting rotation about a top bolt, effectively minimizing moment transfer. The beam hanger was embedded within the wood to provide fire protection for the steel components, ensuring durability and safety under fire exposure.

Figure 6 illustrates the beam-column connection detail, showcasing the design of the slotted holes on the connection plate. These slots were engineered and fabricated by Simpson Strong-Tie to allow rotation along

the major axis, and the bolts were strategically passed through the columns to achieve the final connection configuration. This innovative approach ensured the connection's ability to accommodate the desired rotation about the top bolt, effectively reducing moment transfer while maintaining structural integrity.

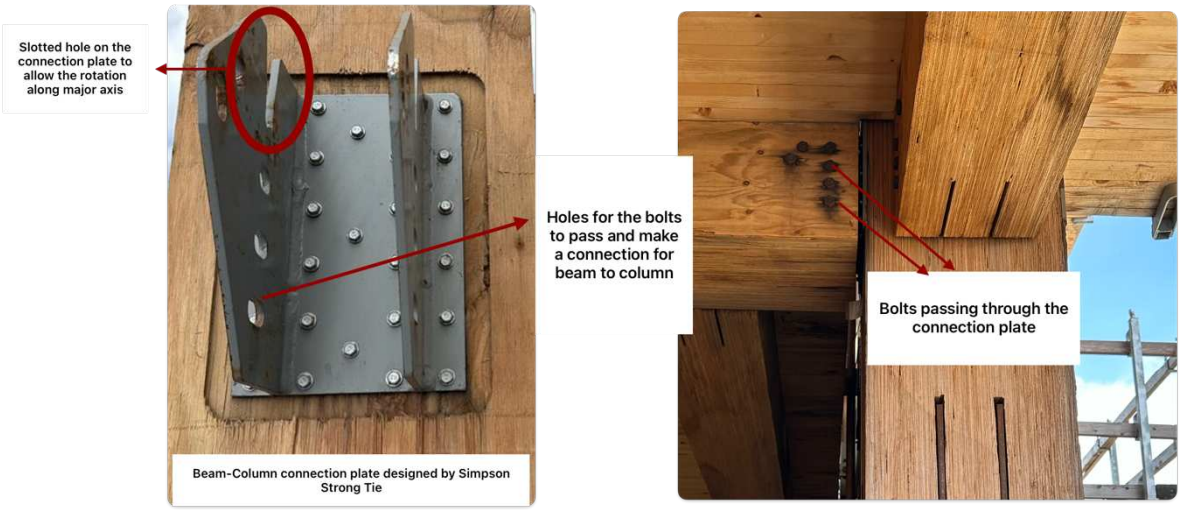

Figure 6: Beam-Column Connection Detail

3.3 Lateral System

The lateral force-resisting system (LFRS) for the NHERI TallWood Project was specifically designed to control drift and minimize damage to both structural and non-structural components. A comprehensive description of the lateral system design, including preliminary design, performance verification using nonlinear response history analysis, and the calculation of demand-to-capacity ratios for all limit states, can be found in Wichman (2023). A brief overview is provided here.

The building was designed for a site in Seattle, Washington, classified as Site Class C soil. Using the ATC Hazards by Location Tool (ATC, 2016), short-period (SMS) and one-second (SM1) risk-adjusted Maximum Considered Earthquake (MCER) spectral acceleration values were determined to be 1.65g and 0.72g, respectively. Additionally, Uniform Hazard Spectra (UHS) were generated for various hazard levels (return periods, RP), as shown in Figure 7. Seattle's seismic hazard is distinct due to contributions from both crustal faults and the Cascadia Subduction Zone, resulting in interplate and intraplate earthquakes.

The UHS were developed using the USGS 2014 US earthquake source model (USGS, 2017a) and were generated for a site with a time-averaged shear-wave velocity of 500 m/s to a depth of 30 meters (USGS, 2017b). A site-specific MCER spectrum was also developed in accordance with ASCE/SEI 7-16 Section 21.2.1.1

Figure 8 presents the elastic acceleration response spectra for the suite of ground motions used in the NHERI Converging Design shake table testing program, scaled to match target spectra for five hazard levels: 43-year (SLE), 225-year, 475-year, 975-year, and the risk-targeted Maximum Considered Earthquake (MCE_R). For each hazard level, the solid line represents the mean spectrum of the selected records, and the dashed line shows the corresponding target spectrum. Individual motions are plotted in light colors to illustrate the record-to-record variability.

The spectra extend up to 3 seconds to cover the building's fundamental as well as higher mode effects. Close alignment between the mean and target spectra across the period range of interest confirms that the ground motion suites are representative of the intended seismic hazard levels. The scaling process for the Converging Design project followed the same methodology applied in the NHERI TallWood program, enabling direct comparison of the structural performance between the two buildings under hazard-consistent seismic input.

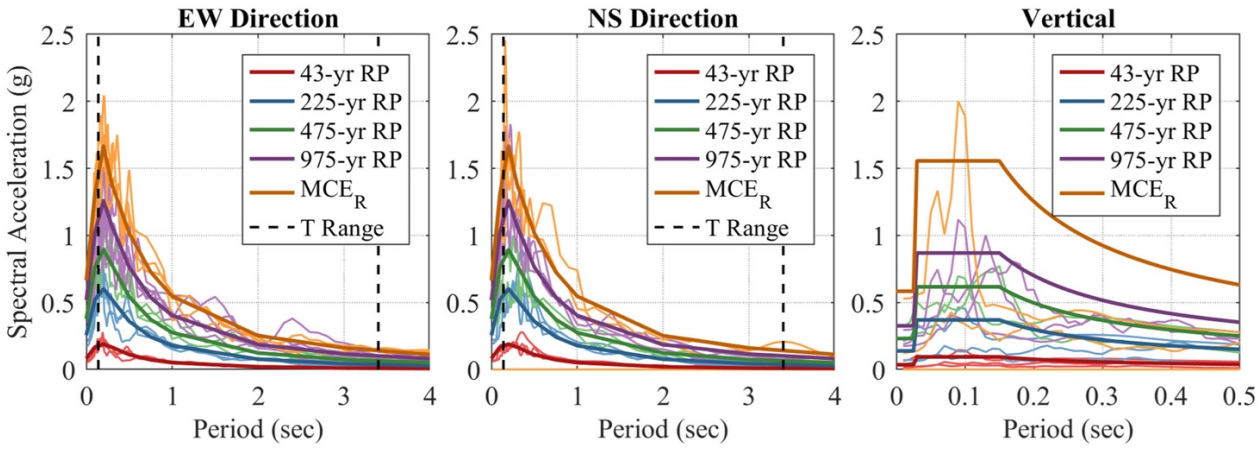

Figure 7:Response Spectrum at the Different Hazard Levels Considered for design and Implemented in Testing. (Data from Wichman 2023.)

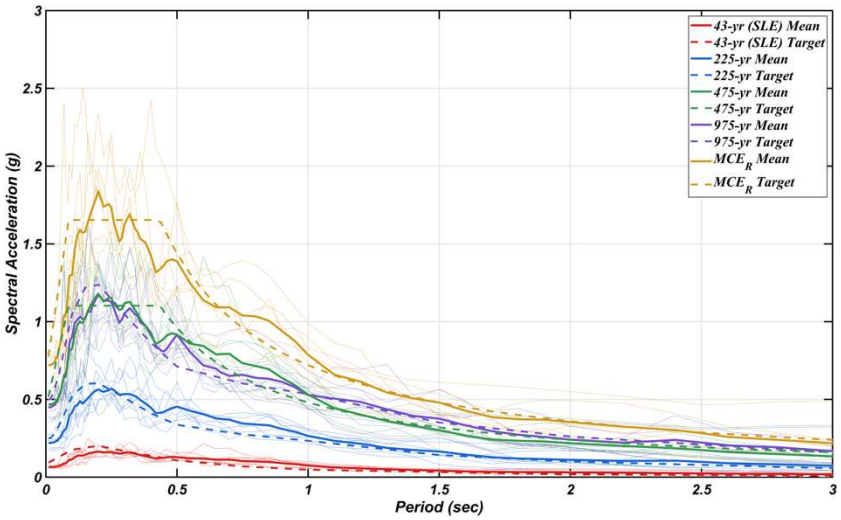

Figure 8: Response Spectrum of NHERI Converging Design Project

After defining the hazard levels, maximum damage states for the structural systems and connections were identified for each hazard level, and corresponding maximum drift limits were set. These drift targets also served as design constraints for non-structural systems, including facades, interior walls, and stairs. These systems were tested under 3D motions in a full-scale setting for the first time. Collaboration with experienced industry partners ensured that these target damage states were met and later validated (see Wichman et al., 2022, Uarac et al., 2024).

3.3.1 Post-Tensioned Rocking wall

The main lateral force-resisting system (LRFD) for both the 10-story and 6-story projects consists of four post-tensioned rocking walls, which provide lateral support to the floors. These floors measure approximately 35 ft by 35 ft. The post-tensioned rocking walls were positioned between two bounding columns and connected to each other using U-shaped Flexural Plates (UFPs), which served as energy dissipation devices. The walls were attached to the diaphragm through slotted shear key connections, allowing rotational and vertical movement. This design effectively decouples the diaphragm from the rocking walls, enabling controlled rocking behavior during seismic events.

The walls are balloon-framed and extend 2.5 ft above the roof level to accommodate the post-tensioning system. As illustrated in Figure 9, the bottom section of the rocking wall includes several key features. The wall is post-tensioned onto a steel foundation beam, which is, in turn, post-tensioned to the shake table platen. To prevent crushing, the wall edges are reinforced with steel armor, while wall shoes at the base restrict movement and ensure controlled rocking at the desired location.

The rocking walls are flanked by two bounding columns, one on each side, bolted to the same steel foundation beam using a true pin connection engineered by Simpson Strong-Tie. These bounding columns are connected to the rocking walls via UFPs, which dissipate energy during seismic events while maintaining the structural integrity of the system.

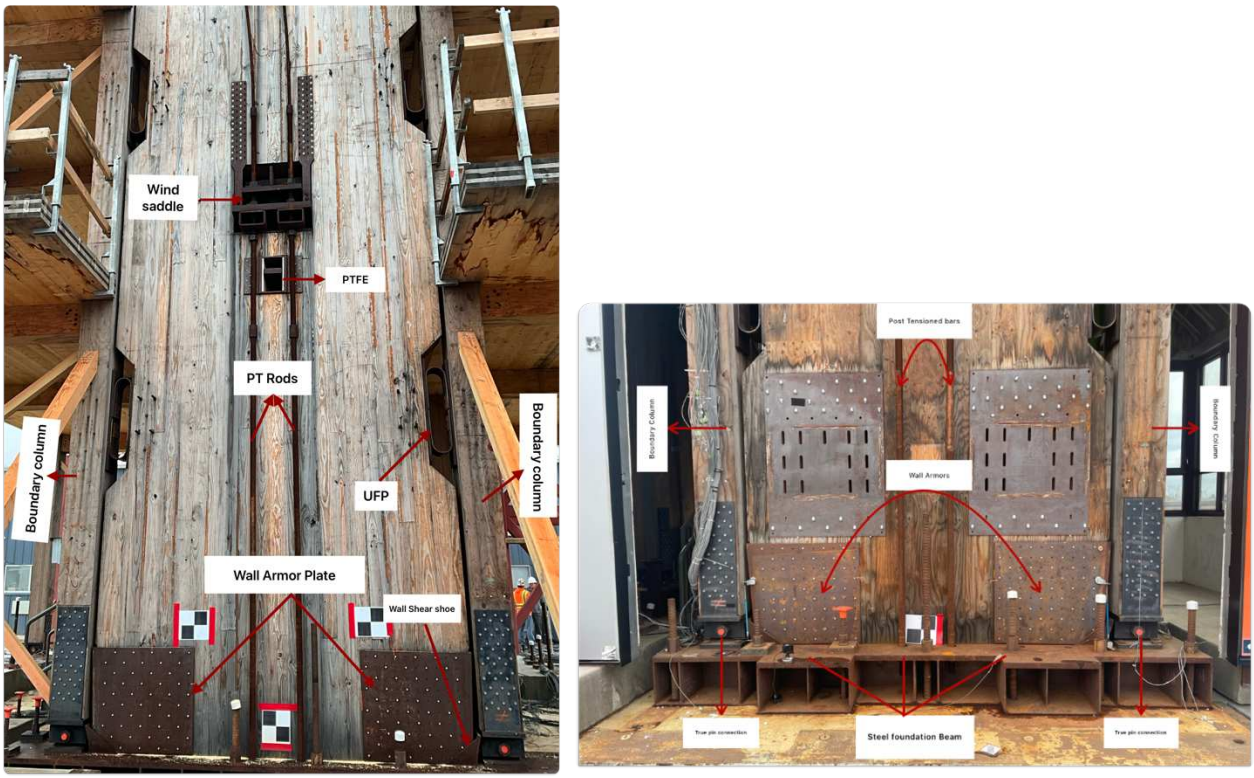

Figure 9: Rocking Wall Detail

To ensure stability during construction, the lower three stories of the building were specifically designed to handle the moment capacity due to wind loading from the upper floors. In this design, special considerations were made for the lower floors, particularly in the use of post-tensioned rods and energy dissipation devices, which were incorporated to enhance the wall's performance. During the construction phase, a wind saddle connection was introduced as a temporary anchorage point for the post-tensioned rods. This wind saddle connection as shown in Figure 10 was customized for different wall materials, considering the varying bearing strengths of each wood type. For the CLT wall, the wind saddle featured both a bearing connection and additional drag straps, which were bolted to the connection and screwed into the wall panels at a 45-degree angle. These straps helped distribute the post-tensioned load across the wall. The MPP wall, on the

other hand, utilized a simpler design with just the bearing connection, as the MPP wall provided a stronger bearing capacity compared to the CLT wall.

Each of the four rocking walls featured wind saddles, with a jacking saddle positioned at the top to facilitate the post-tensioning of rods after the initial wall panels were installed. These wind saddles were designed to endure wind forces of up to 50 mph, ensuring the stability of the building during construction. Each wall was equipped with four post-tensioned rods supplied by Simpson Strong-Tie Strong-Rod® ATS-HSR. The rods had a diameter of 2 inches for the first two floors and 1-1/4 inches for the subsequent floors.

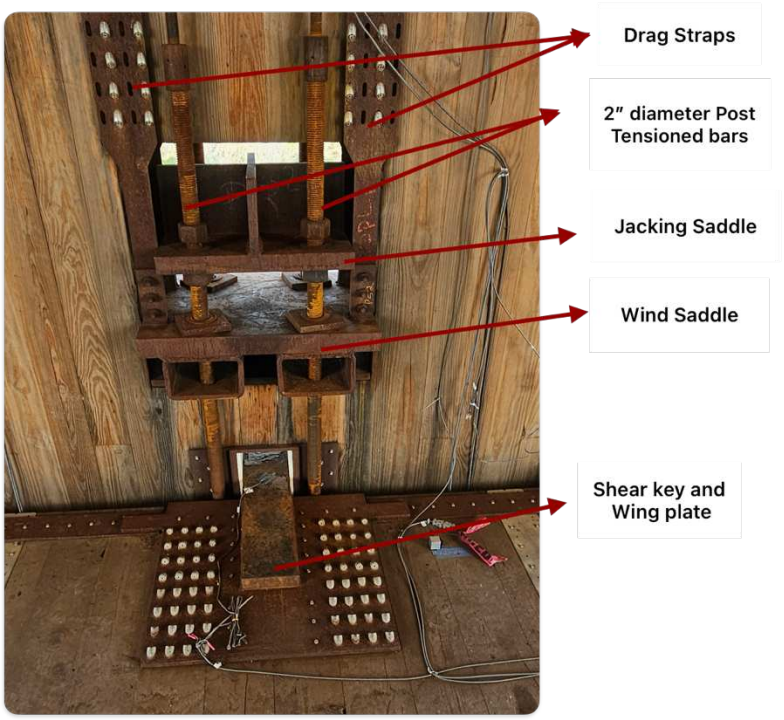

Figure 10: Wind Saddle Detail

The rods, segmented into 12-foot sections, were connected using Simpson Strong-Tie Strong-Rod® coupler nuts, as illustrated in Figure 11. Each rod was post-tensioned to a force of 50 kips, achieving a total post-

tensioning force of 200 kips per wall. This configuration provided the necessary tensioning capacity to ensure structural integrity under seismic loading conditions.

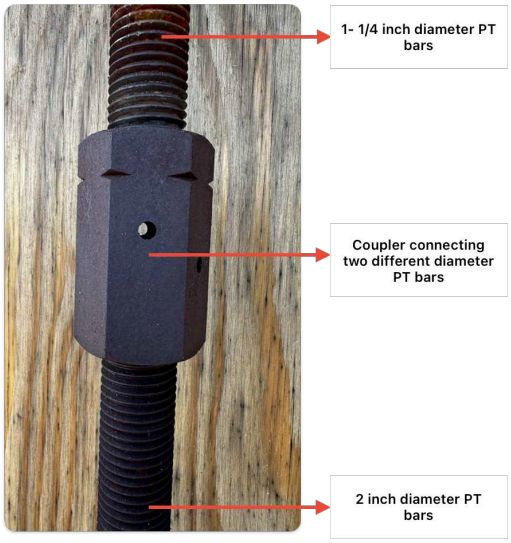

Figure 11: Post Tension Bar Connection Detail

To connect the rocking walls to the adjacent bounding columns, U-shaped Flexural Plates (UFPs) were used. These UFPs were attached to knife plates using bolts, and the knife plates were connected to the wood members via dowel connections. Additionally, each wall was supported by an out-of-plane brace connection, which helped the wall stay in plane during lateral movement. These braces, designed and manufactured by Simpson Strong-Tie, were installed on both sides of the wall at each floor. The brace system featured a built-up steel connection that screwed into the walls and included slotted holes to allow for the rocking motion of the walls without obstruction. On the diaphragm, a plate was fastened with 45-degree screws, and the plate was welded to two perpendicular legs, which were then attached to the wall

connection using bolts that passed through the slotted holes. The detailed design and layout of this connection are illustrated in Figure 12.

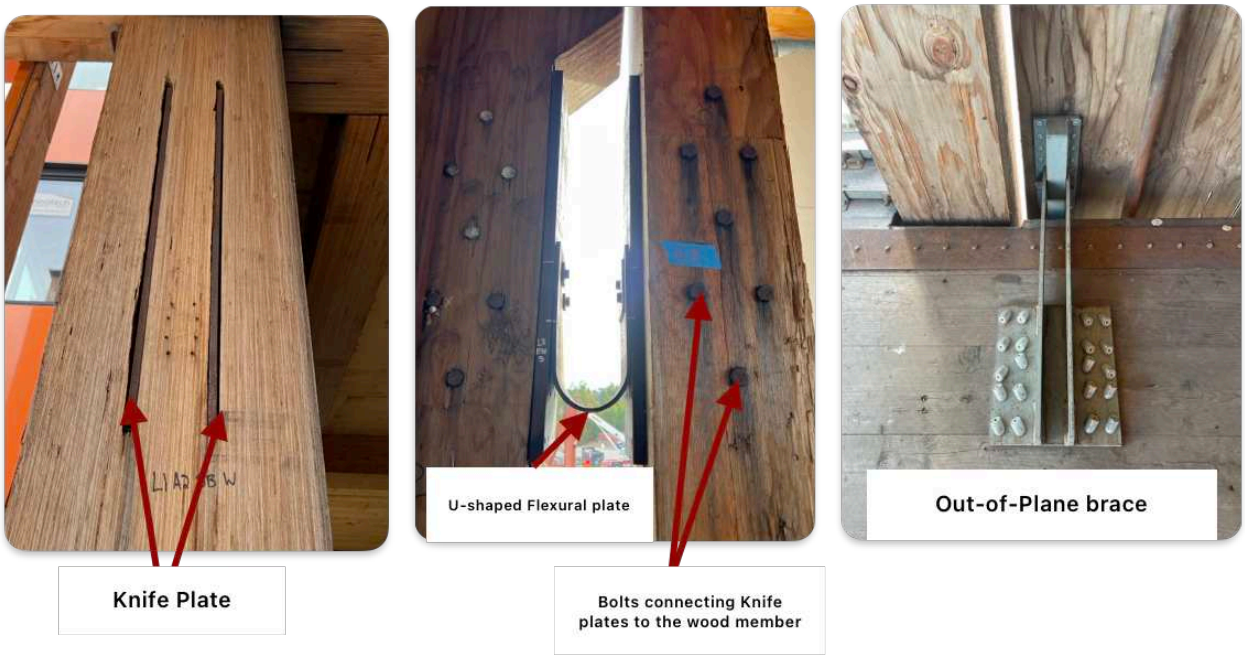

Figure 12: UFP's and Out of Plane Wall Connection Detail

The splice connections for the rocking walls were designed to accommodate both tension (uplift) and shear forces, ensuring structural continuity across stacked wall segments. While the steel splice system had the capacity to resist both types of demands, its primary role varied by location on the wall with tension (uplift) resistance more critical near the base and shear transfer more dominant at intermediate levels (details are available in Kontra et al 2025; and Field et al 2025). Due to deviations observed in the as-built conditions compared to the original design, modifications were made to these connections to maintain performance integrity. The final configuration utilized epoxy-dowel systems in conjunction with bolted steel splice plates. Epoxy rods extended into the adjoining panels to resist tension, while staggered reinforcing screws enhanced shear capacity and durability. These adjustments ensured the splice assemblies fulfilled structural performance objectives while accommodating field deviations. The finalized details and layout of these connections are illustrated in Figure 13.

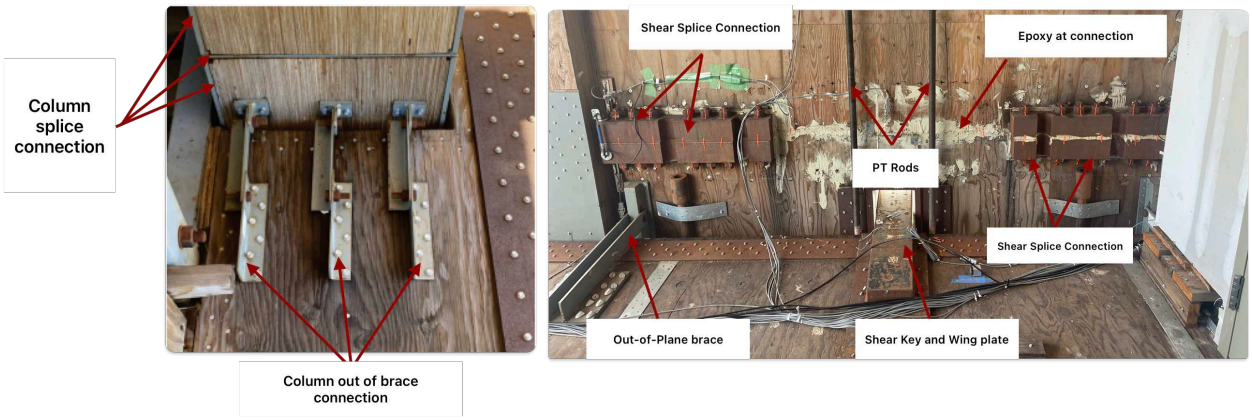

Figure 13: Column Out of Brace Connection and Wall Splice Connection Detail

Two distinct types of rocking walls were incorporated into the project, differentiated by their material composition and dimensions. The north and south elevations utilized 9-ply Cross-Laminated Timber (CLT) walls with a thickness of 12 3/8 inches, while the east and west elevations employed Mass Ply Panels (MPP) with a thickness of 9 3/16 inches. Detailed technical specifications and design considerations for both wall types are elaborated upon in the subsequent sections

3.3.1.1 Cross Laminated Timber (CLT)

Cross-Laminated Timber (CLT) is a large-scale, prefabricated, engineered wood panel made from solid-sawn lumber. CLT panels vary in type based on the number of layers of kiln-dried lumber boards that are stacked on top of each other. These layers are arranged at 90-degree angles to one another, meaning they alternate directions and are bonded together with structural adhesives as illustrated in Figure 14. The panels are then pressed to form solid, straight, rectangular shapes. CLT panels offer several advantages, such as low carbon emissions, high fire resistance, seismic durability, and faster installation, making them widely used for structural panels, floors, and roofs.

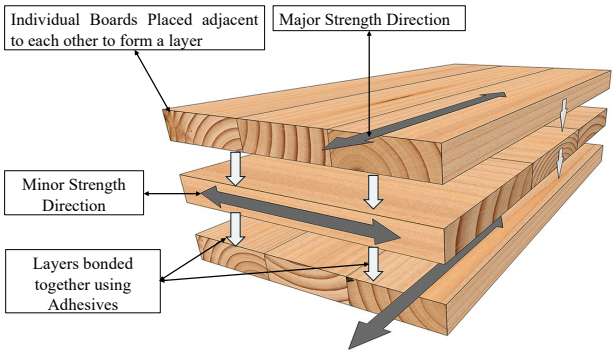

Figure 14: CLT Panel Manufacturing Detail

The CLT panels used for both projects are custom-made 9-ply panels, designed to meet specific requirements for resisting demand forces.

The wood panels consist of MSR-rated lumber with a grade of 2400f-2.0E in the major direction of the CLT. In the minor direction, the wood used is Southern Pine, No. 1 visual grade lumber. The properties used for designing these panels were obtained from the American Wood Council (AWC, 2018) and are presented in the Table 3.

Table 3: CLT Panel Design Parameters

CLT Panel Design Parameters	
Panel Thickness (b_w)	12.375 in
Panel Length (L_w)	117.125 in
Tapered Panel length (L_{wt})	113.125 in
Total Wall Height (H_w)	1374 in 1374 in NHERI TallWood , 846 in NHERI Converging design
Flexural Stress (F_b)	2400 Psi Major Direction, 1000 Psi Minor direction
Compressive Stress (F_c)	1975 Psi Major direction, 1400 Psi Minor direction
Tensile Stress	1925 Psi Major direction, 650 Psi Minor direction

3.3.1.2 Mass Plywood Pannels (MPP)

Mass Plywood Panels (MPP) are a relatively new mass timber product developed by Freres Lumber in Oregon. These panels are created by assembling and gluing multiple layers of Structural Composite Lumber (SCL), resulting in large, strong, and versatile panels that can reach dimensions of up to 12 feet in width and 48 feet in length. Unlike traditional plywood, MPP uses thinner layers of veneer that are carefully aligned to optimize strength and efficiency. This method not only makes MPP lighter and more cost-effective but also sustainable, as it utilizes less wood fiber while maintaining high structural performance. This makes MPP ideal for various applications, including floors, walls, and roofs in mass timber buildings.

The MPP panels used for both projects were donated by Freres Lumber and were 9-inch-wide, grade F16 panels, as defined by APA (2021). The term "plank" or "flatwise" orientation refers to loading perpendicular

to the glue line, while "joint" or "edgewise" orientation refers to loading parallel to the glue line. The table below explains the material properties and design values of the panels.

Table 4: MPP Panel Design Parameters

MPP Panel Design Parameters	
Panel Thickness (b_w)	9.1875 in
Panel Length (L_w)	105.125 in
Tapered Panel length (L_{wt})	101.125 in
Total Wall Height (H_w)	114.5 ft NHERI TallWood, 70.5 ft NHERI Converging design
Flexural Stress (F_b)	1900 psi Joist, 1250 psi Plank
Compressive Stress (F_c)	2400 psi
Tensile Stress	1300 psi
Major EI_{eff}	1.385E+09 lb-in^2 / ft
Major GA_{eff}	3420000 lb/ft

3.4 Diaphragms

The NHERI TallWood building incorporated various types of mass timber panels on different floors to collect diverse data regarding the properties of each panel type. As shown in the Figure 15, the first two floors utilized 5-ply Cross Laminated Timber (CLT) panels, while the 4th and 5th floors were constructed with Glue Laminated Timber (GLT) panels. The 6th floor featured Nail Laminated Timber (NLT) panels, and Dowel Laminated Timber (DLT) panels were used on the 7th floor. The top four floors were made with Veneer Laminated Timber (VLT) panels.

In the NHERI Converging Design project, the same building structure and diaphragm configuration were used; however, the top four floors (VLT panels) were removed for the experiment. The differences in the remaining panels are discussed in detail below.

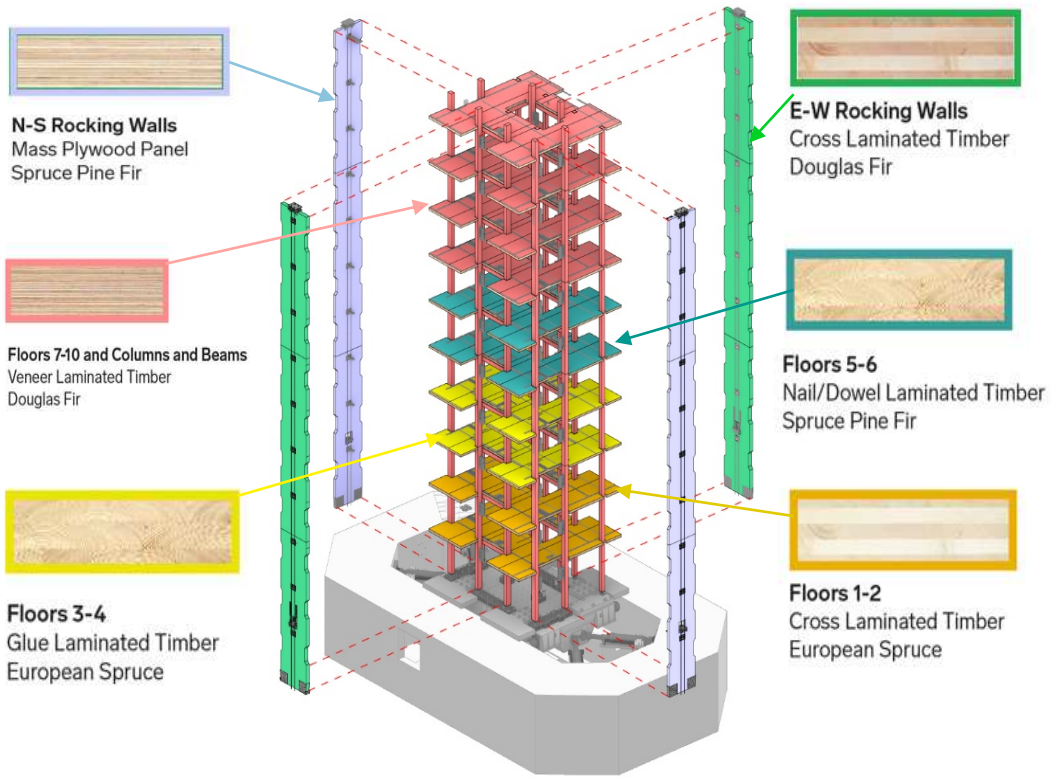

Figure 15: Mass Timber Structural Element Detail (Graphic Courtesy of LEVER Architecture)

3.4.1 Glue-Laminated Timber (GLT)

Glue-Laminated Timber (GLT) is an engineered wood product manufactured by bonding individual layers of timber with adhesives, with all laminations aligned parallel to the length of the member, as illustrated in Figure 16. Unlike Cross-Laminated Timber (CLT), GLT is governed by its own set of standards, distinct from the PRG-320 guidelines. It adheres to American testing standards, primarily ASTM D3737-18e1, which establishes the allowable properties for structural glued laminated timber (Glulam).

The parallel grain alignment in GLT necessitates additional sheathing to enhance strength in the out-of-plane direction. GLT is celebrated for its innovative application in construction, offering a higher strength-to-weight ratio compared to steel, along with increased stiffness and strength relative to conventional lumber of the same size. These properties, combined with its cost efficiency and improved performance, make GLT an ideal material for a variety of applications, ranging from residential beams to complex curved arches in large-scale structures spanning over 500 feet.

Figure 16: Glue Laminated Timber Manufacturing Detail

Glulam, a stress-rated beam, is composed of wood laminations ("lams") bonded with moisture-resistant adhesives, with the grain direction running parallel to the member's length. GLT is versatile, available in both standard and custom sizes, and is classified into four appearance categories: premium, architectural, industrial, and framing, enabling its use in a diverse range of structural and aesthetic applications.

3.4.2 Nail-Laminated Timber (NLT)

Nail-Laminated Timber (NLT) is an engineered wood product constructed from dimensional lumber oriented on edge and mechanically fastened together using nails or screws, as illustrated in Figure 17. Unlike other mass timber products such as Cross-Laminated Timber (CLT) or Glue-Laminated Timber (GLT), NLT lacks a universal manufacturing standard or defined set of tolerances. Instead, its production

relies on guidelines established by manufacturers, which specify essential quality control measures, tolerances, and checks to ensure performance consistency (Binational Softwood Lumber Council, 2007).

Figure 17: Nail Laminated Timber Manufacturing Detail.

3.4.3 Dowel-Laminated Timber (DLT)

Dowel-Laminated Timber (DLT) is a mass timber product composed of dimensional lumber oriented on edge and joined using hardwood dowels inserted via friction, as shown in Figure 18. Like Nail-Laminated Timber (NLT), DLT is classified as a specialty mass timber product and does not currently adhere to any standardized industry-wide manufacturing protocols or tolerances. Instead, its properties and grading criteria are defined by manufacturers, with Structure Lam serving as a primary producer. Detailed specifications for DLT, including its structural grade and performance characteristics, are provided in their product manual (Structure Craft, 2021).

The production of DLT involves taking structurally graded lumber, which is finger-jointed and moulded into precise shapes, and laminating it into large panels in a controlled factory environment. These panels are assembled using hydraulic presses, and hardwood dowels are friction-fitted into pre-drilled holes within the lamellas. The differing moisture content between the hardwood dowels and softwood planks induces swelling in the dowels and shrinkage in the planks, generating the friction necessary to secure the laminations.

Typically, sheathing is pre-installed, and exposed surfaces are finished prior to delivery to the construction site. A defining characteristic of DLT is its all-wood composition, which eliminates the need for metal fasteners, nails, or adhesives, distinguishing it from other mass timber products.

Figure 18: Dowel Laminated Timber Manufacturing Detail

3.4.4 Laminated Veneer Lumber (LVL)

Laminated Veneer Lumber (LVL) is an engineered wood product created from dried, graded wood veneers, strands, or flakes, which are layered and bonded together using high-strength adhesives under heat and pressure. A representative cross-section of LVL is illustrated in Figure 19. Classified as a structural composite lumber product, LVL production is not governed by PRG-320 standards; instead, it is subject to other relevant ASTM standards. The primary standard applicable to LVL is ASTM D5456-18, which provides specifications for evaluating structural composite lumber products (APA-The Engineered Wood Association, 2023).

ASTM D5456-18 accounts for the complexities inherent in the manufacturing process of structural composite lumber and establishes guidelines for manufacturers, regulatory authorities, and end-users. These guidelines ensure consistent evaluation of the structural capabilities of LVL and similar composite products (American Society for Testing and Materials (ASTM), 2019).

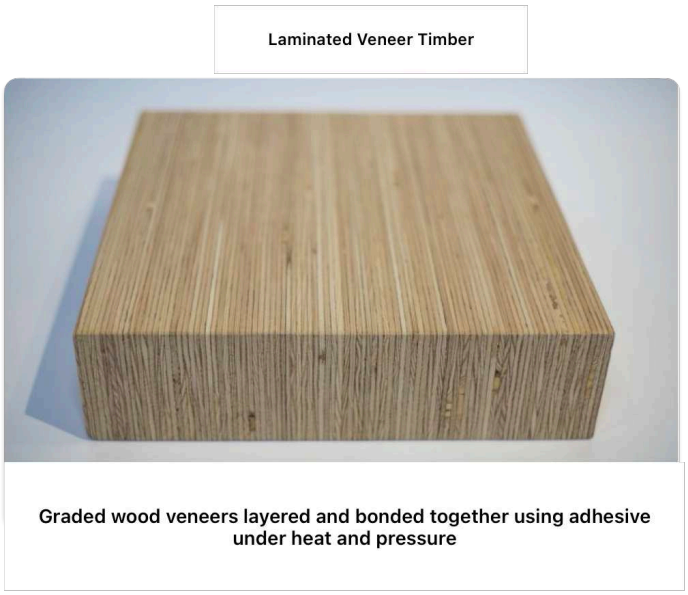

Figure 19: Laminated Veneer Timber Manufacturing Detail

3.4.5 Veneer Laminated Timber

Veneer Laminated Timber (VLT) is an engineered mass timber product constructed from layers of 1-1/16 inch Laminated Veneer Lumber (LVL), featuring cross-band veneers laminated in parallel. Each LVL layer is bonded using high-strength adhesives, with the number of layers varying between two and twelve depending on the application. A representative cross-section of VLT is shown in Figure 19.

VLT is assessed in accordance with PRG-320 standards, similar to Mass Plywood Panels (MPP), ensuring its suitability for use in structural applications. In addition, VLT must comply with ASTM standards applicable to structural composite lumber, including those governing the evaluation and performance of LVL products (APA-The Engineered Wood Association, 2023).

Chapter 4 Construction and Deconstruction.

4.1 Overview

This chapter provides information on the construction processes of the NHERI TallWood Project and the NHERI Converging Design Project. It outlines the challenges encountered during construction and how these challenges were overcome on-site. Additionally, it discusses the construction timelines for both projects and concludes with a description of the final deconstruction process.

4.2 Construction of NHERI TallWood Project

The NHERI TallWood Project's lateral and gravity systems, including panels and columns, were delivered to the site according to the specified dimensions, allowing for direct installation. Due to construction constraints, the process was carried out in three major steps.

The process began with the preparation of the foundation, as illustrated in Figure 20(B), where concrete was poured to integrate the extended portions of the exterior walls. Following this, the cantilever concrete foundations were lifted onto the shake table, and post-tension rods were installed to secure them firmly to the table, as shown in Figures 20(C) and 20(D).

Once the cantilevered concrete foundations were properly positioned and post tensioned, steel foundation beams were installed on all four sides of the shake table to serve as the base for the bounding columns and rocking walls. These beams, as shown in Figure 20(E), provided the necessary structural support for the lateral force-resisting system. The steel foundation beams were then post-tensioned to the shake table foundation, ensuring stability and alignment, as demonstrated in Figure 20(F).

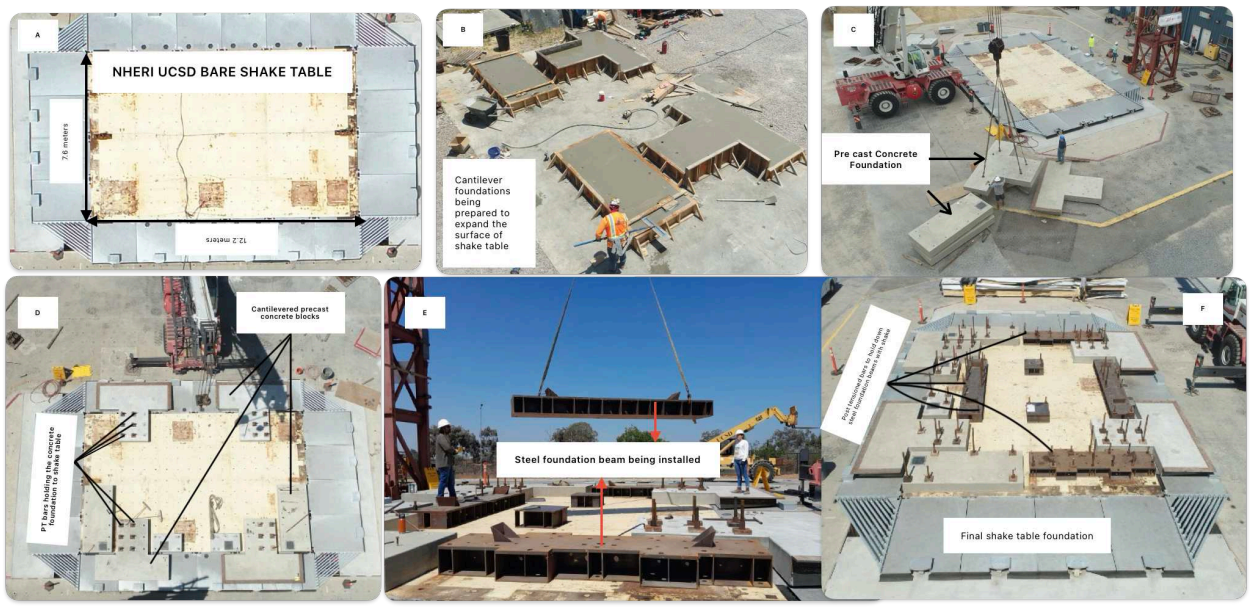

Figure 20: Preparation of Shake Table Foundation

The construction process began with the installation of the staircase for the top two stories, as shown in Figure 21(A). The stairs, preassembled off-site and generously donated by the CS Group, were set in place to provide vertical access during construction. Following the stair installation, the columns for the bottom three stories were erected and temporarily braced to maintain stability until the beams were positioned, as shown in Figure 21(B). Afterward, the diaphragms were installed sequentially, with the first two floors utilizing CLT panels and the third floor using GLT panels, as shown in Figures 21(C) and 21(D). Upon completing the diaphragm for the third floor, the modular stair for that floor was installed, facilitating continued access for construction activities.

Simultaneously, a team of carpenters prepared the splice connections for the rocking walls. To address construction constraints, the 10-story rocking wall system was divided into three sections for ease of transportation. Each section was equipped with splice connections featuring metal plates at the ends of the wall panels, serving as couplers. These steel plates rested on top of panel cutouts, while epoxy tension rods were embedded through panel holes to ensure strong connections. Multiple epoxy rods were utilized to resist shear forces between the panels.

Once the four rocking walls were positioned within the bottom three stories, they were temporarily post-tensioned to the foundation, as shown in Figure 21(F), providing necessary lateral resistance during construction for typical wind loading in San Diego, CA. This temporary post-tensioning allowed the rocking walls to function as an equivalent shear wall system. Following their placement, shear keys were installed in the slotted holes of the rocking walls to secure them to the diaphragm. These shear keys enabled the walls to rock freely while remaining connected to the diaphragm.

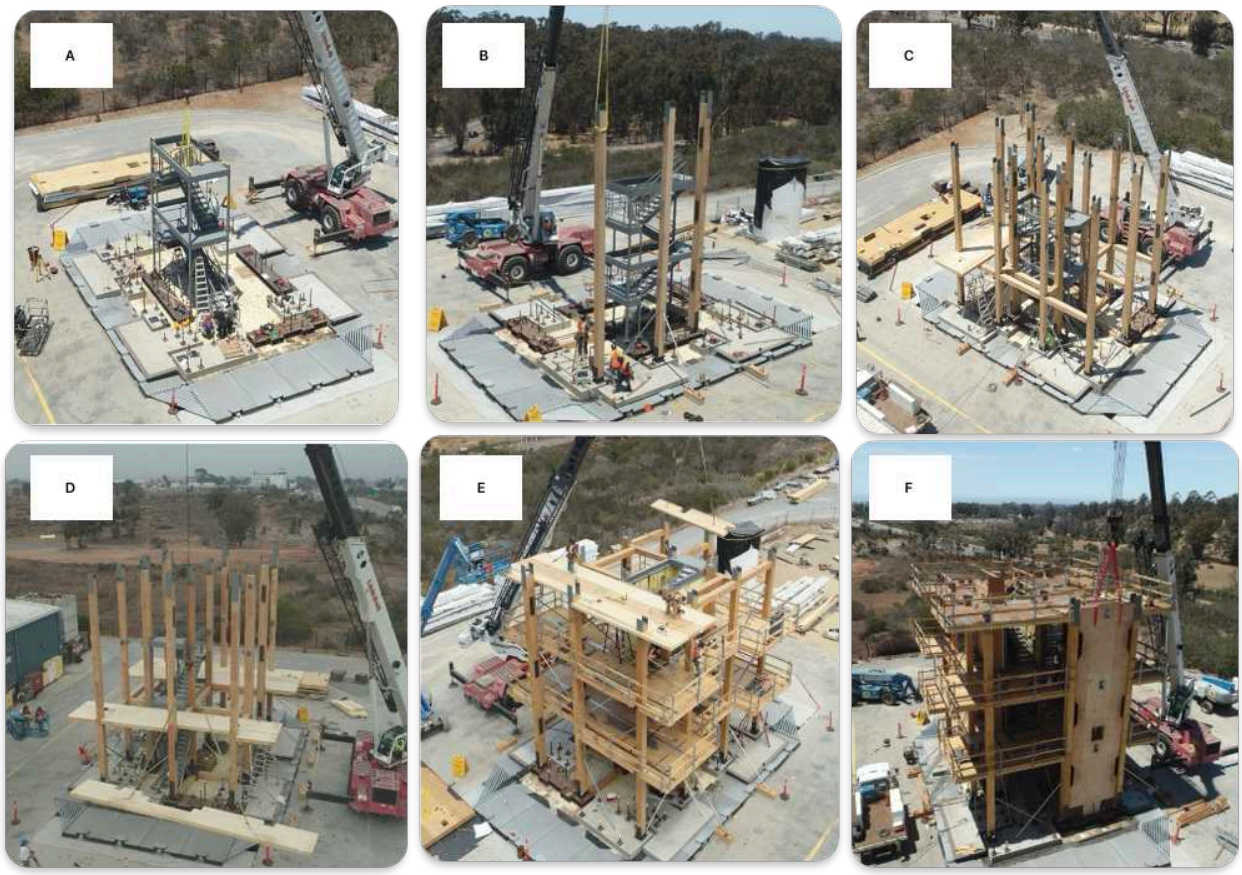

Figure 21: Construction of Bottom 3 Stories of NHERI Tallwood Specimen

Two types of shear keys were employed in the building, each tailored to the diaphragm's construction type. For floors without sheathing on the floor panels, the shear key connection consisted of a tongue plate welded to a wind plate. This assembly was secured to the diaphragm panel using Simpson Strong-Tie SDCF screws installed at a 45-degree angle to mitigate the turning moment induced by the shear key, as shown in Figure 22(A). For floors with sheathing on top of the panels, such as Nail-Laminated Timber (NLT), Dowel-

Laminated Timber (DLT), and Glue-Laminated Timber (GLT) floors, an alternative shear key connection was utilized, as illustrated in Figure 22(B).

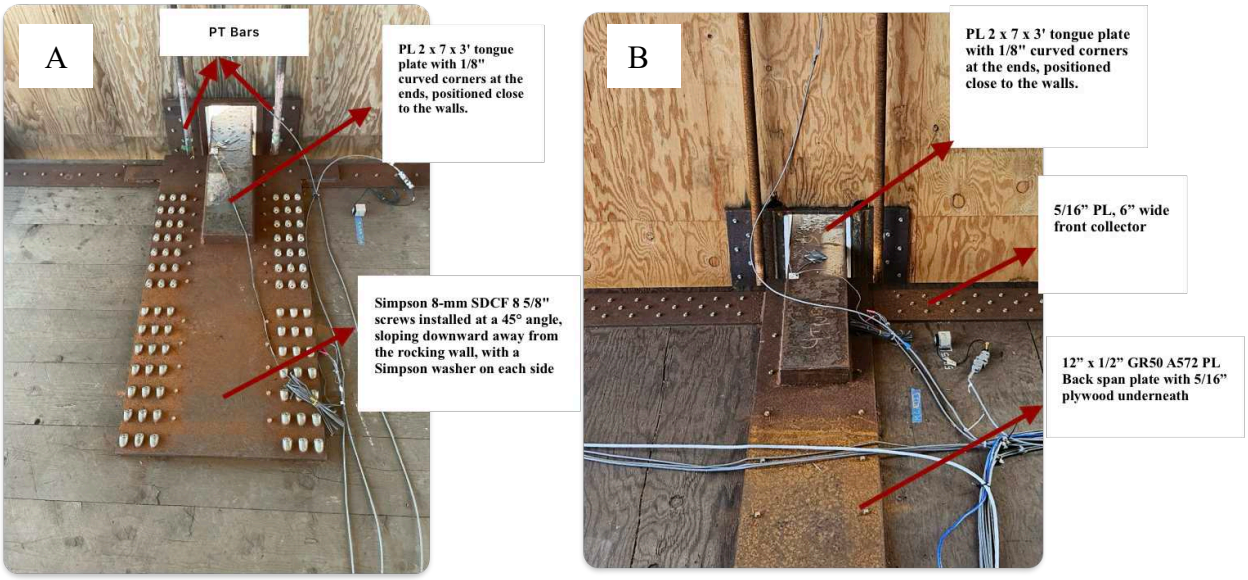

Figure 22: Shear Key Connection Detail

An essential energy dissipation device installed in the building is the U-shaped Flexural Plate (UFP). For each rocking wall panel, a total of 26 UFPs were installed. In the bottom three stories (corresponding to the first wall panel), each UFP cutout accommodated two UFPs, as illustrated in Figure 23(A). For the stories above the third, each cutout was equipped with one UFP, as shown in Figure 23(B). The increased number of UFPs in the bottom three stories provided enhanced lateral support for the building during construction. The UFP cutouts were precision-machined using CNC technology at the DR. Johnson Lumber fabrication facility in Riddle, Oregon.

The installation process involved inserting knife plates into the center of the rocking wall and the adjacent bounding column. The UFP device was then slid into the gap between the two knife plates and secured with bolts. To facilitate installation, the UFPs featured slotted holes on the bounding column side. Once the UFPs were bolted into place, weld washers were added to establish a fixed connection, ensuring the device's stability and performance during seismic events.

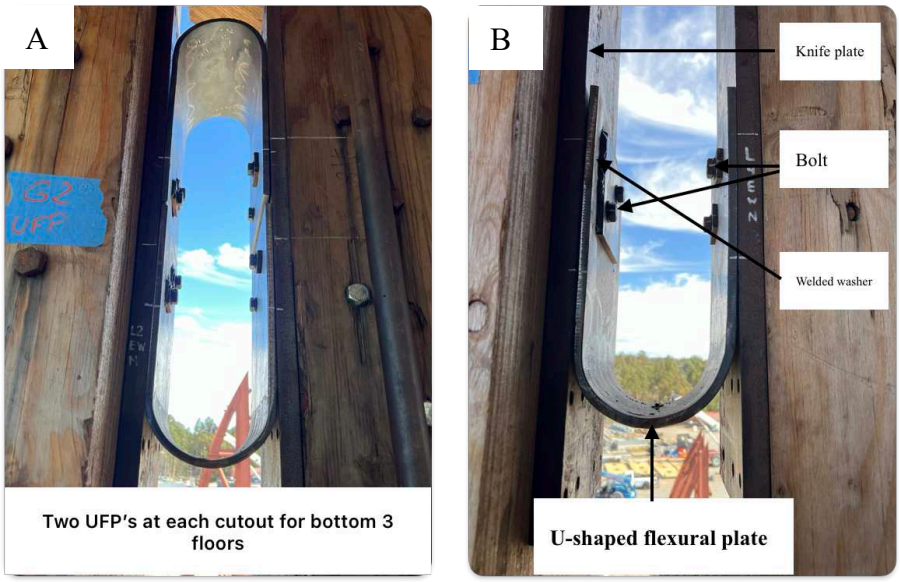

Figure 23: UFP Connection Detail

After the rocking wall panels were secured to the foundation, as shown in Figure 24(A), and the diaphragm hardware installation was completed, the construction transitioned into the second phase. The first step of this phase involved the installation of the precut columns and beams for Level 5, accompanied by the modular staircase installation, as shown in Figure 24(B). Following this, GLT panels were placed for Level 5, as depicted in Figure 24(C), while NLT panels were installed for Level 6. Upon reaching Level 6, two safety towers were positioned on the south side of the building, and another modular staircase was added to provide access to the subsequent levels.

The second phase of construction encompassed four floors, following steps similar to those used for the bottom three stories, as shown in Figures 24(D) and 24(E). Once the frames and floors were completed, the second set of wall panels was lifted and connected to the previously installed bottom wall panels using the connection details outlined earlier. The detailed steps of this phase mirrored the processes used in the

construction of the lower three floors, allowing for a streamlined approach that expedited the overall construction timeline, as shown in Figure 24(F).

Figure 24: Construction of Floor 4 to Floor 8 of NHERI TallWood Specimen

The building erection progressed after the second set of rocking wall panels was securely connected to the bottom panels, with epoxy rod connections requiring 24 hours to cure under summer conditions in San Diego, CA, using CI-GV Structural Injection Epoxy Gel from Simpson Strong-Tie. Following this, another stair module was installed, and the final set of columns was lifted and positioned, as shown in Figure 25(B). Once the columns and beams were in place, diaphragms for floors 9 and 10 were lifted by crane and installed, as illustrated in Figure 25(C). Subsequently, the final segment of rocking wall panels was lowered into place and connected to the lower panels, with the last set of roof panels installed thereafter. At this stage, the major structural components were completed, as shown in Figure 25(E). The construction process for this phase mirrored the methods used for the bottom three stories, ensuring efficiency and consistency in execution. The contractors then shifted their focus to the diaphragm hardware and the installation of PT

bars. After the PT bars were post-tensioned, the leveling bolts at the base connections were removed, enabling the base to function as a true pin connection as per the design.

Figure 25: Final Stage of Construction of NHERI Tallwood Specimen

4.3 Deconstruction of Four Stories of the NHERI TallWood Project to Create the Six-Story Converging Design Test Building

4.3.1 Overview

This section discusses the deconstruction of the top four floors of the NHERI TallWood Project and the subsequent construction of the NHERI Converging Design Project specimen, which was essentially the NHERI TallWood specimen with the top four floors removed. Figure 26 below illustrates an overview of the deconstruction process and the transformation of the test specimen from 10 stories to six stories.

Figure 26: Overview of Deconstruction of NHERI TallWood Specimen to NHERI Converging Design Specimen.

4.3.2 Preparation Days

During the preparation days, workers concentrated on readying the structure for the crane operations, undertaking several crucial tasks to ensure the safe and efficient removal of structural elements. These preparations included drilling holes into the panels to facilitate easier lifting with the crane, unscrewing one side of the spline elements, and cutting the collector straps that were positioned transversely to the panel direction. Additionally, extra holes were drilled to serve as crane pick points, and the long screws attaching the panels to the beams were unscrewed. These meticulous preparations ensured that the structural elements could be removed safely and efficiently during the crane days.

4.3.3 Crane Days

On crane days, a 140-ton Link-Belt crane was employed to facilitate the systematic deconstruction of the building's structural elements. The operation was executed with precision to ensure the safe removal of components while maintaining efficiency. The first stage focused on the removal of modular stair units, which had been specifically designed for ease of disassembly. These units were detached from the floor

diaphragms and the corresponding modules below before being hoisted out using the crane. The modular design significantly expedited the removal process and minimized disruptions to the overall deconstruction sequence.

Following the removal of the stair units, the outer diaphragm panels were carefully detached as shown in Figures 27 A and 27 B. These panels were unscrewed from their spline elements, and additional crane pick points were drilled into them to enable safe lifting. Once the necessary preparations were completed, the crane hoisted the panels out of position. Worker safety was a primary consideration during this stage, with fall protection measures in place to ensure secure handling, particularly during the detachment from the beams.

The deconstruction process then moved to the inner diaphragm panels, which remained connected to the beams and columns. These panels were removed as modular units, with beams detached from the columns via bi-axial connections specifically designed for ease of disassembly. In cases where the disconnection of beams proved challenging, contractors opted to cut the beams to expedite the process, thereby releasing the columns for removal. This step was essential for dismantling the integrated structural system efficiently.

Once the diaphragm panels were fully removed, attention turned to the remaining beams and columns. Where beam-to-column connections could not be quickly unfastened, the connections were severed to streamline the operation. Additionally, column splice connections were either disassembled or, in the absence of splices, columns were cut above the diaphragm level for extraction. This pragmatic approach ensured the safe and rapid removal of the remaining structural framework.

Figure 27: Deconstruction Sequence Detail

The final stage of deconstruction involved the cantilevered shear wall panels. To remove these elements, the post-tensioned rods securing the walls were first severed. Subsequently, the walls were cut with a chainsaw while being supported by the crane to prevent uncontrolled movement. Once detached, the walls were carefully lowered from the structure. Any energy dissipation devices attached to the walls were disconnected during this phase, completing the deconstruction process with meticulous attention to detail. This methodical and technically precise deconstruction process highlighted the importance of pre-engineered connections and modular design elements, ensuring a safe and efficient dismantling of the building's structural components.

Chapter 5 Instrumentation

5.1 Overview

This chapter outlines the instrumentation setup employed across both projects, with a particular focus on the structural systems. The following sections provide a detailed analysis of the instrumentation layout, covering global, gravity, and lateral instrumentation strategies. Each section highlights the types of instruments used, their placement, and the key objectives of each instrumentation group, aiming to capture comprehensive data on the structural behavior during testing.

5.2 Instrumentation Setup

Both the TallWood and Converging Design test specimens were extensively instrumented, utilizing over 700 sensor channels, with many common channels and sensors remaining from Tallwood to Converging Design, to capture the structural and nonstructural responses of the building. In addition to these sensors, approximately 50 high-definition cameras including GoPro and Internet Protocol (IP) cameras were strategically installed throughout the structure to visually document the building's The instrumentation focused on capturing global structural responses such as floor-level accelerations and displacements, while also monitoring localized behaviors. Targeted sensors were installed at critical structural components, including the rocking walls, beam-column connections, and the base of both gravity and bounding columns, to record force demands and deformations. For nonstructural systems, instrumentation was placed at movement joints and interface locations to track displacements and deformations, enabling a comprehensive evaluation of component interaction under dynamic loading.

The camera setup provided valuable visual data to validate assumptions about structural and nonstructural performance and to support detailed post-test analysis. A summary comparison of the number and types of instruments used in both projects is presented in Figure 28.

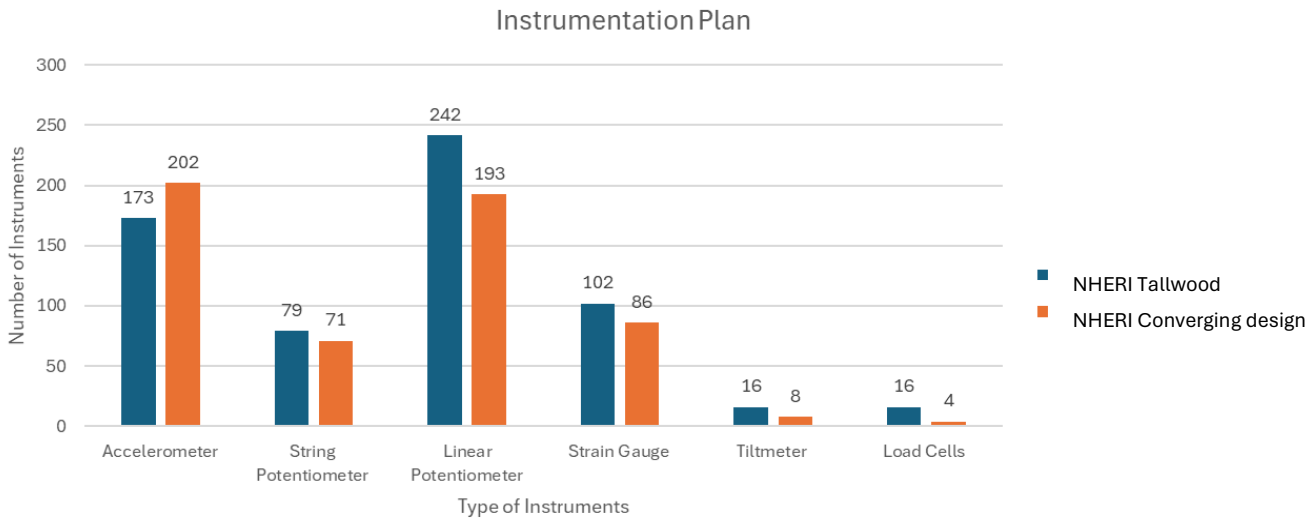

Figure 28: Instrumentation Comparison Between Two Projects

5.3 Types of sensors and channels

This section explains the major subgroups of the building instrumentation plan, detailing the expected findings and the instruments used to achieve these results. The instrumentation plans for both projects are included in the appendix for reference. In total, 733 instruments were used in the NHERI TallWood Project, while 600 instruments were utilized in the NHERI Converging Design Project. These instruments were distributed across the entire structure, and the types used in both projects included accelerometers, linear potentiometers (linear pots), string potentiometers (string pots), push potentiometers (push pots), tiltmeters, load cells, and strain gauges.

The naming of the instruments followed a systematic convention to ensure clarity and minimize errors in data collection. Each instrument in the NHERI TallWood Project was assigned a unique three-digit identifier, starting from 001 and ending at the total number of instruments used. For the NHERI Converging Design Project, an amendment was made to include a "C" prefix in the instrument names to distinguish them from the earlier project and prevent duplication or confusion in the instrumentation setup. This naming convention simplified channel labeling and facilitated efficient data management.

To better understand the scope of instrumentation, the setup is broken down into major categories below, focusing on gravity and lateral systems.

5.3.1 Gravity System Instrumentation

The gravity system instrumentation was designed to monitor displacements and accelerations in various components of the gravity system, including beam-column connections, column bases, column-diaphragm connections, and column splices. These instruments provided critical data on the structural response under seismic and static loads. The detailed instrumentation plans for the NHERI TallWood Project can be found in Bush et al. (2023), while those for the NHERI Converging Design Phase 1 are described in Uarac et al. (2024).

5.3.1.1 Beam-Column Connections

Linear potentiometers were strategically installed to capture the relative rotation between beams and columns, providing essential data on the rotational behavior at these connections. These devices were mounted on L-shaped steel brackets, with one end affixed to the beam and the other securely attached to the column face parallel to the beam. This configuration ensured precise measurement of the angular displacement resulting from structural deformations. A similar instrumentation approach was applied to monitor rotations between beams and diaphragms, enabling a comprehensive understanding of the rotational interactions in both the X and Y directions. Figure 29 illustrates the detailed setup, highlighting the placement and alignment of the linear potentiometers to achieve accurate and reliable data acquisition.

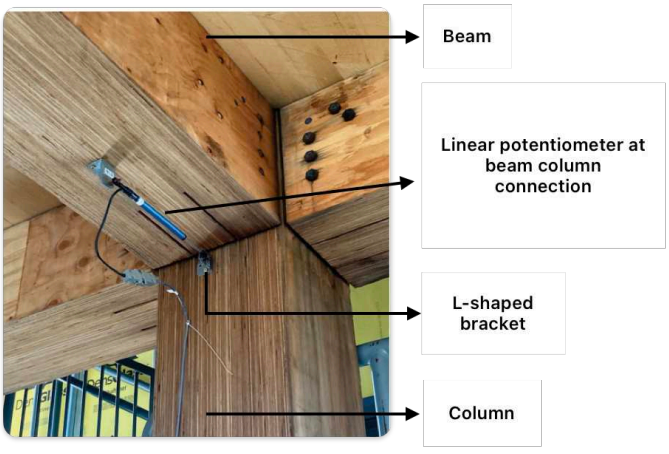

Figure 29: Instrumentation Detail at Beam Column Connection

5.3.1.2 Column Bases

The column bases, which were designed as true pin connections (see section 3.2 Figure 5), were instrumented to monitor pin movement and rotational behavior at the interface between the columns and the foundation. Linear potentiometers were strategically installed on the column faces relative to the foundation to capture these movements with high precision. The installation process involved the use of L-shaped brackets and magnets to securely attach the potentiometers to the foundation, while screws or additional magnets were used to fix them to the column faces.

Fourteen column bases were instrumented, with three faces of each column monitored. One face of each column was left without instrumentation to avoid interference with the adjacent rocking wall system. Instrumentation included all eight bounding columns, as these directly interfaced with the lateral force-resisting system, and two gravity columns were selected to provide insights into rotational behavior within the gravity system. This setup ensured a comprehensive understanding of the dynamic behavior at the column bases under seismic loads.

The instrumentation layout and mounting details are shown in Figure 30, which illustrates the positioning of the linear potentiometers and their attachment mechanisms. This configuration facilitated the collection of high-fidelity data necessary for assessing the performance of the column base connections.

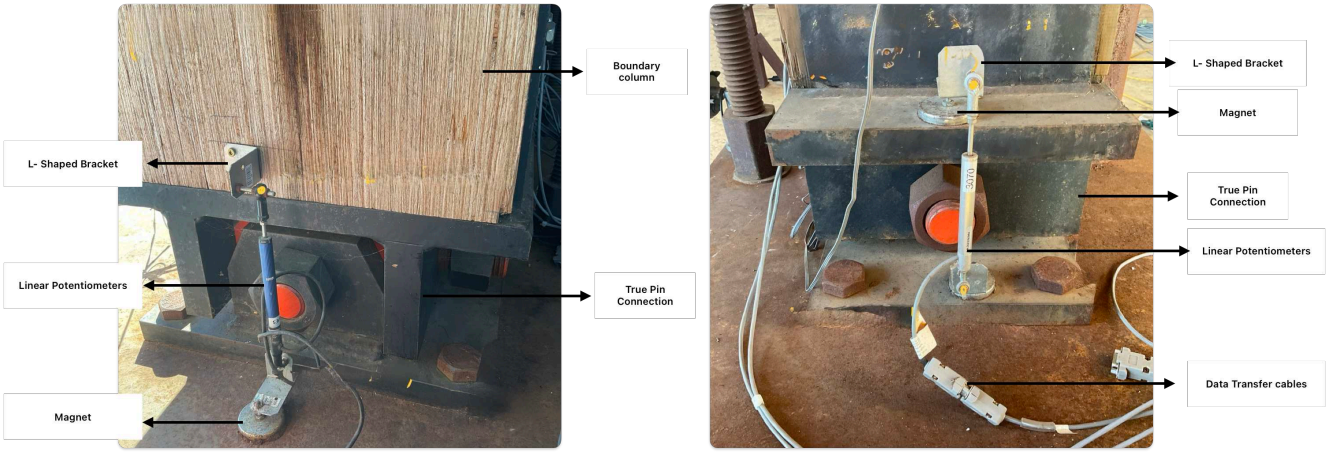

Figure 30: Instrumentation Detail at Column Base Connection

5.3.1.3 Column-Diaphragm Connections

Push potentiometers were installed parallel to the columns and oriented toward the diaphragms to measure relative movement between these structural elements accurately. These devices captured the translational displacements occurring at the column-diaphragm interfaces during dynamic loading conditions.

The potentiometers were mounted on a custom 2x4 framework, which was securely attached to the columns. Careful attention was given to eliminate any gaps between the columns and the diaphragms, ensuring that the measurements reflected actual relative displacements without interference from unintended gaps or misalignments. This setup was implemented on two faces of both gravity and bounding columns that interfaced directly with the diaphragms. The detailed instrumentation layout, including the placement and mounting configuration of the push potentiometers, is illustrated in Figure 31.

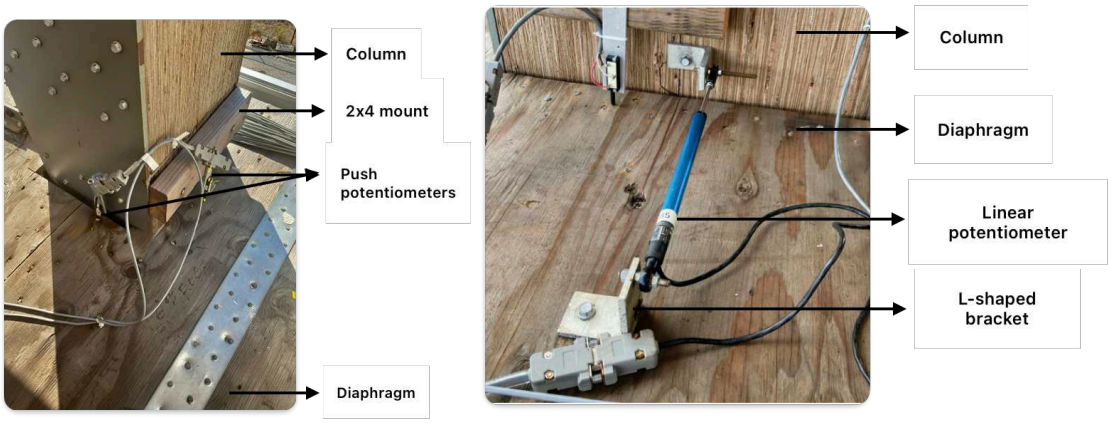

Figure 31: Instrumentation Detail at Column Diaphragm Connection

5.3.1.4 Column Splices

Push potentiometers were installed at column splice connections to monitor potential separation at these critical structural interfaces. These instruments were carefully mounted on plywood strips that bridged the splice, with one end affixed to the upper column and the other end pressed into the lower column using a spring-loaded mechanism. This configuration ensured consistent contact and reliable measurements of relative movement at the splices.

Instrumentation was concentrated at Level 4, where the first splice connection experienced the highest loads due to its position in the structural hierarchy and its role in distributing seismic forces. The detailed instrumentation layout, including the placement and mounting configuration of the push potentiometers, is illustrated in Figure 32.

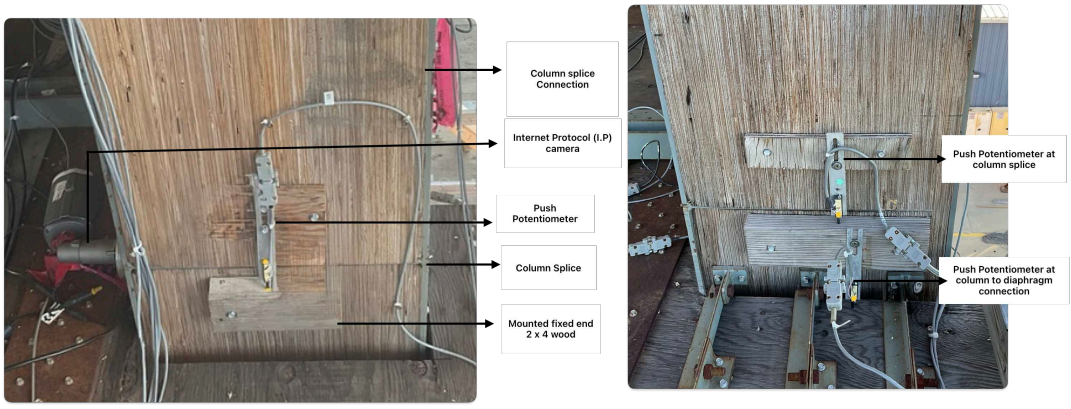

Figure 32: Instrumentation Detail at Column Splice Connection

5.3.2 Lateral System Instrumentation

The lateral system instrumentation was more extensive and included accelerometers, linear potentiometers, string potentiometers, tiltmeters, load cells, and strain gauges. Instrumentation was applied on all levels, with the number of instruments varying to meet project requirements. Detailed instrumentation plans for the lateral system are included in the appendix. To enhance clarity, this section is divided into seven categories: wall bases, wall splices, post-tensioned bars, UFPs, shear keys, and wall out-of-plane braces.

5.3.2.1 Wall Bases

Linear potentiometers were installed along the base of the rocking walls to accurately measure uplift during seismic excitation. Additionally, potentiometers were positioned on the wall faces to monitor strain, providing critical data on the wall's response under dynamic loading. The installation process employed L-shaped brackets and magnets for secure and precise placement. One end of the potentiometer was affixed to the armor plate of the rocking wall, while the other was connected to the foundation plate. This

configuration ensured reliable measurements by maintaining a stable setup while accommodating the wall's motion. The wall base instrumentation setup is shown in Figure 33.

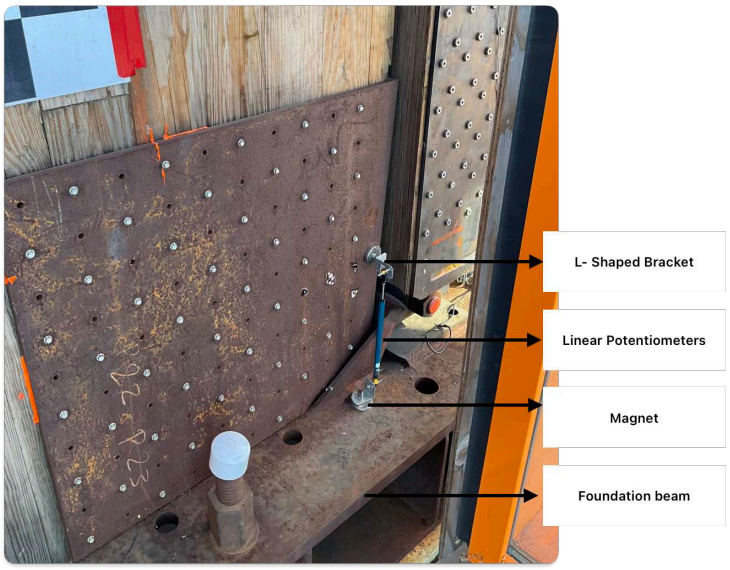

Figure 33: Instrumentation Detail at the Base of the Wall

5.3.2.2 Wall Splices

Push potentiometers and linear potentiometers were installed to monitor separation and strain at critical wall splice connections in both the NHERI TallWood and NHERI Converging Design Projects. These instruments were strategically installed at Levels 4 and 8 in the NHERI TallWood Project and at Level 4 in the NHERI Converging Design Project to capture the behavior of the splice connections under seismic loading. Push potentiometers were used to measure separation between wood and steel interfaces, ensuring detailed observations of any potential detachment at these critical junctions. Concurrently, linear potentiometers recorded strain data in both the wood and steel plates, providing a comprehensive understanding of the forces acting on these materials.

Additional linear potentiometers were installed to monitor shear and strain at the wood-wood and wood-steel interfaces, capturing the dynamic interaction between these elements during seismic activity. This dual instrumentation approach ensured a holistic understanding of the structural behavior at splice connections.

Figure 34 demonstrates the detailed instrumentation setup used on the exterior and interior faces of the splice connections, highlighting the placement and orientation of the potentiometers for optimal data collection.

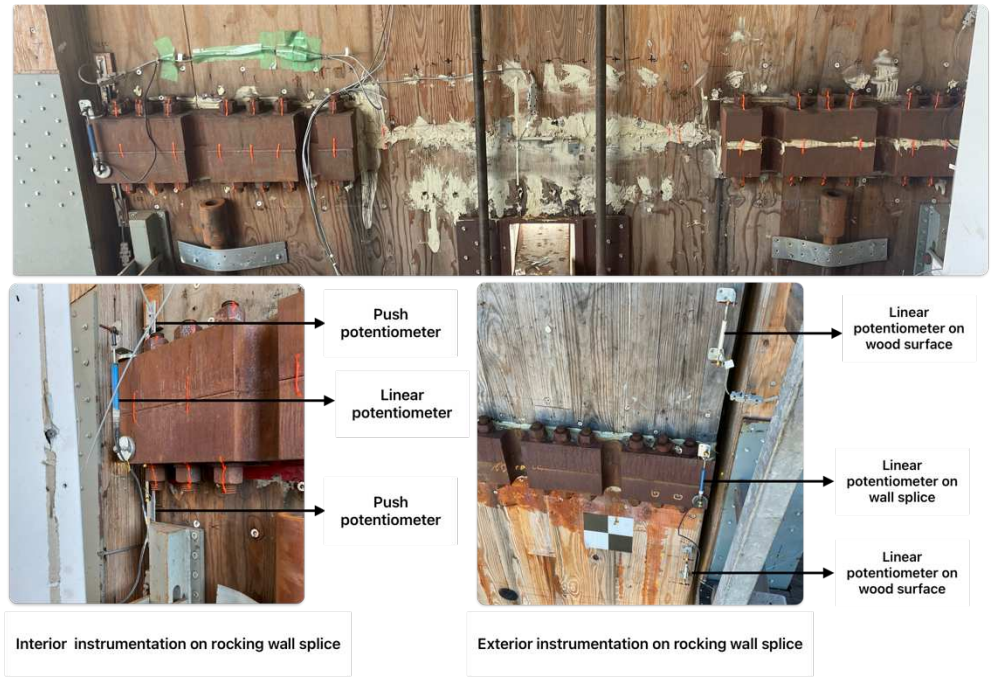

Figure 34: Instrumentation Detail at Wall Splice Connection

5.3.2.3 U-shaped Flexural Plates (UFPs)

String potentiometers were installed on the bounding columns and connected to the rocking walls to measure displacements in the U-shaped Flexural Plates (UFPs). These devices utilized thin wires extending from the string potentiometers, which were anchored to screws on the rocking walls. This setup allowed for precise measurement of displacement and provided insights into the performance and deformation of the UFPs during seismic loading. To complement this, linear potentiometers were subsequently added to monitor relative movement between the rocking walls and bounding columns, ensuring a comprehensive analysis of their interaction.

Figure 35 illustrates the instrumentation setup used to monitor the behavior of the UFPs, highlighting the placement of string potentiometers and the integration of linear potentiometers to capture detailed movement data.

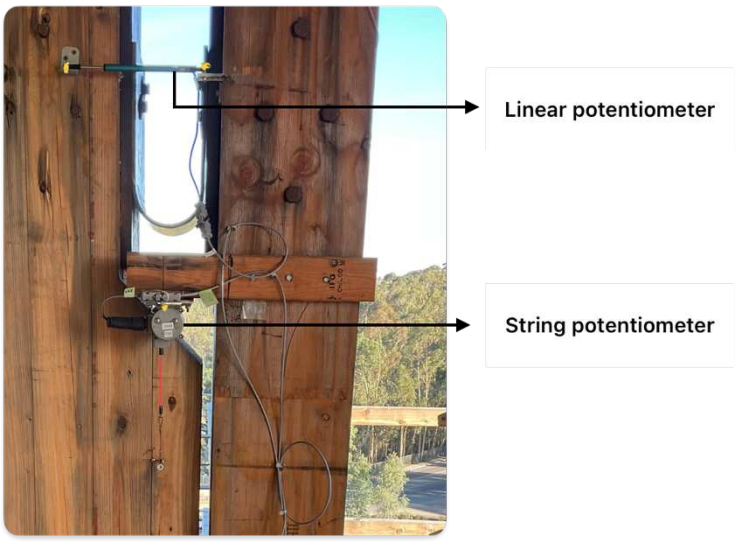

Figure 35: Instrumentation Detail at the UFP's

5.3.2.4 Post-Tensioned Bars

Load cells were installed at the base and roof levels of the post-tensioned (PT) bars to monitor forces throughout the construction and testing phases. Each PT bar was further instrumented with four strain gauges, enabling continuous monitoring of strain during the entire testing process. These strain gauges were strategically positioned to provide detailed insights into the distribution of forces along the PT bars. The load cells ensured precise measurement of post-tensioning forces, a critical parameter for evaluating the structural performance of the rocking wall system under seismic loads.

Figure 36 demonstrates the instrumentation setup, including the PT bars, the configuration of the load cells, and the placement of the strain gauges, offering a comprehensive view of the system used to monitor the post-tensioning forces effectively.

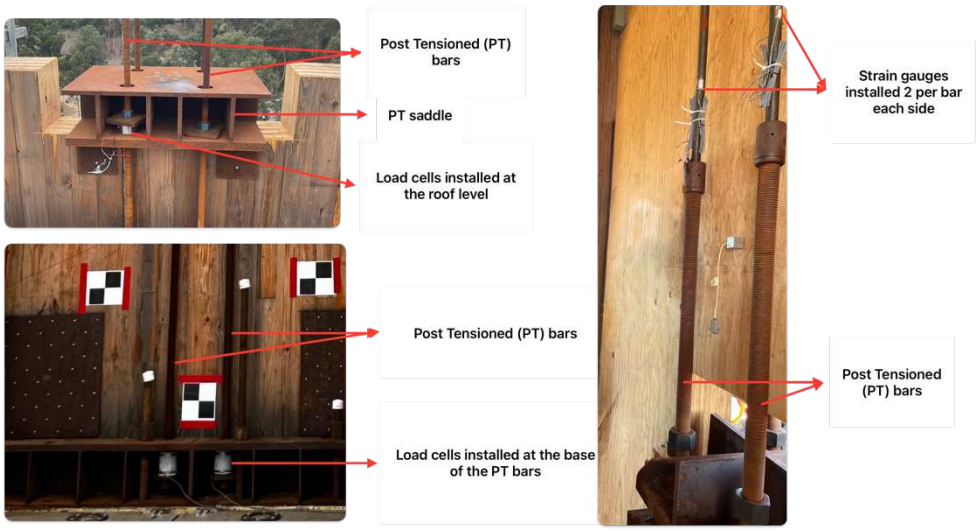

Figure 36: Instrumentation Detail of PT Bars.

5.3.2.5 Shear Keys

String potentiometers were attached to wall faces and tongue plates to monitor displacements. As shown in Figure 37 string potentiometers were configured vertically and at 45-degree angles to capture both in-plane and out-of-plane movements. Strain gauges on tongue plates monitored shear forces, with instruments positioned at mid-span between the wall face and the diaphragm edge.

Figure 37: Instrumentation Detail on Shear Keys

5.3.2.6 Wall Out-of-Plane Braces

Strain gauges were installed on the legs of the wall out-of-plane braces to accurately measure axial forces. These gauges were strategically positioned at the midpoint of each brace leg, capturing both vertical and horizontal orientations. To provide comprehensive data, instrumentation was applied at Levels 2, 3, 4, 6, 8, and 9, with alternating setups between the North and West walls in the NHERI Tallwood . Level 6 received full instrumentation on both walls, as this level was anticipated to experience the maximum out-of-plane forces during seismic testing and later was changed in NHERI Converging Design the approach remained the same and was instrumented until Level 6.

Figure 38 illustrates the instrumentation setup for the out-of-plane rocking wall brace connections, detailing the placement of the strain gauges and their orientation relative to the brace legs. This setup was essential for understanding the force distribution and behavior of the braces under lateral and out-of-plane loads.

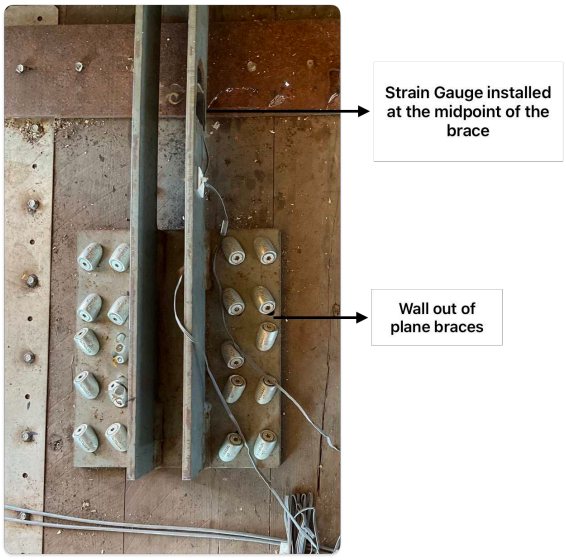

Figure 38: Instrumentation Detail at the Wall out of Plane Brace Connection

5.3.3 Global System Instrumentation

The global system instrumentation comprised two types of instruments: accelerometers and string potentiometers. These instruments were strategically installed throughout the building based on the project's requirements and sensor limitations. The global instrumentation was further divided into three

primary categories according to the type of instruments used and the intended outcomes: accelerations, inter-story displacements, and global displacements. Each category is described in detail below. It should be noted that instruments for global displacement measurements could not be installed throughout the entire building height due to resource constraints.

5.3.3.1 Accelerometers

Accelerometers were installed on each floor to measure floor accelerations in a systematic and strategic manner. These devices were positioned to capture global building accelerations in all three directions: east-west (X-axis), north-south (Y-axis), and vertical (Z-axis). On each floor, accelerometers were placed at the approximate Center of Mass (CoM) to measure accelerations in the X and Y directions. Additionally, vertical accelerometers were installed to monitor Z-axis movements as shown in Figure 39.

To specifically address potential vertical vibration modes, Z-direction accelerometers were placed on the northeast and southwest cantilevers. Furthermore, two of the largest floor spans were selected, and Z-direction accelerometers were positioned at the midpoints of these spans to capture vertical vibrations at these critical locations.

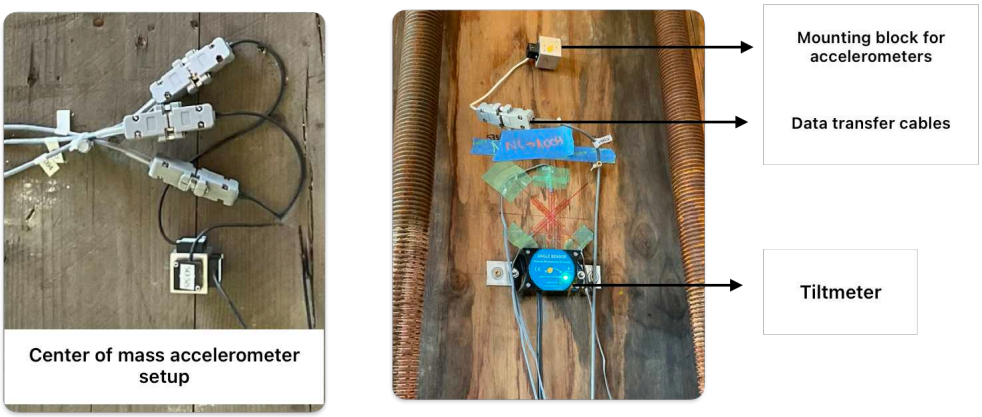

Figure 39: Instrumentation Setup for CoM Accelerometers and Tiltmeter

Triaxial accelerometers were also installed at the CoM on every floor to provide comprehensive data on accelerations in all three directions. On Level 1, six triaxial accelerometers were installed: two on the shake table to aid in building calibration and four on the T-shaped concrete foundations to monitor the response

of the cantilevered portions of these foundation pieces. The two accelerometers on the shake table represented two different brands to ensure consistent calibration between them. These sensors were placed near the CoM to align with the other triaxial accelerometers positioned throughout the height of the building.

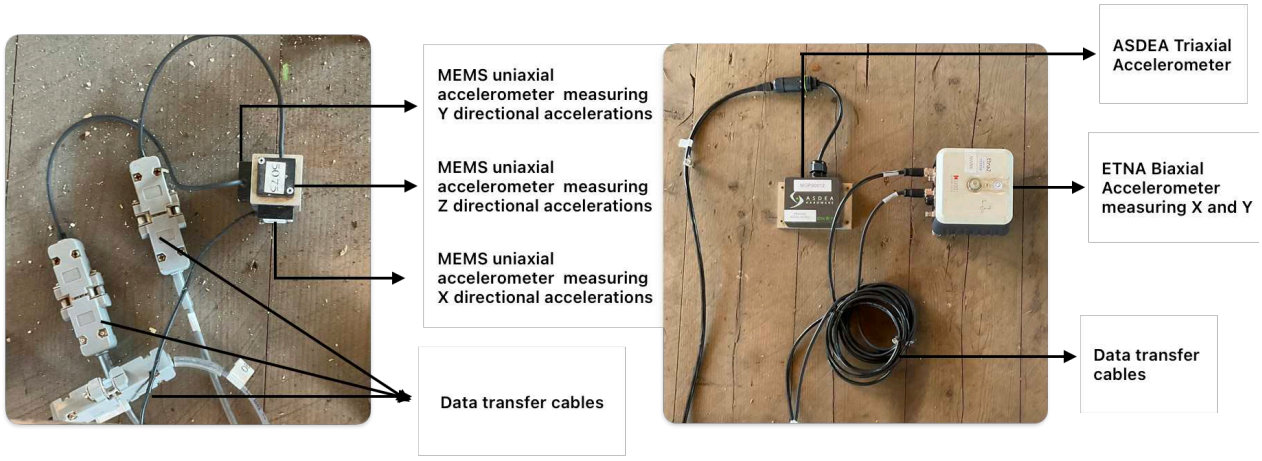

Figure 40: Types of Accelerometers

The accelerometers were securely mounted using machined blocks threaded onto lag screws, which were then fastened into the floor diaphragms. This setup ensured precise and stable placement for reliable data collection.

5.3.3.2 Interstory Displacements

Interstory displacements were measured using string potentiometers installed between the floor diaphragms and adjacent ceilings. These devices recorded the relative motion between successive floors, providing essential data on interstory drift during seismic events. The string potentiometers were installed in both the X and Y directions on all floors, except Levels 4 and 5, where conflicts with nonstructural walls prevented their installation.

To minimize potential directional errors, the locations of the string potentiometers and their anchoring eyebolts were alternated in the plan view on each level. The potentiometers were mounted on angled wooden blocks, with thin wires connecting the strings to eyebolts anchored on the ceiling or beam.

For the NHERI Converging Design Project, an amendment was made to the instrumentation setup, and the string potentiometers used for interstory displacement measurements were removed. This decision was based on data lags observed in the readings due to the longer lengths of the wires. Removing these instruments addressed accuracy concerns and improved data reliability for subsequent testing phases.

5.3.3.3 Global Displacements

Global displacements were measured using string potentiometers that connected the building to external safety towers. These instruments provided critical insights into the overall lateral displacements of the structure during seismic testing.

In the Y-direction, string potentiometers were installed on six floors, with two per floor connecting to the safety towers located on the south side of the building as shown in the Figure 41. On the upper levels, the potentiometers were placed at the far corners of the building to capture any potential torsional behavior. On the lower two floors, the potentiometers were placed at the inner corners of the building to avoid interference with the exterior nonstructural facade. This required the fabrication of extension beams to connect the potentiometers to the safety towers, which were positioned at the exterior corners of the building.

Figure 41: Global Displacement Instrumentation Setup

In the X-direction, string potentiometers were installed on only two levels due to height and location constraints of the safety tower on the east side of the building. Each level had one string potentiometer to measure displacement along the X-axis.

The installation process involved mounting the string potentiometers to the diaphragms using steel angle brackets and connecting the strings to eyebolts attached to magnets on the safety towers. This setup ensured stable connections and reliable data collection.

For the NHERI Converging Design Project, the global displacement instrumentation was modified. On the south side, two string potentiometers were installed up to the roof level following the same methodology as the NHERI TallWood Project. On the west side, one string potentiometer was installed per floor up to Level 3, which was the maximum height reachable by the safety tower.

Chapter 6 Testing and Data Processing

This chapter provides an overview of the testing process for the NHERI TallWood and Converging Design Projects, with a detailed focus on Phase 1 of the Converging Design Project, which involved U-shaped Flexural Plates (UFPs) as energy dissipation devices. The chapter outlines the test setups, the seismic simulations conducted, and the methods employed to process and interpret the gathered data. Additionally, comparisons between the two projects are discussed to highlight advancements in testing protocols and structural design approaches.

6.1 The NHERI TallWood Project

The NHERI TallWood Project involved an extensive series of tests on a full-scale 10-story mass timber building to evaluate its seismic performance. A total of 88 tests were carried out, encompassing ground motion simulations, white noise excitations, and controlled low-level excitations. These tests explored seismic scenarios at various hazard levels, including service-level earthquakes (SLE), design-level earthquakes (DE), and maximum-considered earthquakes (MCER).

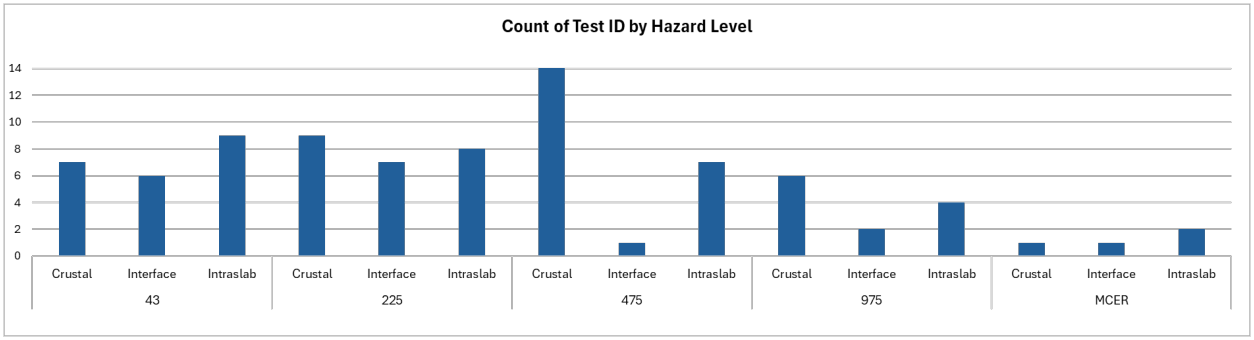

Figure 42: NHERI TallWood's Count of Tests based on Hazard Level

The testing protocol utilized multi-directional force applications, with seismic inputs delivered in uniaxial (X or Y), biaxial (XY), and triaxial (XYZ) configurations. This approach provided a comprehensive understanding of the building's response under realistic multi-axial seismic forces. Ground motions included crustal events like Northridge and Loma Prieta and subduction events such as Maule and Ferndale, scaled progressively from elastic-level motions to high-intensity MCER conditions. The maximum input

PGA reached 0.76 g, representing the extreme seismic demands that structures might face in high-hazard regions.

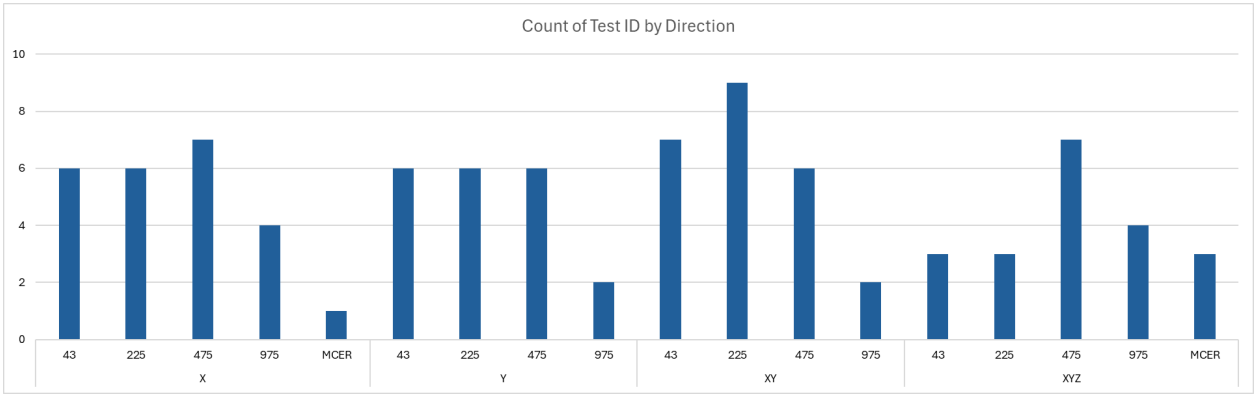

Figure 43: NHERI TallWood's Count of Test Based on Direction

White noise excitations were conducted before and after each seismic event to track changes in stiffness and damping. Inspections between tests documented any damage, such as connection deformation or cracking, and assessed the functionality of non-structural components. The findings validated the efficacy of the post-tensioned mass timber rocking wall system, which exhibited excellent energy dissipation and re-centering capabilities while sustaining minimal damage under severe seismic loads.

6.2 The NHERI Converging Design Project: Phase 1

Building upon the successes of the NHERI TallWood Project, Phase 1 of the NHERI Converging Design Project focused on investigating the seismic performance of U-shaped Flexural Plates (UFPs) as energy dissipation devices in a six-story mass timber building. This phase aimed to optimize the design of mass

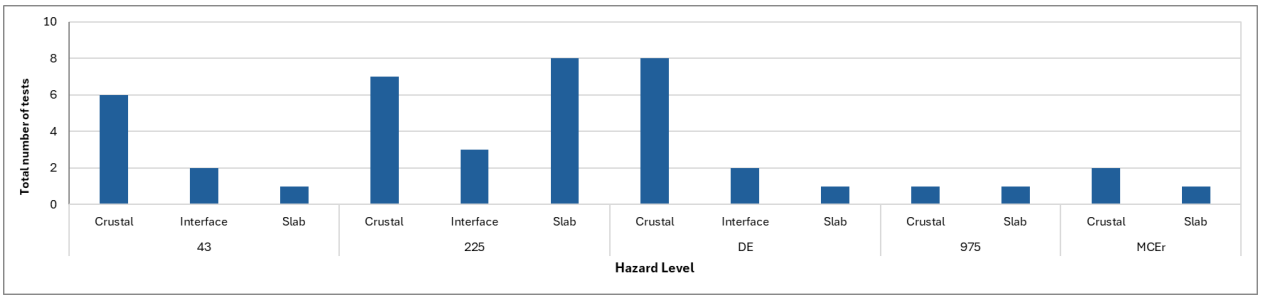

Figure 44: NHERI Converging Design's Count of Tests based on Hazard level

timber structures by validating the UFP system's ability to achieve an effective balance between energy dissipation, re-centering capability, and sustainability. The testing protocol incorporated a mix of earthquake source types, including crustal, interface, and slab earthquakes, which represent distinct seismic origins and characteristics. Crustal earthquakes are shallow events originating near tectonic plate boundaries or fault lines, often generating high-frequency ground motions. Interface earthquakes occur at the interface between subducting and overriding tectonic plates, typically producing long-duration and lower-frequency motions. Slab earthquakes, on the other hand, originate deeper within the subducting plate and are characterized by their complex frequency content and often widespread impact. These diverse seismic sources were combined with hazard levels such as the 43-year return period, 225-year return period, Design-Level Earthquake (DE), 975-year return period, and Maximum Considered Earthquake Risk-Targeted (MCER).

Phase 1 involved 43 ground motion tests, executed in both uniaxial and multi-directional configurations (XY and XYZ), mirroring the comprehensive approach of the NHERI TallWood Project. These tests simulated seismic intensities ranging from low-level service events to extreme MCER-level earthquakes, as shown in the accompanying figures. The figures highlight the distribution of tests across various directional configurations and hazard levels, demonstrating a thorough investigation of potential seismic scenarios. Peak ground acceleration (PGA) values reached up to 0.79 g during the most extreme scenarios,

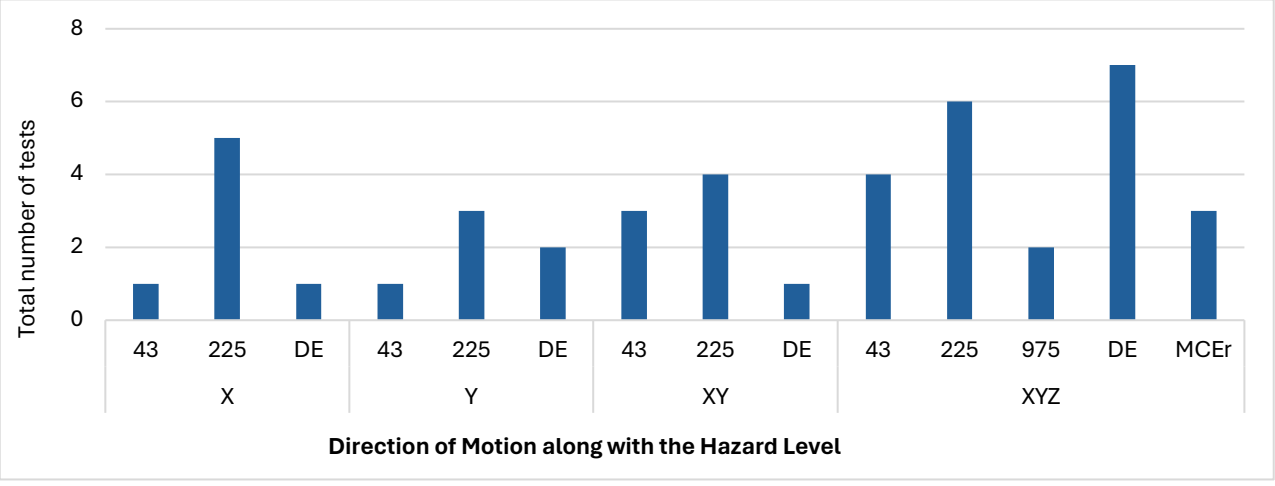

Figure 45: NHERI Converging Design's Count of Test Based on Direction

underscoring the rigorous nature of the testing and the UFP system's capacity to withstand significant seismic demands effectively.

To monitor changes in the building's dynamic properties, white noise excitations were performed before and after each ground motion test. These tests provided critical insights into variations in the structure's stiffness and damping characteristics over time. Detailed inspections were conducted between tests to identify and document any structural or non-structural damage, offering valuable feedback on the UFP system's performance under varying seismic demands.

6.3 Comparison of Testing Protocols

The NHERI TallWood and Converging Design Projects share several testing methodologies, including the use of ground motions scaled to hazard levels, white noise excitations to track structural properties, and meticulous inspections between tests. However, the Converging Design Project, particularly in Phase 1, introduced focused evaluations of innovative lateral systems like UFPs, emphasizing multi-objective optimization. While the TallWood Project explored a single lateral system across its tests, the Converging Design Project's investigated additional energy dissipation devices. Both projects achieved high PGA inputs during MCER tests, with TallWood reaching 0.76 g and Converging Design achieving 0.79 g, demonstrating the robustness of mass timber systems under extreme ground motions.

6.4 Data Processing

This section will provide an overview of how the raw data achieved from all the instruments were processed to provide useful engineering demand and other quantities.

6.4.1 Data Processing of Accelerometers

The data acquired from the accelerometers during the shake table tests underwent a comprehensive processing protocol to ensure the accuracy and reliability of the results. The initial step involved baseline

correction, which was employed to eliminate low-frequency drift and offsets in the raw acceleration signals, ensuring that the data reflected only the dynamic response of the structure during seismic events. To mitigate artifacts caused by abrupt transitions at the start and end of the signal, a half-cosine tapering function was applied to the first and last one second of the acceleration data, thereby smoothing the edges and minimizing noise interference. Subsequently, zero-padding was introduced to enhance the frequency resolution of the data. This process involved extending the signal length by appending zeros, typically at 20 times the sampling frequency, thereby facilitating better filtering and spectral analysis.

The processed acceleration data were then subjected to a 4th order bandpass Butterworth filter with cutoff frequencies of 0.1 Hz and 50 Hz. This filtering step effectively removed low-frequency noise, such as environmental disturbances, and high-frequency noise, including sensor artifacts, retaining only the frequencies pertinent to the building's seismic response. Following filtering, the acceleration data were integrated using the 4th order Runge-Kutta method to compute velocity, providing insights into the rate of structural movement during seismic excitation. The velocity data were subsequently baseline-corrected to remove residual drift and offsets, ensuring that the signal accurately represented the structure's dynamic behavior.

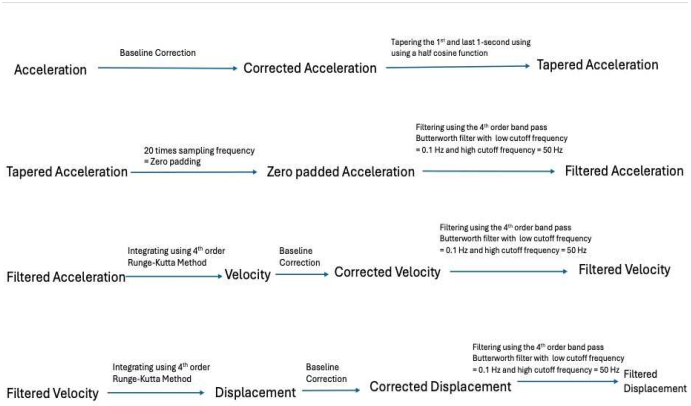

Figure 46: Data Processing Methodology

The velocity data were then integrated a second time using the Runge-Kutta method to calculate displacement, a critical metric for assessing structural deformation under seismic loading. As with the acceleration and velocity data, a baseline correction was applied to the displacement signal to eliminate any

offsets, ensuring that the processed displacement started and ended at zero. The displacement data were further filtered using the same 4th order bandpass Butterworth filter to remove any residual noise, yielding a clean and reliable signal. Throughout the processing sequence, quality assurance measures were implemented, including cross-referencing the processed accelerometer data with other measurement devices, such as string potentiometers and strain gauges, to validate consistency and accuracy. This rigorous data processing protocol ensured that the final acceleration, velocity, and displacement data accurately reflected the dynamic response of the structure, providing a robust basis for analyzing its seismic performance and resilience.

6.4.2 Data Processing of String Potentiometers

The data obtained from the string potentiometers, which were installed to measure interstory drifts and global displacements, underwent a systematic processing protocol to ensure accurate representation of the building's structural deformations during testing. The raw voltage signals recorded by the potentiometers were first converted to displacement values using calibration factors determined during pre-test setups. Since string potentiometers are prone to noise, especially at high frequencies, the displacement data was filtered using a 4th order low-pass Butterworth filter with a carefully chosen cutoff frequency to remove extraneous noise while retaining the essential dynamic response of the structure. The baseline correction was applied to eliminate any offsets caused by sensor drift or initial misalignment, ensuring that the displacement data accurately started and ended at zero when the structure returned to its initial position. Further adjustments were made for any non-linearities in the potentiometer readings, typically by applying a polynomial correction based on the calibration data. The processed displacement data was then smoothed to reduce any abrupt fluctuations caused by minor inconsistencies in the potentiometer readings. The final displacement signals provided a clear representation of interstory and global deformations, critical for assessing the structure's drift and torsional responses under seismic loading.

6.4.3 Data Processing of Linear Potentiometers

Linear potentiometers, used for measuring localized displacements in key structural components, such as wall-panel connections and energy dissipation devices, required a similar yet distinct data processing approach. The raw voltage readings from the potentiometers were converted to displacement values using calibration coefficients determined during the pre-test setup. Baseline correction was applied to remove any offsets introduced by the initial positioning of the potentiometers. Given their sensitivity to high-frequency noise, the displacement data was filtered using a 4th order low-pass Butterworth filter, ensuring the elimination of irrelevant noise while preserving the dynamic response of the components under study. Non-linearities in the potentiometer output, often caused by slight misalignments during installation, were corrected using calibration data and polynomial fitting techniques. After processing, the displacement data was smoothed to reduce abrupt variations and provide a consistent time history of movement. These refined signals were critical for evaluating localized behaviors, such as joint rotations, sliding, and deformation of energy dissipation devices, under seismic excitation.

Chapter 7 Results

This chapter presents the results obtained from the shake table tests, focusing on some comparisons of the seismic response of the NHERI TallWood and NHERI Converging Design projects. The data was processed using the instrumentation techniques described earlier, and the outcomes were analyzed to evaluate key parameters, including accelerations, displacements, inter-story drift ratios, and base shear. Through a comparative analysis, the behavior of both buildings was examined under similar ground motions, although the tests featured slightly different PGA values.

The acceleration time histories and peak accelerations recorded at key points in both structures are analyzed to understand their dynamic behavior. These insights help illustrate how each building responds to seismic loads and the effectiveness of the lateral force-resisting systems in dissipating energy and maintaining stability. Absolute and relative displacements are also compared to assess the deformation patterns and re-centering capabilities of the two structures.

Inter-story drift ratios are evaluated to determine compliance with seismic performance criteria, highlighting the differences in flexibility and stiffness between the NHERI TallWood and NHERI Converging Design buildings. Furthermore, base shear forces are analyzed to understand the distribution of seismic loads and the role of the lateral systems in managing these forces.

This chapter aims to synthesize the test results and provide a comprehensive understanding of the seismic performance of mass timber structures, contributing to the broader goal of optimizing mass timber design for high- and mid-rise applications in seismic regions. The findings offer valuable insights into dynamic behavior, energy dissipation, and overall performance of these innovative systems.

7.1 Accelerations

7.1.1 NHERI TallWood Analysis

The acceleration time series of the NHERI TallWood structure under the Ferndale MCEr ground motion, shown in the Figure 47, illustrate the structure's dynamic response at three key levels: Floor 2, Floor 6 (Mid-height), and the Roof. The plots show acceleration data in both the X and Y directions for each of these levels.

At the second floor, located just above the shake table, the acceleration amplitudes remain relatively low, reflecting the minimal amplification near the base of the structure. This behavior is expected due to the direct transmission of ground motion to the lower stories, where structural deformation is limited and acceleration closely follows the input motion.

At mid-height (Floor 6), the acceleration amplitudes increase significantly compared to the input motion as one would expect. The accelerations at this level are amplified, which is a typical characteristic of tall, flexible buildings where mid-height floors are more susceptible to the effects of higher modes of vibration. The increased amplitude at Floor 6 demonstrates the participation of higher vibrational modes, amplifying the seismic response at this intermediate level.

At the roof level, the accelerations decrease in amplitude when compared to Floor 6. Although the roof still experiences noticeable accelerations, these are lower than those at the mid-height, which is typical of structures that exhibit higher-mode participation at intermediate levels. Overall, the acceleration profiles highlight the complex modal behavior of the NHERI TallWood structure under strong ground motion, particularly the presence of higher-modes.

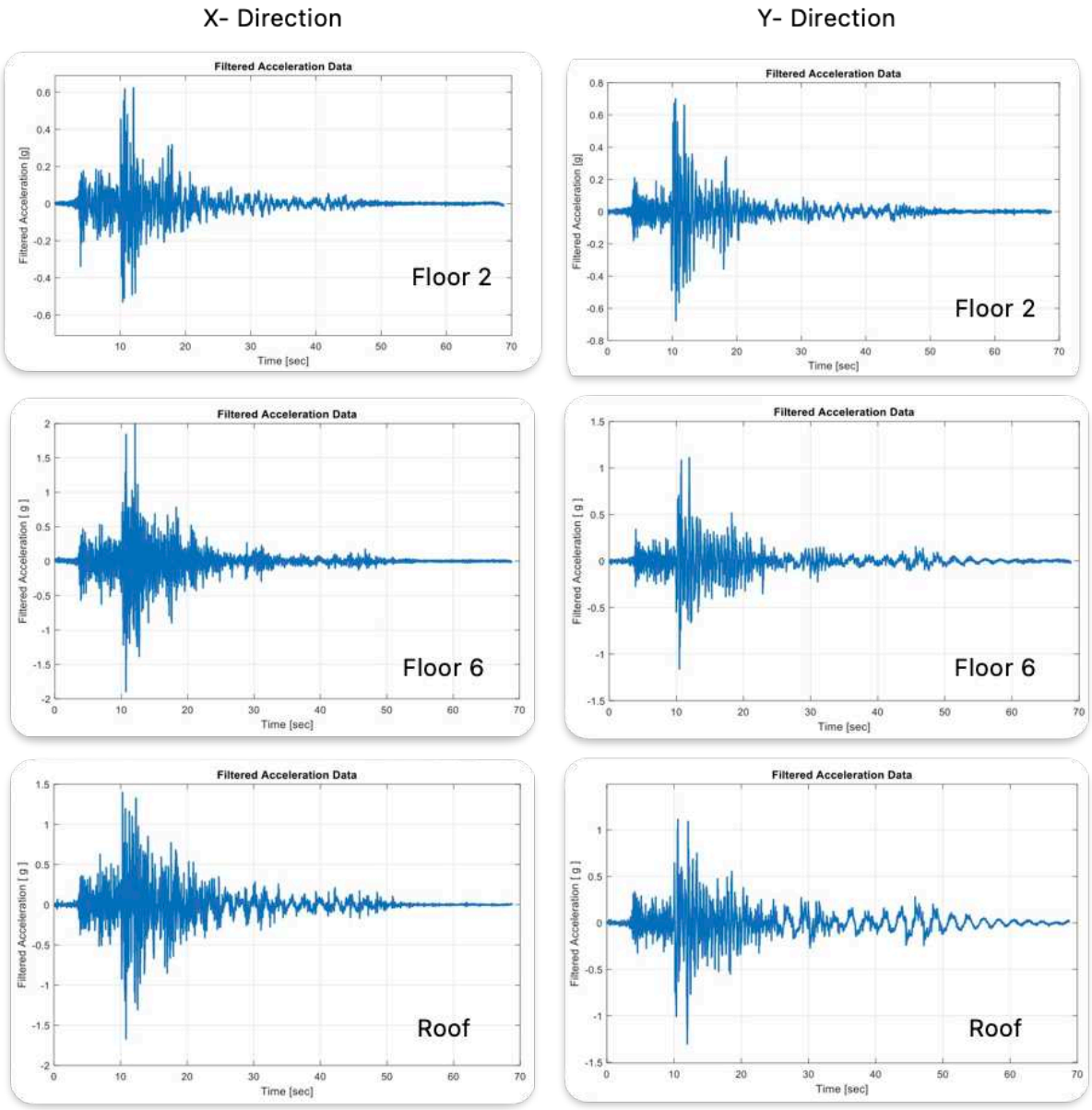

Figure 47: NHERI Tallwood Acceleration Time history at Various Levels.

7.1.2 NHERI Converging Design Analysis

The seismic response of the NHERI Converging Design structure under the same (note the scaling approach was different but very close motion) Ferndale MCEr ground motion was characterized by lower acceleration amplification and less higher-mode participation compared to the NHERI TallWood structure, as illustrated in Figure 48.

Now, consider both structures just above mid-level, i.e. sixth story for Tallwood, and now 4th story for Converging Design. At Level 4 the response demonstrates moderate dynamic amplification which less pronounced increase in amplitude compared to Tallwood structure. The frequency content remains relatively uniform, indicating limited excitation of higher vibration modes at these near mid-heights. The time history plots show smoother acceleration profiles and more consistent frequency content in both X and Y directions, indicating that the response remains largely governed by the fundamental mode. The absence of high-frequency components suggests that higher-mode excitation at this level is limited.

At the roof level, peak accelerations are observed, as expected in taller buildings during seismic events However, these peaks are notably lower than those seen in the NHERI TallWood structure, further confirming the first-mode dominated behavior and the reduced dynamic amplification in the Converging Design structure. The NHERI Converging Design structure also displays reduced directional variability in its response, with comparable acceleration amplitudes in both X and Y directions. This indicates a more uniform structural behavior under bidirectional ground motion excitation, again probably due to higher modes being more pronounced in Tallwood.

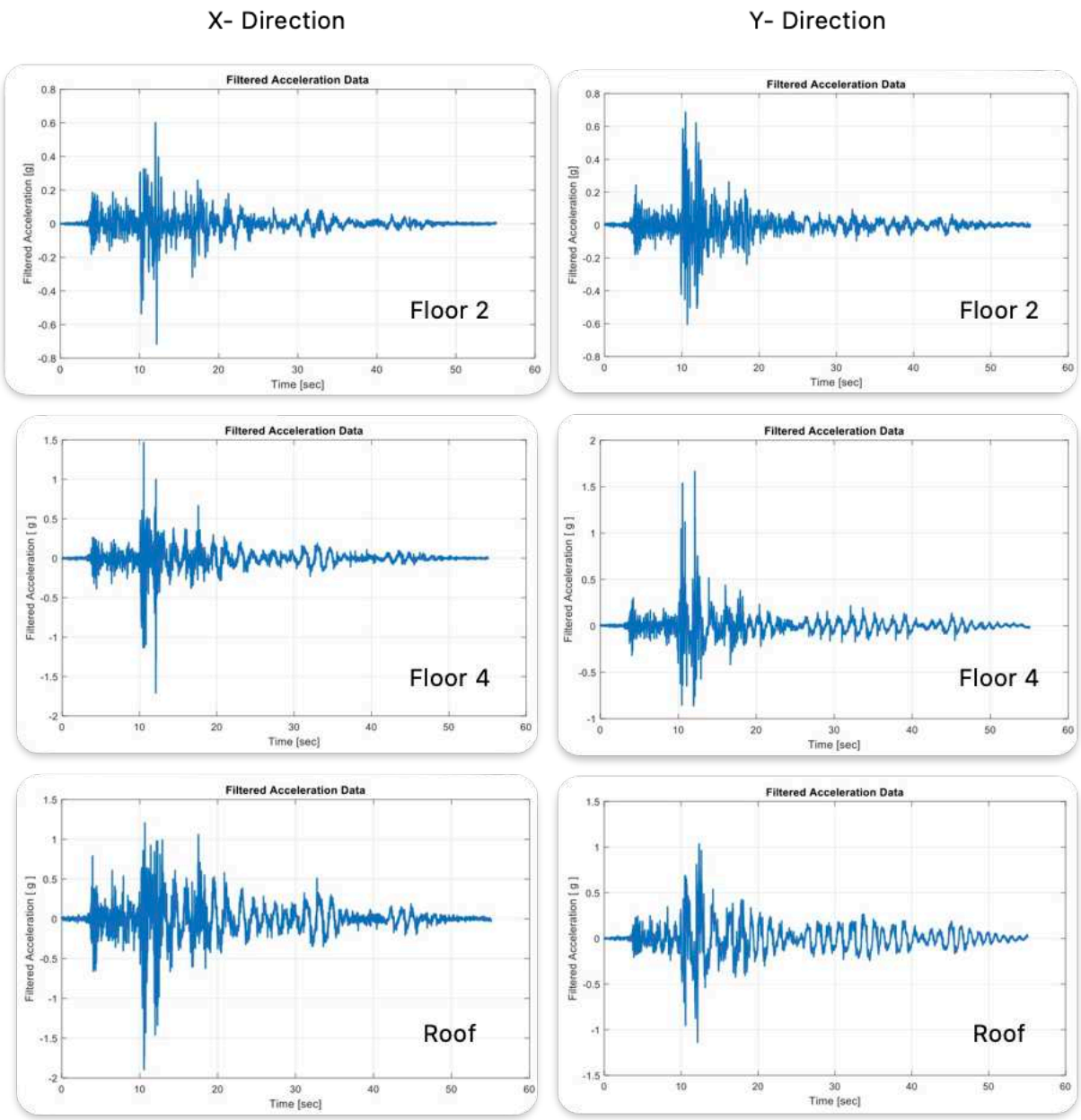

Figure 48: NHERI Converging Design Acceleration Time History at Various Levels

7.1.3 Comparison of NHERI TallWood and NHERI Converging Design

The seismic response of the NHERI Converging Design structure under the Ferndale MCEr ground motion exhibits key differences compared to the NHERI TallWood structure. While both buildings show dynamic amplification of accelerations from the base to the roof as expected, the Converging Design structure exhibits lower peak accelerations at the roof level, especially in the Y direction. Additionally, the frequency

content of the Converging Design remains relatively uniform across different elevations, indicative of a potentially stiffer structural system in contrast to the TallWood structure. These are not unexpected behaviors given the differences in height and therefore period of vibration, but nonetheless quantified herein.

On the other hand, the NHERI TallWood structure shows greater amplification of accelerations at mid-height, with a richer frequency spectrum observed at both mid-height and roof levels. This reflects the presence of higher-mode effects, indicating that the TallWood structure excited higher modes, as one would expect due to its increased height and stories compared to Converging Design. Some of these differences may have been influenced by design strategy but more likely the structural configurations, i.e. 10 versus six stories.

7.2 Displacement

7.2.1 NHERI TallWood: Displacement Analysis

Figure 49 shows the displacement time histories at Floor 2, Floor 7, and the roof level of the NHERI Tallwood structure under the Ferndale MCEr ground motion. Displacement refers to the lateral displacement of each floor level with respect to the moving shake table base. This measure isolates the building's deformation from the imposed ground motion.

At the second floor (first story above the shake table), displacement amplitudes in both the X and Y directions remain relatively small. The recorded peak relative displacements are approximately ±0.79 inches in the X direction and ±1.2 inches in the Y direction. The slightly larger response in the Y direction may reflect a combination of directional flexibility and the ground motion record in that direction.

At mid-height (Floor 7), the displacement amplitudes increase, with peak values reaching approximately ±6 inches in the X direction and ±5.7 inches in the Y direction. The time histories at this elevation indicate a more complex dynamic response characterized by both amplitude and frequency variation. This behavior suggests contributions from both the fundamental mode and higher vibration modes. The multi-modal interaction is especially evident in the Y direction, where displacements are larger and exhibit prolonged motion following the peak shaking.

At the roof level, the TallWood structure experiences the largest relative displacements, reaching approximately ±10.2 inches in the X direction and ±11 inches in the Y direction. The response is initially dominated by the first mode, as indicated by the smooth and large-amplitude motion, but transitions into a more irregular pattern with visible higher-frequency oscillations in the middle of the record. Minimal residual displacements following the ground motion suggest effective re-centering capability of the rocking wall system.

X-Direction Y- Direction

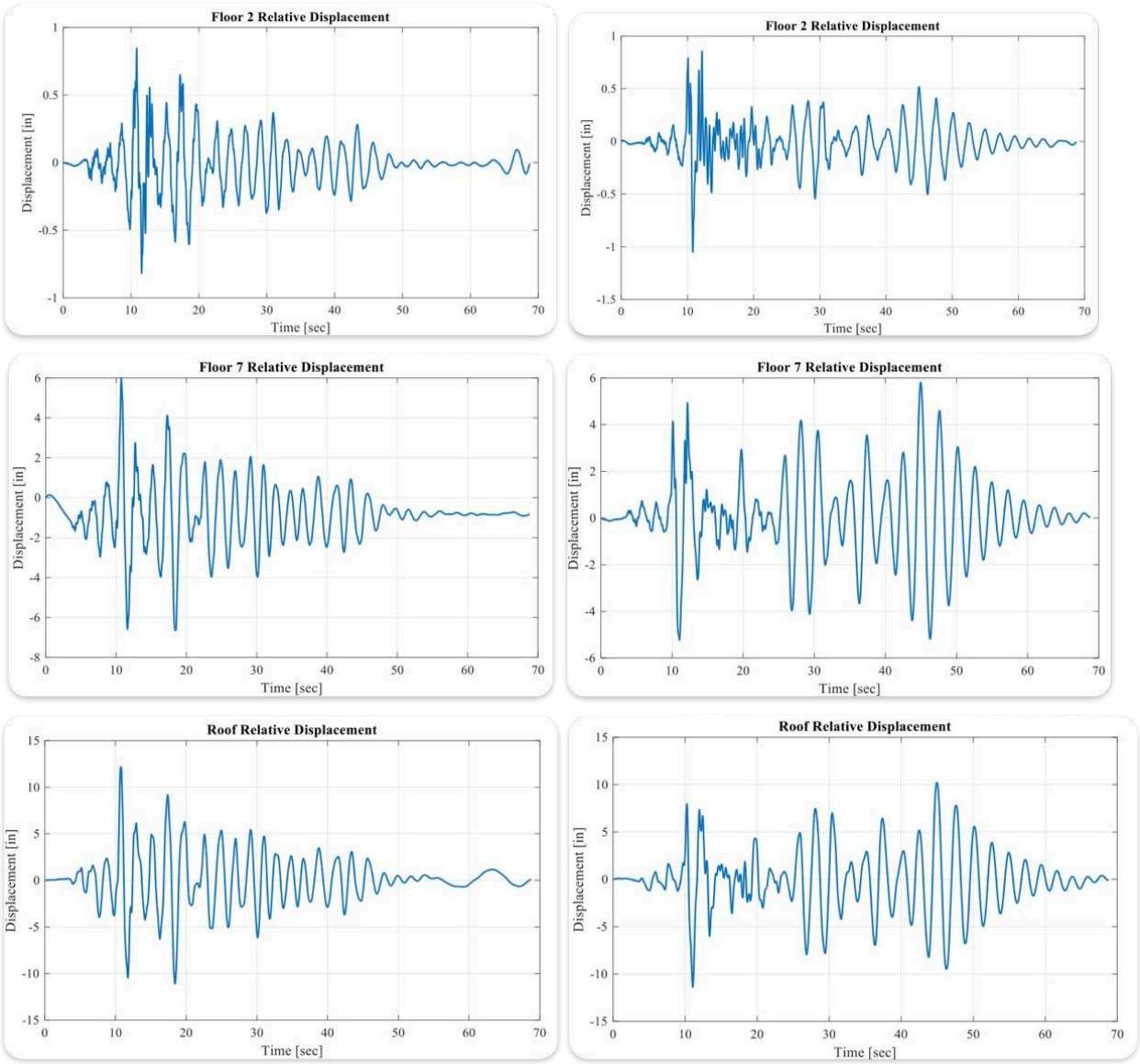

Figure 49: NHERI Tallwood Displacement at Various Floor Levels

7.2.2 NHERI Converging Design Displacement Analysis

Figure 50 illustrates the relative displacement time histories at the Floor 2, mid-height (Level 4), and Roof levels of the NHERI Converging Design structure subjected to the Ferndale MCEr ground motion. Relative displacement refers to the lateral motion of each floor with respect to the moving base.

At the second floor (first story above the foundation), the lateral displacements are less then 2% limit, with peak amplitudes reaching approximately ±1.2 inches in the X direction and ±1.7 inches in the Y direction. The slightly larger response in the Y direction may reflect a combination of directional flexibility and the ground motion record in that direction.

At mid-height which is level 4, the displacements increase to approximately ±4.8 inches (X) and ±6.0 inches (Y). The displacement time histories here exhibit a smoother, lower-frequency response, dominated by the fundamental mode. Minor deviations in displacement response indicate the presence of higher-mode contributions, particularly in the Y direction.

At the roof level, the peak displacements grow significantly to approximately ±9 inches in the X direction and ±12.5 inches in the Y direction. These time histories display the largest amplitudes. While the overall response is consistent with a dominant first-mode behavior, the presence of high-frequency content especially later in the time series reflects higher-mode participation. This is particularly notable in the Y direction.

The observed increase in displacement amplitude with height, along with some lower frequency content, underscores the importance of capturing higher-mode effects in performance-based seismic design. The NHERI Converging Design structure exhibits some multi-modal dynamic response under strong ground motion.

X- Direction Y- Direction

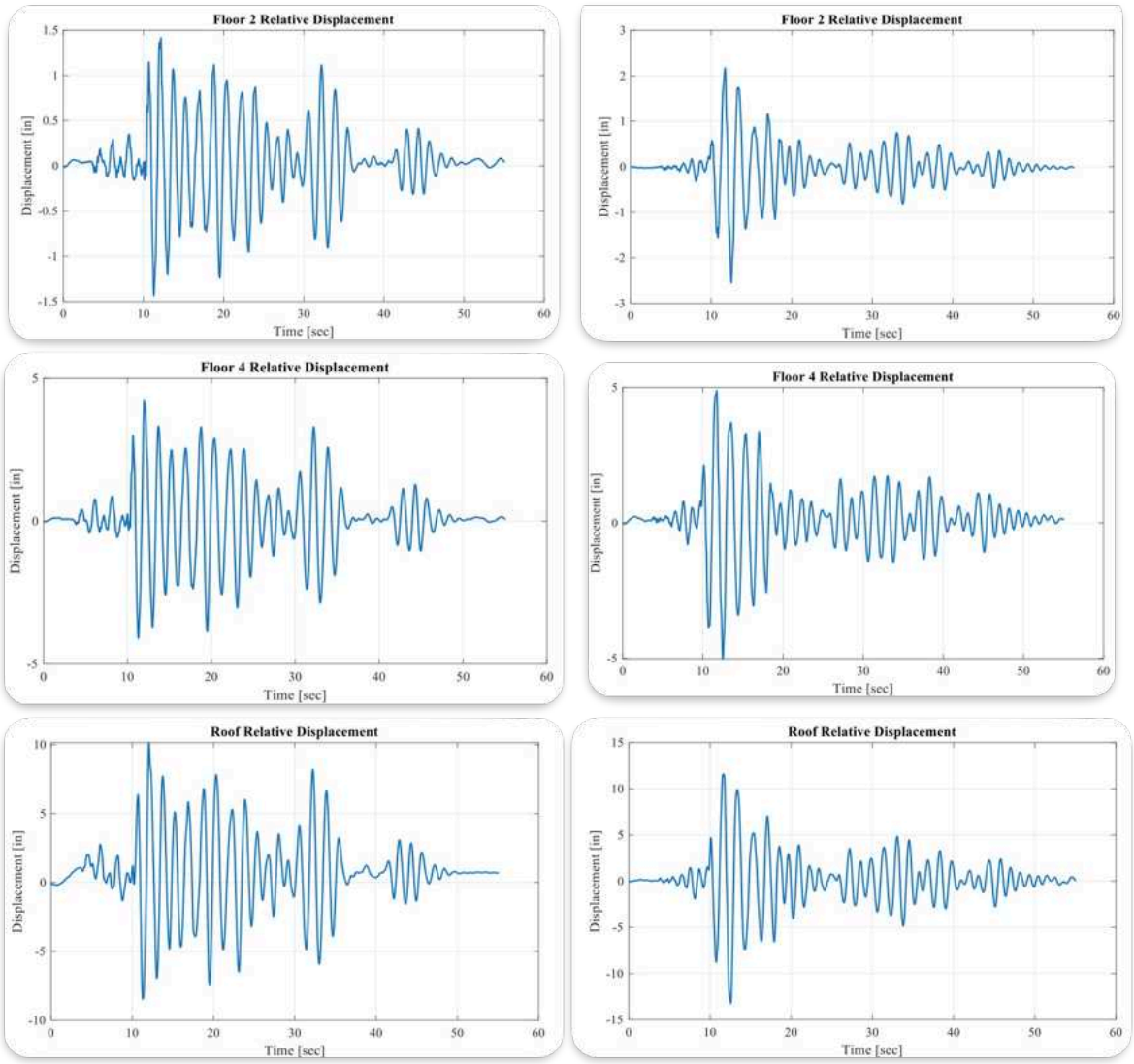

Figure 50: NHERI Converging Design Displacement at Various Floor Levels

7.2.3 Comparison of NHERI TallWood and NHERI Converging Design

The displacement data for both the NHERI TallWood and NHERI Converging Design structures under the Ferndale MCEr ground motion show notable differences in their dynamic responses because of their different heights, story counts, and dynamic properties. At the second floor (first story above the foundation), both structures show displacements below about 2%. The Converging Design structure

exhibits slightly larger peak relative displacements approximately ±1.2 inches in X and ±1.7 inches in Y compared to ±0.76 inches in X and ±1.2 inches in Y for TallWood.

At mid-height (level 6), the TallWood structure displays significant displacement amplification, with peak values reaching ±6 inches (X) and ±5.7 inches (Y).

While at the mid height (level 4), the Converging Design structure shows peak displacements of approximately ±4.8 inches (X) and ±6.0 inches (Y). The displacement time series in Converging Design appear to indicate the dominant role of the fundamental mode. While the term 'mid-height' is used here to characterize the response at central elevations, it is important to note that the absolute position and modal behavior associated with this level differ between the two buildings. Given their different total heights, story counts, and dynamic properties, direct comparison at mid-height should be interpreted with caution.

At the roof level, the two buildings show differing dynamic characteristics. The TallWood structure reaches peak roof displacements of ±10.2 inches (X) and ±11.0 inches (Y), while the Converging Design structure records higher amplitudes of approximately ±9.0 inches (X) and ±12.5 inches (Y). While both structures exhibit dominant first-mode behavior at the roof, the TallWood building shows additional higher-mode contributions, evident from displacement time series complexity and mid-height amplification and the Converging Design structure exhibits a stronger first-mode-dominated response with roof-level displacement.

Overall, this comparative behavior seeks to highlight some of the influence of system height, stiffness distribution, and dynamic characteristics. TallWood, being taller and more flexible, exhibits notable mid-height amplification due to higher-mode effects, whereas the Converging Design structure demonstrates a more concentrated roof-level response aligned with first-mode dominance.

7.3 Displacement Profile and Inter Story Drift

7.3.1 NHERI Tallwood X and Y Direction

Relative Displacement Profiles

The upper portion of Figure 51 presents the relative displacement (with respect to Floor 1) across all floors at selected points in time. These profiles capture the instantaneous deformation shape of the structure during dynamic response and help visualize the modes.

In the X direction Figure 51 A, the early profile at T = 12.73 s (blue) exhibits a near-linear increase in displacement with height, indicative of a first-mode dominated response. However, subsequent profiles (T = 10.37 s, 12.32 s, 14.78 s) reveal distinct inflection points, particularly around Floor 6–7, where curvature changes direction. This curvature reversal signals the onset of second-mode excitation, which causes displacement concentration and localized deformation at mid-height.

In the Y direction Figure 51 C, similar mode transitions are observed. The early time profile (T = 10.51 s, orange) again follows a smooth, upward-increasing pattern, consistent with first-mode behavior. However, profiles at T = 10.58 s, 12.87 s, and 13.05 s show pronounced deformation around Floor 6, with the purple profile (13.05 s) exhibiting an S-shape a strong indicator of higher-mode participation.

Interstory Drift Time Histories

The bottom plots in Figure 51B and 51 D show the interstory drift time history at Floor 6, which emerges as a critical story in both X and Y directions based on the displacement profiles.

In the X direction Figure 51 C, the Floor 6 interstory drift peaks shortly after 10 seconds, reaching up to 1.4%. This aligns with the time instants where displacement curvature is most pronounced near Floor 6, suggesting a strong correlation between mode shape distortion and localized drift demand.

In the Y direction Figure 51 D, the interstory drift response of Floor 6 follows a similar pattern, with significant peak drift amplitudes occurring between 10–20 seconds. Notably, this period also corresponds to when mode transitions are observed in the Y-direction displacement profiles.

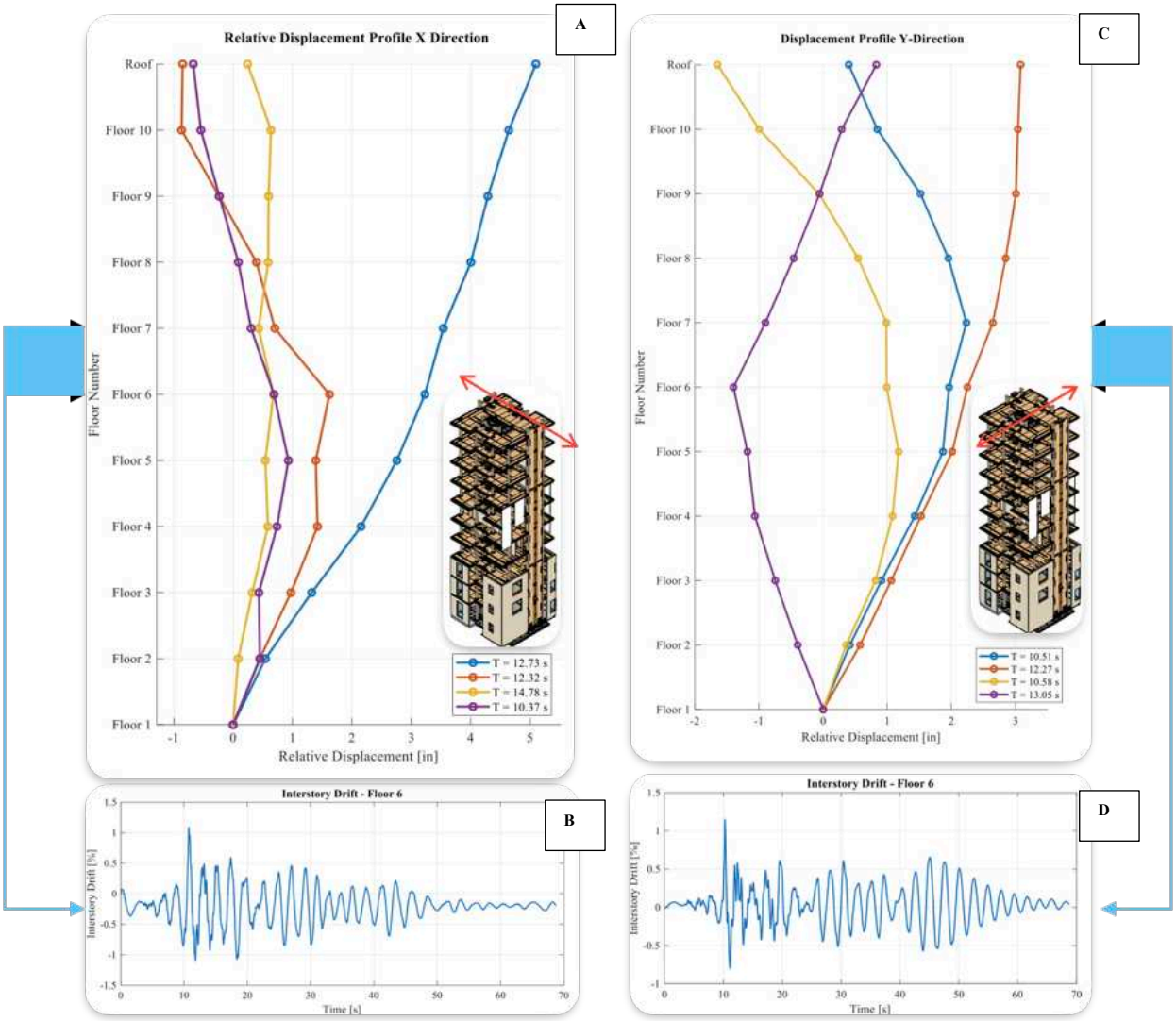

Figure 51: NHERI Tallwood Displacement Profile at various Time and IDR Time Series

7.3.2 NHERI Converging Design X and Y Direction

Figure 52 presents a comprehensive comparison of the relative displacement profiles and interstory drift histories in the X and Y directions for the six-story mass timber structure. The plots illustrate key time instants during the seismic excitation where modal behavior and local deformation demands are most prominent.

Relative Displacement Profiles

Figure 52 A and Figure 52 C illustrates the relative displacement profiles at selected time instants. These profiles capture the instantaneous deformation shape of the structure during dynamic response and help visualize the modal contributions.

In the X-direction Figure 52 A, the displacement profile at T = 18.35 s (blue curve) demonstrates a classic first-mode dominated behavior, with a smooth, monotonic increase in displacement from the base to the roof. In contrast, the profiles at T = 30.05 s, 39.58 s, and 46.43 s (orange, purple, and yellow curves) show distinct inflection points near Floor 4, suggesting participation of higher vibration modes. The S-shaped deformation around mid-height is indicative of second-mode activation, leading to a localized increase in curvature and potential concentration of drift demand.

In the Y-direction Figure 52 C, a similar evolution is observed. The profile at T = 9.97 s again reflects a dominant first-mode shape, while the later time instants (T = 12.96 s, 19.47 s, and 54.48 s) exhibit noticeable flattening or reversal in curvature near Floor 6, signifying that the seismic response involves higher-mode contributions in the Y direction as well.

These instantaneous mode shapes confirm that the building exhibits a multi-modal response under tri-axial ground motion input, with local amplification of deformation at different story levels depending on the direction and time of excitation.

Interstory Drift Time Histories

The bottom plots in Figure 52 B and Figure 52 D display the interstory drift time histories for Floor 4 (X direction) and Floor 6 (Y direction), which are the critical stories identified from the displacement profiles.

For Floor 4 Figure 52 B, the interstory drift reaches peak amplitudes of up to 1.4% between 10–20 seconds, aligning well with the time instants where higher-mode inflection was observed in the displacement

profiles. The early onset of high-frequency oscillations followed by decay suggests transient higher-mode excitation and subsequent damping.

Similarly, the Floor 6 drift in the Y-direction Figure 52 D peaks slightly after 10 seconds, also exceeding 1.8%, indicating significant local deformation demand. This matches the displacement behavior at the top-right of the figure, where several time instants exhibit substantial curvature at Floor 6.

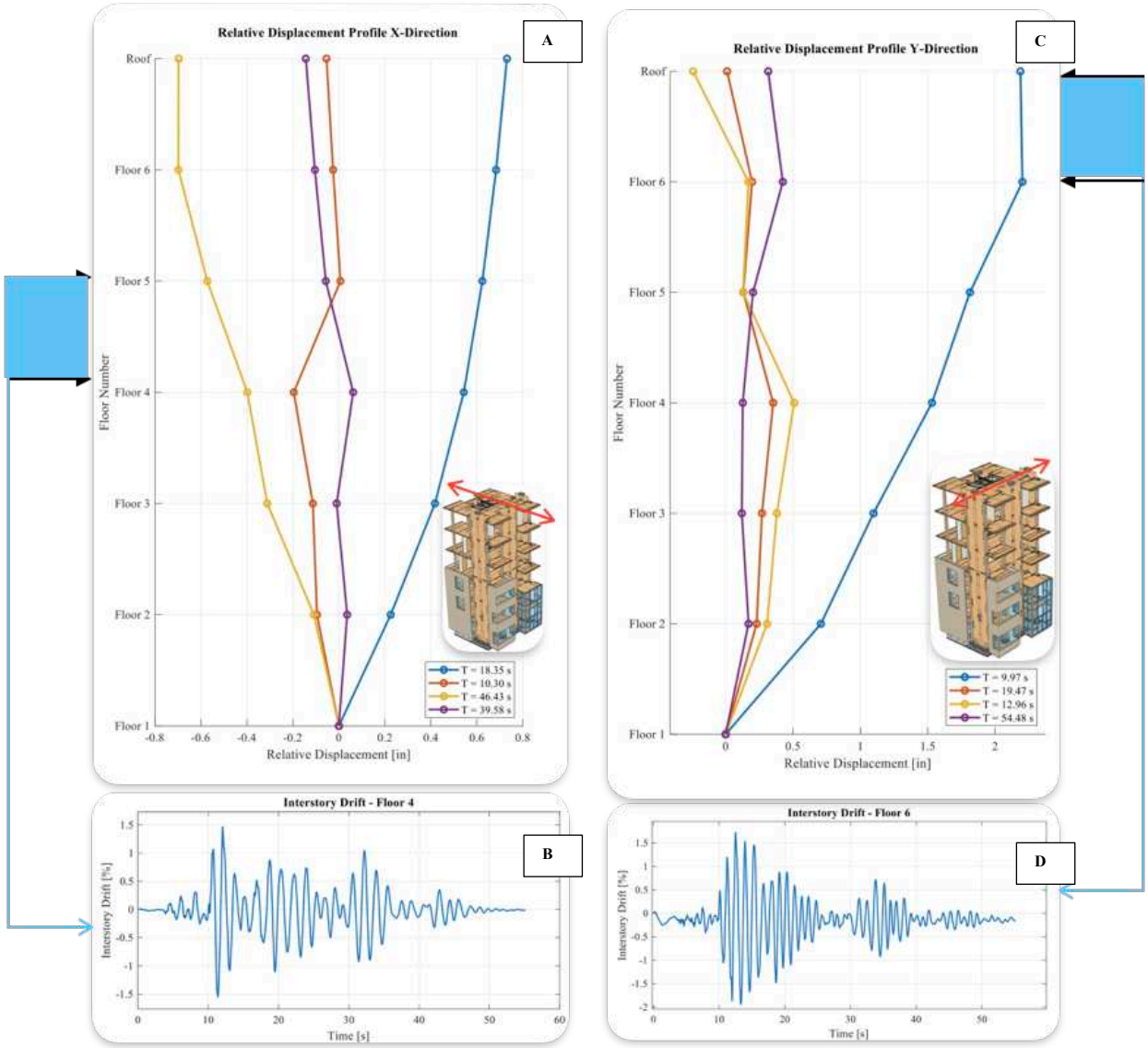

Figure 52: NHERI Converging Design Displacement Profile at various Time and IDR Time Series

7.4 Base Shear

7.4.1 NHERI TallWood: Base Shear Analysis (X Direction)

The base shear response of the NHERI TallWood structure in the X direction under the Ferndale MCEr ground motion reveals pronounced dynamic behavior, characterized by large amplitude variations during the initial phase of the seismic excitation. The NHERI Tallwood had the seismic weight of approximately 611 kips, based on the distributed floor mass. As illustrated on the Figure 51, during the first 10 seconds, which corresponds to the most intense phase of the ground motion, the base shear reaches a peak amplitude of approximately ±170 kips. This indicates the significant inertial forces transmitted to the base of the structure due to the interaction of the ground motion with the building's dynamic properties. When normalized by the total seismic weight, the peak base shear corresponds to a Normalized Base Shear (NBS) of approximately 27.2 %, indicating that more than one quarter of the building's weight was resisted at the base as lateral seismic force during peak shaking.

As the test progressed beyond 10 seconds, the amplitude of the base shear begins to diminish, reflecting the structure's dynamic response to the decaying input motion. Between 10 and 20 seconds, secondary peaks are observed, likely influenced by the excitation of higher vibration modes. Beyond 20 seconds, the response has a gradual decay in amplitude, with smaller fluctuations persisting until approximately 50 seconds. This behavior suggests effective energy dissipation mechanisms, such as material damping and structural deformation, which help reduce the inertial forces over time. The periodic nature of the base shear indicates the dominant influence of the structure's fundamental vibration mode, although higher modes

contribute to the transient response during the initial phases of shaking, and then less so after about 20 seconds.

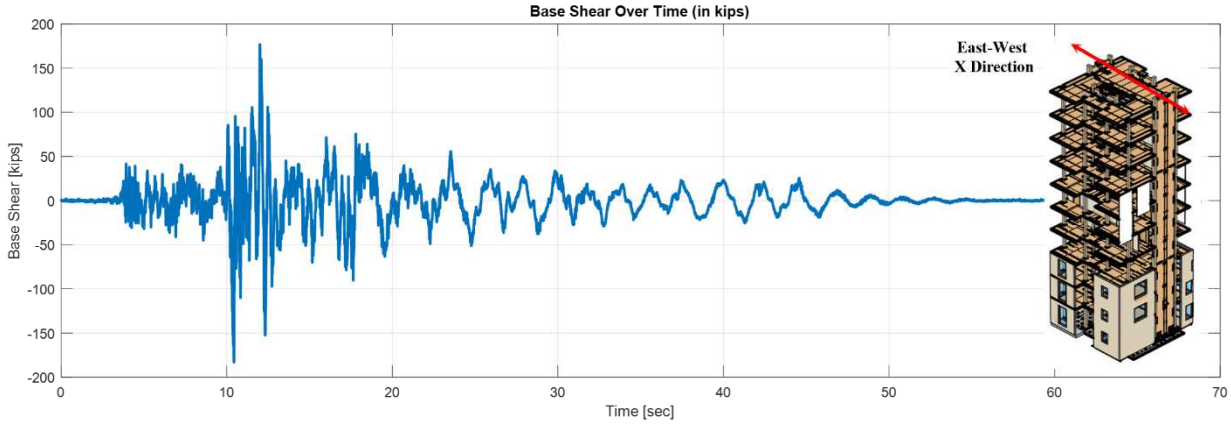

Figure 53: NHERI Tallwood Base Shear X Direction

7.4.2 NHERI TallWood: Base Shear Analysis (Y Direction)

The base shear response of the NHERI TallWood structure in the Y direction under the Ferndale MCEr ground motion exhibits significant dynamic activity, with a more pronounced amplitude compared to the X direction. The NHERI Tallwood had the seismic weight of approximately 611 kips, based on the distributed floor mass. As illustrated in Figure 52, during the initial 10 seconds, which corresponds to the most intense phase of the seismic input, the base shear reaches a peak amplitude of approximately ±210 kips. When normalized by the total seismic weight, the peak base shear corresponds to a Normalized Base Shear (NBS) of approximately 34.4 %, indicating that more than one quarter of the building's weight was resisted at the base as lateral seismic force during peak shaking. The spectral acceleration in Y direction reaches approximately 0.43g compared to 0.36g in X direction which likely resulted in the higher peak base shear recorded in Y direction (see Figure 6).

As the test progressed beyond 10 seconds, the amplitude of the base shear reduced in magnitude but continued to exhibit time-varying response, reflecting the decaying ground motion and the dynamic

interaction with the structural system. Between 10 and 20 seconds, secondary peaks are observed, which are slightly more prominent than in the X direction indicating greater excitation of higher vibration modes. After 20 seconds, the base shear response continues to diminish steadily. By approximately 50 seconds, the base shear flattens out into smaller variations, suggesting effective energy dissipation and the structure's capacity to reduce force demands over time. The response pattern reflects dominance of the structure's fundamental mode, with additional contributions from higher modes during earlier phases of the motion.

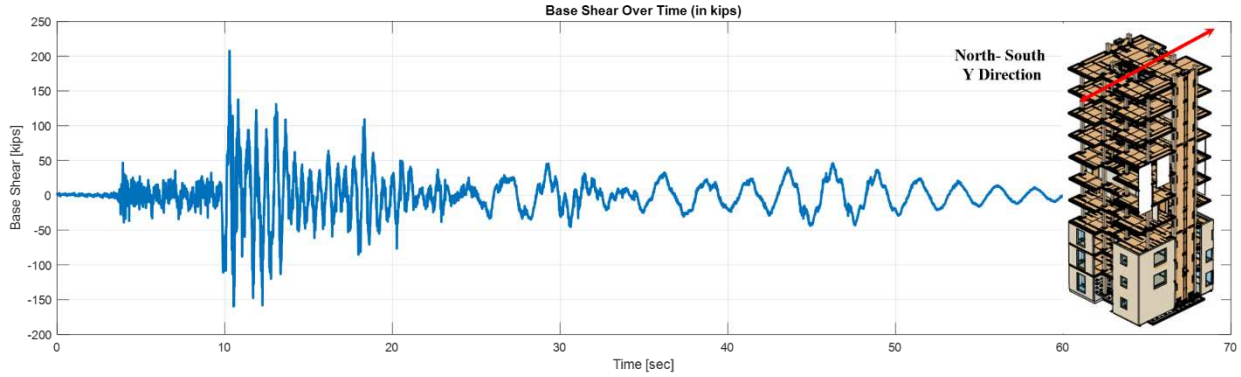

Figure 54: NHERI Tallwood Base Shear Y Direction

7.4.3 NHERI Converging Design: Base Shear Analysis (X Direction)

The base shear response of the NHERI Converging Design structure in the X direction under the Ferndale MCEr ground motion exhibits significant dynamic activity, with prominent peaks during the initial phase of the seismic event. The NHERI Converging Design had a seismic weight of approximately 328 kips, based on the distributed floor mass. As illustrated in Figure 53, during the first 10 seconds, the base shear reaches a peak amplitude of approximately ±137 kips, reflecting the inertial forces generated as the seismic energy interacts with the structure's mass and stiffness. This phase corresponds to the most intense portion of the ground motion, where the structure experiences the greatest lateral force demands. When normalized by the total seismic weight, the peak base shear corresponds to a Normalized Base Shear (NBS) of approximately 41.7%, indicating that nearly half of the building's weight was resisted at the base as lateral seismic force during peak shaking.

Beyond the initial phase of strong seismic input, the base shear amplitude decreases but remains dynamic, characterized by transient force variations governed by the structure's modal behavior. Between 10 and 20 seconds, distinct secondary peaks are evident, likely resulting from the activation of higher vibration modes. After 20 seconds, the amplitude of the base shear response gradually attenuates, reflecting effective energy dissipation through damping and inelastic deformation. These variations in base shear highlight the influence of both the fundamental and higher-mode responses, which contribute to the overall seismic performance of the structure.

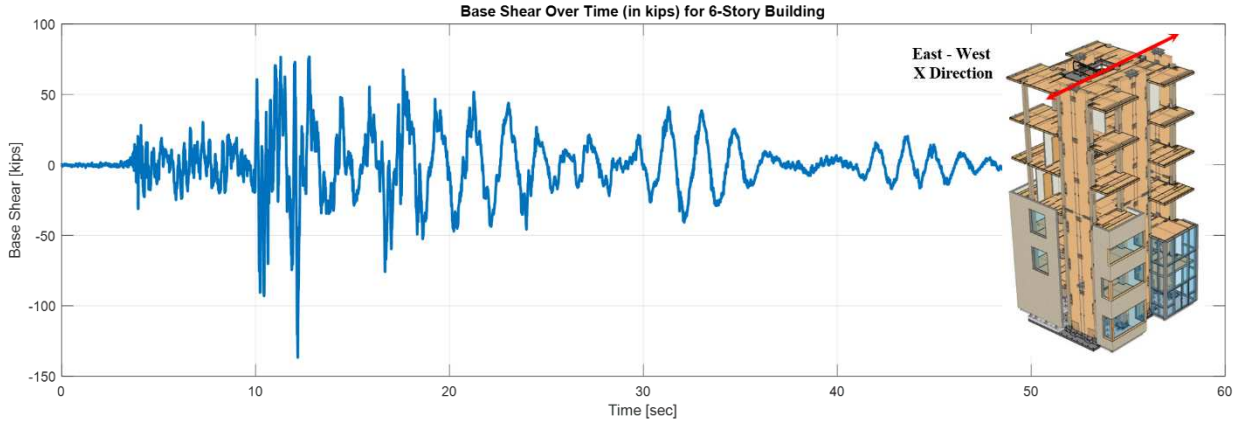

Figure 55: NHERI Converging Design Base Shear X Direction

7.4.4 NHERI Converging Design: Base Shear Analysis (Y Direction)

The base shear response of the NHERI Converging Design structure in the Y direction under the Ferndale MCEr ground motion displays similar trends to the X direction but with slightly higher peak values. The NHERI Converging Design had a seismic weight of approximately 328 kips, based on the distributed floor mass. As illustrated on Figure 54, during the initial 10 seconds, the base shear reaches peak amplitudes of approximately ±160 kips, reflecting a higher force demand in the Y direction. This increased amplitude may indicate directional differences in the structure's stiffness or variations in the ground motion intensity along the Y axis. When normalized by the total seismic weight, the peak base shear corresponds to a Normalized Base Shear (NBS) of approximately 48.7%, indicating that nearly half of the building's weight

was resisted at the base as lateral force during peak shaking. The spectral acceleration in Y direction reaches approximately 0.43g compared to 0.36g in X direction which likely resulted in the higher peak base shear recorded in Y direction (see Figure 6).

As the seismic event progresses, the base shear exhibits a gradual reduction in amplitude but remains oscillatory. Between 10 and 20 seconds, the secondary peaks are more pronounced than in the X direction, highlighting potential differences in the excitation of vibration modes. The response persisted beyond 20 seconds but demonstrates a longer response, which may be attributed to directional stiffness properties or lower damping level in this direction for some unknown reason.

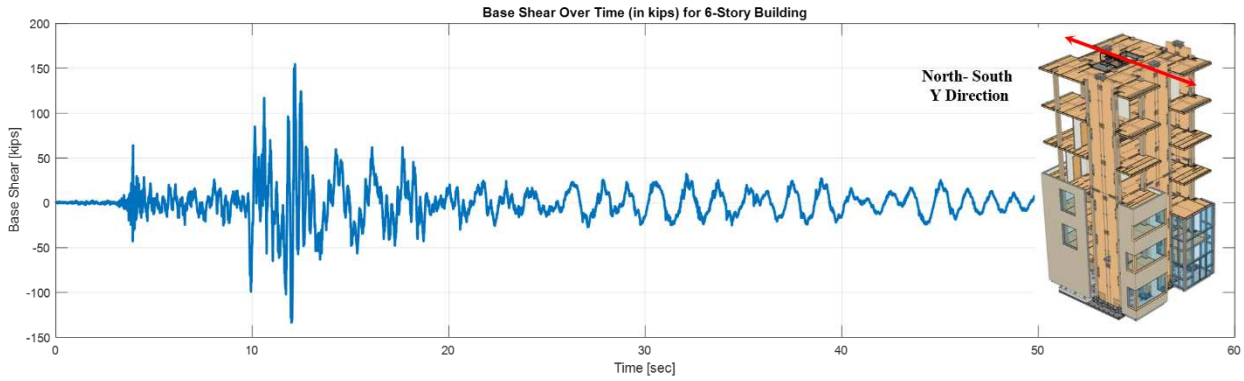

Figure 56: NHERI Converging Design Base Shear Y Direction

7.4.5 Comparison of Base Shear Responses: NHERI TallWood vs. NHERI Converging Design

The base shear responses of the NHERI TallWood and NHERI Converging Design structures under the Ferndale MCEr ground motion reveal notable differences in their dynamic behavior, highlighting the impact of structural height and potentially design strategy on seismic performance. In the X direction, both structures exhibit a peak base shear during the initial phase of the ground motion, but the NHERI TallWood structure reaches a lower peak of approximately ±170 kips, corresponding to a Normalized Base Shear (NBS) of 27.8%, while the Converging Design structure experiences a higher peak of approximately ±137 kips with an NBS of 41.7%. This suggests that the Converging Design attracted a greater proportion of its

weight as base shear, potentially due to its stiffer configuration and more efficient force transmission, while the taller and more flexible TallWood structure distributed lateral forces more gradually.

In the Y direction, both structures again show higher base shear responses than in the X direction. The NHERI TallWood records a peak base shear of approximately ±210 kips, yielding an NBS of 34.4%, whereas the Converging Design reaches a peak of approximately ±160 kips, resulting in an NBS of 48.7%. This trend underscores the higher lateral force demands in the Y direction, which may be attributed to elevated spectral acceleration (Sa) in that axis, as seen in Figure 6, and to differences in structural stiffness. The Converging Design shows a more concentrated and efficient dynamic response with quicker attenuation, while the TallWood structure displays prolonged oscillations and greater influence from higher vibration modes, particularly in the Y direction.

7.5 Comparison of Periods: NHERI TallWood vs. NHERI Converging Design

The period comparison between the NHERI TallWood and NHERI Converging Design structures highlights significant differences in their dynamic properties. The NHERI TallWood structure exhibits longer natural periods in both directions, with 1.95 seconds in the X direction and 2.03 seconds in the Y direction. These longer periods are indicative of a more flexible structural system, which results in greater dynamic amplification at higher elevations during seismic excitation. The small difference between the X and Y periods suggests that the structural stiffness is relatively similar in both directions, leading to a balanced response under bidirectional ground motion.

In contrast, the NHERI Converging Design structure demonstrates shorter natural periods, with 1.08 seconds in the X direction and 1.34 seconds in the Y direction. These shorter periods reflect a stiffer structural system, which is designed to minimize lateral deformations and reduce resonance effects. The greater difference between the periods in the two directions indicates that the structure may have varying stiffness characteristics, possibly due to different lateral force-resisting systems or material configurations

along the two axes. As a result, the Converging Design structure is less susceptible to dynamic amplification but experiences higher base shear forces due to its stiffer response.

In addition to observed periods, a comparison with the empirical period estimation from ASCE 7-16 was made. ASCE 7-16 specifies the fundamental period T of timber buildings using the equation

$$T = C_t H_n^x$$

where T is the fundamental period, H_n is the building height, and C_t and x are coefficients dependent on the lateral system. For timber buildings, Ct is specified as 0.028 and x as 0.8. Using this approach, the estimated periods for the NHERI TallWood and NHERI Converging Design structures were 1.04 seconds and 0.78 seconds, respectively substantially lower than the experimentally observed values. This highlights a notable discrepancy between code-based estimations and the actual dynamic response of mass timber rocking wall systems.

These differences in periods correlate strongly with the displacement and acceleration responses observed in both structures. In the X direction, the NHERI TallWood structure's longer periods lead to slightly larger roof displacements and more pronounced higher-mode amplification effects, especially at mid-height levels. The Converging Design structure, with its shorter periods, exhibits a more first-mode-dominated response with relatively controlled displacement profiles. In the Y direction, although the Converging Design structure experiences larger roof displacements, the overall acceleration response remains more regular due to its stiffer lateral system and limited higher-mode participation. These observations highlight how structural flexibility and modal characteristics influence seismic response across directions.

Chapter 8 Summary, Conclusions, and Contributions

This chapter presents summary of the NHERI TallWood and NHERI Converging Design Projects, focusing on the seismic performance of post-tensioned mass timber rocking walls. A comparative evaluation of the two test programs is discussed, highlighting differences in structural behavior, base shear response, drift characteristics, and period estimates. The chapter also assesses the discrepancies between the experimentally measured fundamental periods of mass timber structures and those estimated using ASCE 7-16 equations. Finally, the contributions of this research to seismic design methodologies for mass timber buildings are summarized.

8.1 Summary

The NHERI TallWood and NHERI Converging Design Projects provided a unique opportunity to evaluate the seismic response of mass timber structures at full scale. While both structures incorporated post-tensioned mass timber rocking walls as their lateral force-resisting system, they differed in height, stiffness, and in the detailing and configuration of their energy dissipation components, such as the placement and number of UFPs.

The NHERI TallWood structure was a ten-story building with a height of 34.1 meters, whereas the NHERI Converging Design structure was a six-story building with a height of 20.7 meters. Both buildings were subjected to unidirectional, bidirectional, and triaxial earthquake ground motions at varying hazard levels, ranging from service-level earthquakes to maximum considered earthquake (MCER) intensities. The experimental results demonstrated that structural stiffness and fundamental period characteristics significantly influenced seismic response with seismic performance being good for both.

One of the critical findings from this study, as discussed in Section 7.5, was the discrepancy between the measured fundamental periods of the mass timber buildings and those estimated using ASCE 7-16 guidelines. The code-based empirical formula notably underpredicted the periods for both structures,

indicating limitations in its applicability to mass timber rocking wall systems. This underestimation can lead to conservative seismic force calculations, as base shear is inversely related to period. Consequently, such overestimation of seismic demand may result in overly conservative structural designs and increased construction costs. These observations highlight the need for updated period estimation models that better reflect the dynamic characteristics of modern mass timber systems.

8.1.1 Base Shear Response

The comparison of base shear responses between the NHERI TallWood and NHERI Converging Design structures highlights the influence of structural stiffness and dynamic properties. While the NHERI Converging Design structure exhibited lower absolute base shear forces due to its smaller seismic mass, it demonstrated higher normalized base shear (NBS) compared to the taller NHERI TallWood structure. These observations suggest that taller mass timber buildings tend to experience lower NBS values as a result of period elongation but may still be subjected to higher absolute base shear demands. In contrast, midrise and stiffer configurations like the NHERI Converging Design structure facilitate more direct force transfer and reduced dynamic amplification, contributing to efficient energy dissipation and favorable seismic performance.

8.1.2 Drift Behavior and Period Elongation

The maximum inter-story drift ratios for both structures remained within acceptable limits, demonstrating the effectiveness of post-tensioned rocking walls in controlling lateral deformations. No residual drift was recorded after multiple MCER-level tests, validating the self-centering capability of the system.

However, period elongation was observed over successive tests, attributed to minor crushing at the wall-panel interfaces, softening of nonstructural components, and gradual degradation of connection stiffness. Despite these factors, the post-tensioned system maintained its ability to restore the structure to its original position after each seismic event.

8.2 Contributions to Seismic Design of Mass Timber Buildings

This research contributes to the advancement of seismic design for mass timber buildings by providing large-scale experimental validation of post-tensioned rocking wall systems. The key contributions include:

1. Empirical evidence that ASCE 7-16 underestimates the fundamental periods of mass timber buildings, demonstrating the need for revised period equations that account for the flexibility of post-tensioned rocking walls.
2. Seismic performance evaluation of full-scale mass timber rocking wall structures, offering critical insights into drift control, period elongation, and base shear.
3. Validation of post-tensioned mass timber rocking walls as an effective lateral force-resisting system, showcasing their ability to dissipate energy while maintaining self-centering behavior.
4. Comparative analysis of a ten-story and six-story mass timber structure, highlighting the effects of height and stiffness on seismic response.

8.3 Conclusion

The results of this study confirm that post-tensioned mass timber rocking walls are a viable and resilient lateral force-resisting system for seismic applications. While ASCE 7-16 underestimates the actual fundamental periods of these structures, the experimental results demonstrate that mass timber buildings can effectively manage seismic forces, control drift, and recover functionality after very intense earthquakes.

The findings from this research contribute to the broader adoption of mass timber in high-seismic regions by providing empirical data for performance-based seismic design. Moving forward, the development of updated seismic design provisions and period equations specific to mass timber structures will be essential to ensuring that these buildings achieve optimal seismic resilience while maintaining cost efficiency and sustainability.

REFERENCES

Abed, J., Rayburg, S., Rodwell, J., and Neave, M. (2022). "A review of the performance and benefits of mass timber as an alternative to concrete and steel for improving the sustainability of structures." Sustainability, 14(9), 5570. https://doi.org/10.3390/su14095570

Akbas, T., Sause, R., Ricles, J. M., Ganey, R., Berman, J., Loftus, S., Dolan, J. D., Pei, S., van de Lindt, J. W., and Blomgren, H.-E. (2017). "Analytical and experimental lateral-load response of self-centering posttensioned CLT walls." J. Struct. Eng., 143(6), 04017019. https://doi.org/10.1061/(ASCE)ST.1943-541X.0001733.

American Society of Civil Engineers (ASCE). (2017). Minimum design loads and associated criteria for buildings and other structures (ASCE/SEI 7-16). Reston, VA: American Society of Civil Engineers.

American Wood Council. (2018). National Design Specification (NDS) for Wood Construction. Leesburg, VA: AWC.

Araújo, R. G. A., Simpson, B. G., Barbosa, A. R., Pieroni, L., Ho, T. X., Orozco, G. F., Miyamoto, B., and Sinha, A. (2025). "Experimental and Numerical Simulation of a Three-Story Mass Timber Building with a Pivoting Wall and Buckling-Restrained Boundary Elements." (Submitted to Journal of Structural Engineering).

Araújo, R. G. A. (2022). "Design, experimental testing, and numerical analysis of a three-story mass timber building with a pivoting spine and buckling-restrained energy dissipators." Master's thesis, Oregon State University, Corvallis, OR.

Barbosa, A., Simpson, B., van de Lindt, J., Sinha, A., Field, T., McBain, M., Uarac, P., Kontra, S., Mishra, P., Gioiella, L., Pieroni, L., Pryor, S., and Saxey, B. (2025). "Shake table testing program for mass timber and hybrid resilient structures datasets for the NHERI Converging Design project." DesignSafe-CI. https://doi.org/10.17603/ds2-rh8q-rn95

Blomgren, H.-E., Pei, S., Jin, Z., Powers, J., Dolan, J. D., van de Lindt, J. W., Barbosa, A. R., and Huang, D. (2019). "Full-scale shake table testing of cross-laminated timber rocking shear walls with replaceable components." J. Struct. Eng., 145(10), 04019115. https://doi.org/10.1061/(ASCE)ST.1943-541X.0002388.

Brown, J. R., Li, M., Palermo, A., Pampanin, S., and Sarti, F. (2021). "Experimental testing of a low-damage post-tensioned C-shaped CLT core-wall." J. Struct. Eng., 147(3), 04020357. https://doi.org/10.1061/(ASCE)ST.1943-541X.0002926.

Busch, A. (2023). "Design and Construction of Tall Mass Timber Buildings With Resilient Post-Tensioned Mass Timber Rocking Walls." Ph.D. Thesis, Colorado School of Mines.

Field, T., Barbosa, A. R., Zimmerman, R. B., Pryor, S., Sinha, A., and Higgins, C. (2023). "Experimental and analytical evaluation of the tension capacity of edgewise connected glued-in rods in mass ply panels." *J. Struct. Eng.*, 149(6), 04023074. https://doi.org/10.1061/(ASCE)ST.1943-541X.0003429

Field, T. J., Barbosa, A. R., Sinha, A., McBain, M., Pieroni, L., Uarac Pinto, P. A., Araújo, G. A. R., Mishra, P., Pei, S., and Simpson, B. G. (2025). "Full-scale shake table test of resilient six-story hybrid mass timber and steel structure." *Proc., World Conf. on Timber Engineering (WCTE 2025)*, Brisbane, Australia. https://doi.org/10.52202/080513-0301

Field, T., Barbosa, A. R., Pryor, S., Simpson, B., Uarac, P. P. A., Sinha, A., and van de Lindt, J. W. (2025). “Shake-Table Testing of a Full-Scale Six-story Resilient Mass Timber-Steel Hybrid Building.” Submitted to Journal of Structural Engineering.

Ganey, R., Berman, J., Akbas, T., Loftus, S., Dolan, J. D., Sause, R., Ricles, J., Pei, S., van de Lindt, J. W., and Blomgren, H.-E. (2017). “Experimental investigation of self-centering cross-laminated timber walls.” J. Struct. Eng., 143(10), 04017135. https://doi.org/10.1061/(ASCE)ST.1943-541X.0001877.

Granello, G., Palermo, A., Pampanin, S., Pei, S., and van de Lindt, J. W. (2020). “Pres-Lam buildings: State-of-the-art.” J. Struct. Eng., 146(6), 04020085. https://doi.org/10.1061/(ASCE)ST.1943-541X.0002603

Huang, D. (2023). “Optimized Seismic Design and Dynamic Response Analysis of Mass Timber Rocking Wall Lateral System.” Ph.D. Thesis, Colorado School of Mines.

Iqbal, A., Smith, T., Pampanin, S., Fragiacomo, M., Palermo, A., and Buchanan, A. H. (2016). “Experimental performance and structural analysis of plywood-coupled LVL walls.” J. Struct. Eng., 142(2), 04015123. https://doi.org/10.1061/(ASCE)ST.1943-541X.0001383.

Kontra, S., Mishra, P., Field, T., Barbosa, A. R., Pei, S., van de Lindt, J. W., & Berman, J. (2025). “Design and Performance of Vertical Splice Connections in a Six-Story Mass Timber Rocking Wall System.” *World Conference on Timber Engineering (WCTE) 2025*.

Mar, D. (2010). “Design Examples using Mode Shaping Spines for Frame and Wall Buildings.” In Proceedings of the 9th U.S. National and 10th Canadian Conference on Earthquake Engineering.

McBain, M., Simpson, B., Araújo, R. G. A., Pieroni, L., Barbosa, A. R., van de Lindt, J. W., Sinha, A., Brown, N., Kontra, S., Mishra, P., Gioiella, L., Sorosh, S., Hutchinson, T., Pryor, S., Field, T., and Uarac, P. (2024, September). "Shake table testing of a six-story, full-scale, mass timber rocking wall using buckling-restrained boundary elements as energy dissipators." World Conference on Earthquake Engineering, Milan, Italy.

McBain, M., Pieroni, L., Araújo, G. A. R., Uarac Pinto, P. A., Mishra, P., Kontra, S., Field, T., Barbosa, A. R., Berman, J. W., Pei, S., and Simpson, B. G. (2025). "Response of mass ply panel, self-centering rocking walls with buckling-restrained boundary elements as energy dissipators in shake table testing." *Proc., World Conf. on Timber Engineering (WCTE 2025)*, Brisbane, Australia. https://doi.org/10.52202/080513-0300

Mishra, P., van de Lindt, J. W., Pei, S., Barbosa, A. R., Pryor, S., Berman, J. W., Simpson, B. G., Ryan, K. L., Sinha, A., Uarac, P. A., McBain, M., Field, T., Kontra, S., and Pieroni, L. (2025). "Resilient seismic design of tall mass timber buildings: Comparison of two full-scale tri-axial shake table tests." *Proc., World Conf. on Timber Engineering (WCTE 2025)*, Brisbane, Australia. https://doi.org/10.52202/080513-0714

Palermo, A., Pampanin, S., and Buchanan, A. (2006). "Experimental investigations on LVL seismic resistant wall and frame subassemblies." Proc., 1st European Conf. on Earthquake Engineering and Seismology (ECEES), Geneva, Switzerland.

Pei, S., Ryan, K. L., Berman, J. W., van de Lindt, J. W., Pryor, S., Huang, D., Wichman, S., Busch, A., Roser, W., Wynn, S. L., Ji, Y., Hutchinson, T., Sorosh, S., Zimmerman, R. B., and Dolan, J. (2024). "Shake-table testing of a full-scale 10-story resilient mass timber building." J. Struct. Eng., 150(12), 04024183. https://doi.org/10.1061/JSENDH.STENG-13752

Pei, S., van de Lindt, J. W., Barbosa, A. R., Berman, J. W., McDonnell, E., Dolan, J. D., Blomgren, H.-E., Zimmerman, R. B., Huang, D., and Wichman, S. (2019). "Experimental seismic response of a resilient 2-story mass-timber building with post-tensioned rocking walls." J. Struct. Eng., 145(11), 04019120. https://doi.org/10.1061/(ASCE)ST.1943-541X.0002382.

Pei, S., van de Lindt, J. W., Barbosa, A. R., Berman, J. W., McDonnel, E., Dolan, J. D., Blomgren, H.-E., Zimmerman, R. B., Huang, D., and Wichman, S. (2019). "Experimental seismic response of a resilient 2-story mass-timber with post-tensioned rocking walls." J. Struct. Eng., 145(11), 04019120. https://doi.org/10.1061/(ASCE)ST.1943-541X.0002382.

Pryor, S., Pei, S., van de Lindt, J., and Huang, D. (2024). "Seismically Resilient Connections for Mass Timber Buildings." In Proceedings of 18th World Conference on Earthquake Engineering, Milan, Italy.

Pryor, S., Pei, S., van de Lindt, J. W., and Huang, D. (2024). "Seismically resilient connections for mass timber buildings." Proc., World Conf. on Earthquake Engineering, Tokyo, International Association of Earthquake Engineering.

Roser, W., Wichman, S., Ji, Y.-E., Wynn, S. L., Ryan, K., Berman, J. W., Hutchinson, T. C., and Pei, S. (2023). "Evaluation of Non-structural Walls with Drift-Compatible Details in a 10-Story Mass Timber Building Shake Table Test." In Fifth International Workshop on the Seismic Performance of Non-Structural Elements (SPONSE).

Seyed Hossein Zargar, S., Patricio Uarac, Andre R. Barbosa, Arijit Sinha, Barbara Simpson, John W. van de Lindt, and Nathan C. Brown. "Comparing Optimization Approaches in the Direct Displacement-Based Design of Tall Mass Timber Lateral Systems." https://ascelibrary.org/doi/epdf/10.1061/9780784485248.085

Sorosh, S., Zhang, J., Hutchinson, T. C., Ryan, K. L., Smith, K. W., Kovac, A., Pei, S., Barbosa, A. R., and Simpson, B. (2024, December). “Detailing for seismically resilient steel stair systems: Validation in the mass timber (10 and 6-story) programs (Paper No. 7-2).” 18th U.S.-Japan-New Zealand Workshop on the Improvement of Structural Engineering and Resilience (ATC 15-17 Workshop), San Diego, CA.

Uarac, P. P. A., Barbosa, A. R., Sinha, A., van de Lindt, J. W., and Simpson, B. G. (202X). “Full-Scale Shake Table Testing of a Resilient Six-Story Mass Timber Building with Self-Centering Rocking Walls.” Journal of Structural Engineering.

van de Lindt, J. W., Furley, J., Amini, M. O., Pei, S., Tamagnone, G., Barbosa, A. R., Rammer, D., Line, P., Fragiacomo, M., and Popovski, M. (2019). “Experimental seismic behavior of a two-story CLT platform building.” Eng. Struct., 183, 408–422. https://doi.org/10.1016/j.engstruct.2018.12.079.

Wichman, S. (2023). “Seismic behavior of tall rocking mass timber walls.” Ph.D. thesis, Dept. of Civil and Environmental Engineering, Univ. of Washington.

Wichman, S., Berman, J. W., and Pei, S. (2022). “Experimental investigation and numerical modeling of rocking cross laminated timber walls on a flexible foundation.” Earthquake Eng. Struct. Dyn., 51(7), 1697–1717. https://doi.org/10.1002/eqe.3634.

Zhang, J., Sorosh, S., Hutchinson, T. C., Ryan, K. L., Smith, K. W., Kovac, A., Pei, S., Barbosa, A. R., and Simpson, B. (2024). “Detailing for seismically resilient steel stair systems: Validation in the mass timber (10 and 6-story) programs.” 18th U.S.-Japan-New Zealand Workshop.